



Wireless Laser Speckle Contrast Imaging during DIEP flap breast reconstruction: an evaluation of the first prototype

S.E.M. Teunissen

Master Thesis Technical Medicine
Medical Imaging and Interventions

August 2022

Graduate committee

Chairman: Prof. dr. ir. W. Steenbergen¹

Medical supervisors: Dr. H.A. Rakhorst², dr. D.J. Evers²

Technological supervisor: Prof. dr. ir. W. Steenbergen¹

Process supervisor: A.G. Lovink¹, MSc

External supervisor: B. Wermelink¹, MSc

Daily supervisor: Dr. A. Chizari¹

¹ The University of Twente, Enschede

² Hospital Ziekenhuisgroep Twente, Department of (plastic) surgery, Hengelo

Table of contents

Abstract	2
1. Introduction	3
1.1 Breast cancer and breast reconstructions	3
1.2 Current assessment of the microcirculation during DIEP flap breast reconstruction	4
1.3 Laser Speckle Contrast Imaging	4
1.4 Results from previous LSCI studies.....	5
1.5 Wireless Perfusion Imager	6
1.6 Motion artefacts.....	6
1.7 Aims of the thesis	7
2. Proof-of-concept study.....	8
2.1 Introduction	8
2.2 Materials and methods.....	8
2.3 Results	14
2.4 Discussion	21
2.5 Conclusion.....	25
3. Clinical study	26
3.1 Introduction	26
3.2 Methods.....	26
3.3 Hypothetical results.....	31
3.4 Ethical considerations.....	33
4. Future perspectives and general conclusion	34
5. References	35
6. Appendix.....	38
6.1 Appendix A: Optical flow and Farneback's algorithm	38
6.2 Appendix B: Creating perfusion maps based on optical flow	40
6.3 Appendix C: MATLAB script ECC versus Optical flow	41
6.4 Appendix D: Analysis of the perfusion maps	43
6.5 Appendix E: Visualisation of the displacements between handheld and mounted measurements.....	45
6.6 Appendix F: MATLAB script for the calculations of the velocity and speed	47
6.7 Appendix G: Overzicht indiening documenten aan METC en ALU	49
6.8 Appendix H: Proefpersoneninformatie brief	52
6.9 Appendix I: User Experience Questionnaire	60
6.10 Appendix J: Research protocol	61

Abstract

Background Surgical decisions regarding the improvement of the quality of life of patients that survived breast cancer have become more important as the 10-year survival rate has significantly increased in the last decades. One of the surgical options after a breast cancer survival that is related to a good quality of life is Deep Inferior Epigastric Perforator (DIEP) flap breast reconstruction. Most patients have a postoperative recovery without any severe complications. However, perfusion-related complications are reported to occur in 7%-35% of the patients. To avoid these, the microcirculation is intraoperatively assessed by the surgeon, which depends on the surgeon's experience and is subjective. For a more objective assessment, indocyanine green (ICG) angiography can be applied. But ICG has some disadvantages including intravenous administration and the incapability of the visualisation of changes in the microcirculation after administration. A promising technique that could overcome these disadvantages is Laser Speckle Contrast Imaging (LSCI). LSCI is a real-time and non-contact imaging technique for the visualisation of the perfusion up to a depth of 700 μm in the skin. In several studies, LSCI is considered as a promising technique for perioperative assessment of the microcirculation. However, a limitation of these studies was the use of mounted LSCI devices, making it complicated to use them in the operating theatre. Therefore, the Biomedical Photonic Imaging group of the University of Twente is developing a handheld and wireless system: the Wireless Perfusion Imager (WIPI). However, a handheld device brings another challenge: correct motion artefacts.

Objective This thesis has two main objectives. The first aim is to test, evaluate and improve the WIPI in a proof-of-concept study for the application in a clinical study. The second aim is to organise the clinical study considering the visualisation of the microcirculation with the use of the WIPI during DIEP flap breast reconstruction that is subject to the Medical Research Involving Human Subject Act.

Methods First, the performance of the optical flow algorithm to correct for motion artefacts caused by image misalignment was determined and compared to enhanced correlation coefficient (ECC) maximisation. For the proof-of-concept study, 11 handheld and mounted perfusion measurements were performed to show the effect of background light, the differences in perfusion and displacements between handheld and mounted measurements and the perfusion distribution of the abdomen in a healthy test subject. For the clinical study, the measurement protocol remains the same. Additionally, the WIPI needs to be packed in a sterile bag.

Results The optical flow algorithm shows a similar pattern in displacement compared to ECC maximisation. Background light increases the measured perfusion value. Most of the handheld measurements have approximately 10% higher perfusion values than mounted measurements and the displacements are three to five times as large in handheld measurements than in mounted measurements. Lastly, no accurate measurements can be performed when the laser light is of low intensity at the skin, which is the case at the edges of the perfusion map. Reliable perfusion measurements can therefore only be performed in the centre of the perfusion maps as the laser beam had a Gaussian pattern.

Conclusion The optical flow algorithm shows good performance in aligning the perfusion maps for the application in the clinical study. The multiple perfusion maps show that background light increases the perfusion values and that handheld measurements mostly lead to higher perfusion values compared to mounted measurements. In the perfusion maps, only the measured perfusion values in the centre are reliable as the laser beam had a Gaussian pattern. It is desirable to increase the area in which reliable measurements are possible before starting the clinical study by for example increasing the laser intensity or flatten the Gaussian curve. However, these solutions need to be further researched.

Key words – DIEP flap breast reconstruction, Laser Speckle Contrast Imaging, motion artefacts, optical flow, perfusion.

1. Introduction

1.1 Breast cancer and breast reconstructions

Breast cancer is responsible for 26% of all malignancies in the Netherlands and is therefore the most frequently diagnosed malignancy among Dutch females¹. As the 10-year survival rate has significantly increased in the last decades due to improved treatments, surgical decisions regarding the improvement of the quality of life have become more important²⁻⁴. One of the treatments which is related to a good quality of life is skin-sparing mastectomy followed by breast reconstruction⁵. Breast reconstructions can be performed with the use of autologous tissue or breast implants^{5,6}. Autologous breast reconstructions are superior to implants regarding the aesthetic outcome, long-term satisfaction and quality of life⁷. Moreover, autologous breast reconstructions are recommended in case the remaining breast tissue is of bad quality due to, for example, radiotherapy⁸. The standard for autologous breast reconstruction is the Deep Inferior Epigastric Perforator (DIEP) flap reconstruction, referring to the feeding artery⁶. During this procedure, an abdominal flap, the so-called DIEP flap, is harvested to reconstruct the breast (Figure 1)⁹.

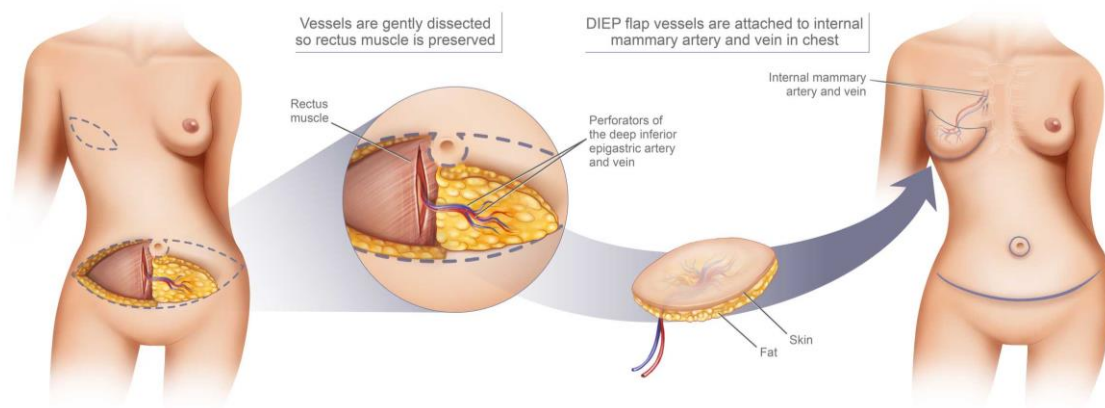


Figure 1 Deep Inferior Epigastric Perforator (DIEP) flap breast reconstruction⁹.

The DIEP flap is supplied by an average of five perforators, which have a broad variety in branching patterns¹⁰. These perforators arise from the Deep Inferior Epigastric Artery, which runs from the lateral side of the rectus abdominis muscle to the umbilicus and eventually penetrates the rectus abdominis muscle to end up in these perforators¹¹. Most perforators are located within 2 cm cranial and 6 cm caudal and between 1 to 6 cm around the lateral sides of the umbilicus¹¹. The locations of the potential perforators for transplantation are marked on the skin before surgery. Also, the contours of the DIEP flap are marked on the abdomen before surgery, as visible as the dashed line in Figure 1. The first part of the surgery consists of raising the DIEP flap at a superficial level until the perforators are visible to find the dominant perforator. When an appropriate perforator is encountered, the surgeon assesses the quality of the perforator and may use Ultrasound Doppler to check whether this perforator is suitable for transplantation¹⁰. After the best perforator is chosen, all other perforators are sacrificed. Then, the DIEP flap can be transplanted to the breast by anastomosing the perforator to the internal mammary artery to complete the breast reconstruction^{12,13}.

Most patients have a postoperative recovery without any severe complications. However, perfusion-related complications, such as wound healing delay or necrosis in for example fatty tissue, are reported to occur in 7%-35% of the patients^{7,14-17}. Perfusion-related complications can occur when the transplanted flap is too large or because of thrombosis or vasospasms in the microcirculation of the flap or in the pedicle. It is important to reduce these complications to an absolute minimum as these complications have been shown to decrease the patient's satisfaction and quality of life⁵. Moreover, necessary revision surgeries lead to the increase of costs, hospital stay and can lead to serious stress for the surgeon involved⁶.

1.2 Current assessment of the microcirculation during DIEP flap breast reconstruction

Currently, to check for thromboses, vasospasms or a too large flap, the microcirculation is intraoperatively assessed by the surgeon by visual evaluation of the skin colour and temperature, capillary refill time and dermal edge bleeding^{8,18}. However, these methods depend on the surgeon's experience and subjective opinion, resulting in potential intra- and inter-observer variabilities¹⁹. For a more objective assessment, indocyanine green (ICG) angiography can be applied for additional evaluation of the perfusion of the DIEP flap²⁰. ICG can give a real-time prediction of the perfusion of tissue that is going to be transplanted and to assess the perfusion of the newly reconstructed breast. The assessment of the perfusion with the use of ICG is based on the area that becomes green on the angiogram and its intensity level. The intensity level corresponds to the amount of ICG and therefore to the amount of blood that perfuses the tissue. The application of ICG has resulted in a decrease in perfusion-related complications²¹. Therefore, nowadays in Ziekenhuisgroep Twente (ZGT), the current assessment of the microcirculatory consists of the combination of the application of ICG and the subjective assessment of the surgeon.

Nevertheless, ICG has some disadvantages^{22,23}. First, it requires the administration of a contrast agent and can therefore cause adverse reactions. However, these are rare and are reported to develop in 0.2% of the exposed patients²⁴. Furthermore, due to the washout of 20 minutes and a half-life time of 150 to 180 seconds, ICG has to be administered multiple times during surgery when assessment of the DIEP flap before and after transplantation is desired^{23,25}. But the time interval between two different administrations should be long enough to avoid an angiogram that includes 'old signal'. Also, changes in perfusion after inflow of ICG due to for example vasospasm or thrombosis can hardly be visualised as ICG is already present in the vascular system. Thus, it is hard to detect an occlusion that is caused by vasospasms or thrombosis just after the inflow of ICG. Lastly, the assessment of the fluorescence intensity does not have a cut-off value (yet) for under-perfused tissue, which makes the assessment subjective²².

1.3 Laser Speckle Contrast Imaging

A promising technique that could overcome the aforementioned disadvantages of ICG is Laser Speckle Contrast Imaging (LSCI). LSCI does not need any contrast agents, the measurements could take place at any convenient time and the measurements only take a few seconds^{18,26}. LSCI is a real-time and non-contact imaging technique for perfusion measurements. These perfusion measurements encounter the velocity and the concentration of the red blood cells. However, the contribution of the velocity and red blood cell concentration to the eventual measured perfusion is unknown. With the use of this technique, the perfusion can be visualised up to a depth of 700 μm in the skin, which corresponds to dermal microcirculation^{8,27,28}.

The principle of LSCI is that it uses backscattered light from tissue that is illuminated with coherent laser light to create a random interference pattern²⁹. This is also known as the speckle pattern³⁰. Moving particles in tissue, for example red blood cells, cause fluctuations in this speckle pattern. This results in blurring speckles when being integrated with a certain exposure time³⁰. The degree of blurring can be correlated to the blood flow, and so to perfusion³¹. The blurring can be measured by calculating the speckle contrast (C), which is defined as the ratio of the standard deviation of the intensity (σ_I) to the mean intensity (I) in a region of interest in an image³²:

$$C \triangleq \frac{\sigma_I}{I} \quad (1)$$

This equation is applied on the raw speckle frames obtained by a mono camera. A window of, for example 9x9 pixels, moves over the raw speckle frame and calculates C for each window, resulting in a contrast map³³. To estimate the perfusion with the use of the contrast, some other variables should

be considered, including exposure time (T) and correlation time (τ_c). Exposure time is typically around 10 ms. Correlation time is the time needed for the speckle pattern to change, i.e., to decorrelate or to turn into a different type of speckle pattern. Therefore, higher perfusion results in shorter correlation times. The speckle contrast is defined as³⁴:

$$C = \sqrt{\frac{\tau_c}{T} + \frac{\tau_c^2}{2T^2} (e^{\frac{2T}{\tau_c}} - 1)} \quad (2)$$

As the correlation time is unknown, the velocity (v_c) needs to be estimated (in arbitrary units). The correlation time is assumed to be inversely proportional to the velocity of the scattering particles³⁴:

$$\tau_c = \frac{\alpha}{v_c} \quad (3)$$

$$\alpha = \frac{\lambda}{2\pi} \quad (4)$$

In this equation, λ is the wavelength of the laser, which is 671 nm. Based on the set exposure time of 10 ms, a graph from a lookup table to obtain perfusion out of contrast, is created to determine the perfusion (velocity) for each measured speckle contrast value (Figure 2).

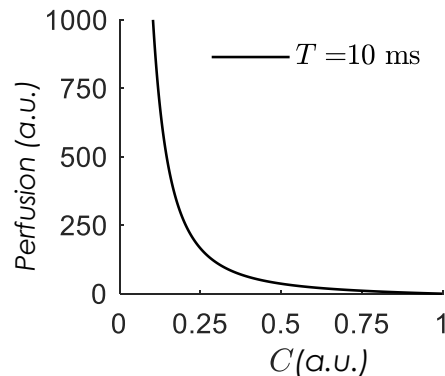


Figure 2 Graph from lookup table for the correlation between speckle contrast and perfusion.

1.4 Results from previous LSCI studies

In several studies, LSCI is already evaluated and considered as a promising technique for perioperative assessment of the microcirculation in colorectal surgery, cerebrovascular surgery and reconstructive surgery^{8,18,19,26,35,36}. The results in reconstructive surgery are of particular interest to this study. Zötterman et al. performed multiple studies regarding the assessment of perfusion in reconstructive surgery, of which a cut-off value was lacking for under-perfused tissue^{8,19,26}. First, their aim was to investigate whether LSCI could be perioperatively applied to identify areas with compromised circulation and thereby to predict areas that have a high risk of developing postoperative necrosis²⁶. They concluded that perfusion below 25 Perfusion Units (PU, arbitrary unit) was a predictor for tissue morbidity within 72 hours after surgery in porcine flap models. Consecutive research started on the perfusion distribution and perfusion-related postoperative complications during DIEP flap breast reconstruction^{8,26}. That study also showed a cut-off value for tissue morbidity, but this was a cut-off value of 30 PU for postoperative flap necrosis.

However, a limitation of these studies was the use of mounted LSCI devices. Due to the inflexibility of these devices, it is complicated to use them in the operating theatre. Therefore, the Biomedical

Photonic Imaging group of the University of Twente is currently developing a handheld and wireless system: the Wireless Perfusion Imager (WIPI). The previous version of this LSCI system, known as handheld perfusion imager (HAPI), was applied in the research to psoriasis lesions and this showed that handheld measurements give similar visual results compared to mounted measurements^{37,38}. Even though a statistically significant difference was found between mounted and handheld measurements because of movement artefacts in handheld measurements, the handheld device is of additionally clinical value in terms of comfortability and flexibility for medical staff and patients. However, the HAPI system still has some disadvantages. The HAPI is less bulky than the already existing mounted LSCI devices, but it is still complicated to perform measurements at the operating room (OR) as the computer and laser must be carried together with the device in a trolley. Moreover, motion artefacts must be manually corrected in postprocessing, which makes analysis time-consuming.

1.5 Wireless Perfusion Imager

The WIPI should be able to overcome the aforementioned disadvantages of the HAPI. A trolley to carry the laser and computer is not necessary anymore since the laser and an onboard computer, which can be controlled by a touchscreen on the top side of the WIPI, are integrated in the device. This makes the WIPI flexible and usable in the OR. The onboard computer enables preview mode, temporary storage of the data after performing a measurement and communication between the WIPI and a laptop via a router to send the data from the onboard computer to the laptop for more computationally expensive calculations. The laptop can be controlled by a touchpad that is attached on the top side of the WIPI. Furthermore, the WIPI contains two cameras: a mono camera for the reception of the backscattered laser light and a colour camera to image the measured area. To ensure similar light settings between multiple measurements, two LEDs are integrated in the system. Figure 3 shows the top view and the front view of the WIPI.



Figure 3 Left: top view of the WIPI. Right: front view of the WIPI with the laser in the left window and the mono camera (left) and colour camera (right) in the right window. Two LEDs are mounted in the upper corners.

1.6 Motion artefacts

As the WIPI is just as the HAPI a handheld system, motion artefacts should be corrected to get a reliable and an accurate measurement³⁹. Motion artefacts could be divided into two types: motion artefacts occurring within the exposure time of the mono camera and motion artefacts due to misalignment between consecutive frames. The first one is complicated to correct as the exact velocity of the displacement within the exposure time is unknown. This makes that handheld measurements have approximately 16% higher measured perfusion values than mounted measurements³⁷. The second type of motion artefacts is correctable and there are several methods described in literature⁴⁰⁻⁴⁴. However, only the studies performed by Lertsakdadet et al. described a method to correct motion artefacts due to image misalignment in handheld LSCI^{43,44}. Their method was based on the use of fiducial markers for the alignment of the speckle frames, but fiducial markers are not preferable in the operating theatre because of the strict rules to take any object into the sterile environment in the OR. A method to correct for artefacts caused by image misalignment that does not need any markers, is

optical flow. Optical flow is the pattern of motion of objects between consecutive colour (RGB) frames, which is caused by relative movement between object and camera⁴⁵⁻⁴⁸. Optical flow estimates the displacement in x and y direction (dx, dy) by measuring the intensities (I) at times (t) and ($t + dt$), i.e., comparing two consecutive images. This is graphically represented in Figure 4. The time between frames is known, as this is the inverse proportion of the sampling rate of the camera. A detailed explanation of the optical flow algorithm is attached in 6.1 Appendix A: Optical flow and Farneback's algorithm.

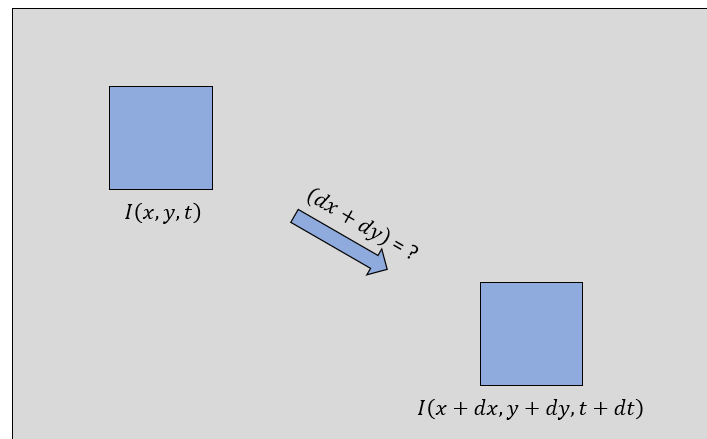


Figure 4 Graphical representation of the optical flow problem. In optical flow, dx and dy are estimated.

1.7 Aims of the thesis

This thesis has two main objectives. The first aim is to test, evaluate and improve the WIPI in a proof-of-concept study for the application in a clinical study. The second aim is to organise the clinical study considering the visualisation of the microcirculation with the use of the WIPI during DIEP flap breast reconstruction that is subject to the Medical Research Involving Human Subject Act. To successfully investigate these objectives, the following research questions are defined for each objective:

Proof-of-concept study

- i. What is the performance of the optical flow algorithm compared to enhanced correlation coefficient maximisation to correct motion artefacts?
- ii. What is the effect of ambient light in the OR and light of the LEDs on the perfusion images?
- iii. What are the differences in perfusion and displacement between handheld measurements and mounted measurements?
- iv. What is the perfusion distribution of the abdomen in a healthy test subject measured with the WIPI?

Clinical study

- i. What is the correlation between the mean perfusion of the newly reconstructed breast during DIEP flap breast reconstruction and the development of perfusion-related complications?
- ii. What is the perfusion distribution of the abdominal flap and the newly reconstructed breast during and after DIEP flap breast reconstruction measured with the WIPI?
- iii. What is the reliability and user-friendliness of the WIPI during surgery?

2. Proof-of-concept study

2.1 Introduction

Before starting the clinical study, a small proof-of-concept study was performed in which the perfusion of the abdomen in one healthy test subject was measured with the WIPI. In this test set-up, a future baseline measurement in the OR was simulated to gain experience in performing measurements with the WIPI. Then, the four research questions which are formulated for this proof-of-concept study can be answered.

2.2 Materials and methods

2.2.1 Materials

In previous chapter 1.5 Wireless Perfusion Imager, Figure 3 shows the top view and front view of the WIPI. To perform measurements with the use of the WIPI, the following materials are required:

- WIPI, which contains:
 - Laser with a wavelength of 661 nm and a negative lens.
 - Camera system, including a mono camera for the perfusion measurements and a colour camera with a focus distance of 30 cm to image the measured area for the application of optical flow
 - Onboard computer, which is the raspberry pi 4. The raspberry pi enables temporary storage of the images, preview mode and communication with the laptop
 - Battery (14.4 V, Li-Ion battery)
 - 2 buttons on the grips, one to start preview mode, one to start measuring mode
 - Touchscreen for the real-time visualisation of the measurements (preview mode) and to control the raspberry pi
 - Touch pad to control the laptop
 - 2 LEDs to light the skin
- External hardware:
 - Laptop for more computationally expensive calculations
 - TP-link router to enable communication between WIPI and laptop

For more details about the WIPI, the Investigational Medical Device Dossier can be consulted in P:\Users\Sacha Teunissen\Manuscripts\2022 METC en ALU aanvragen\2022-05 METC aanvraag ronde 2\D. Productinformatie\IMDD WIPI Version 2 No Track Changes.

2.2.2 Methods

2.2.2.1 Performance of the optical flow algorithm compared to ECC maximisation

Before performing the actual measurements for the proof-of-concept study, the performance of the optical flow algorithm was researched to ensure the resulting perfusion maps were well aligned. Therefore, this algorithm was compared to enhanced correlation coefficient (ECC) maximisation, which was successfully applied in previous study to the HAPI system in psoriasis patients³⁷. In that study, ECC maximisation was directly applied on speckle frames after segmentation of black marker dots on the skin. ECC maximisation is a computationally cheap image registration technique that estimates the 2D geometric transformation to register the input image to the template one^{31,37,49}. However, ECC maximisation needs multiple drawn marks on the skin to properly perform image registration on speckle frames, which is undesirable in a surgical environment. Therefore, the possibilities of optical flow were researched. For a comparison between both algorithms, a measurement with the HAPI system was performed as the WIPI was not ready yet to perform perfusion measurements. This measurement took place in the lab of the Biomedical Photonic Imaging group of the University of Twente in Enschede. For this measurement, a ruler of 1 cm was placed on a test subject's arm to calculate the conversion factor between RGB frames and speckle frames in postprocessing (Figure 5). Furthermore, five dots were marked on the skin for the application of ECC maximisation. After the placement of the ruler and drawing the dots on the arm, a handheld measurement with the use of the

HAPI system was performed. The framerates of the colour camera and mono camera were both 30 Hz and the measurement took 10.9 seconds, resulting in 328 RGB frames and speckle frames. The gain of the colour camera was 0 dB, whereas the gain of the mono camera was 10 dB. The exposure time was 10 ms for both cameras.

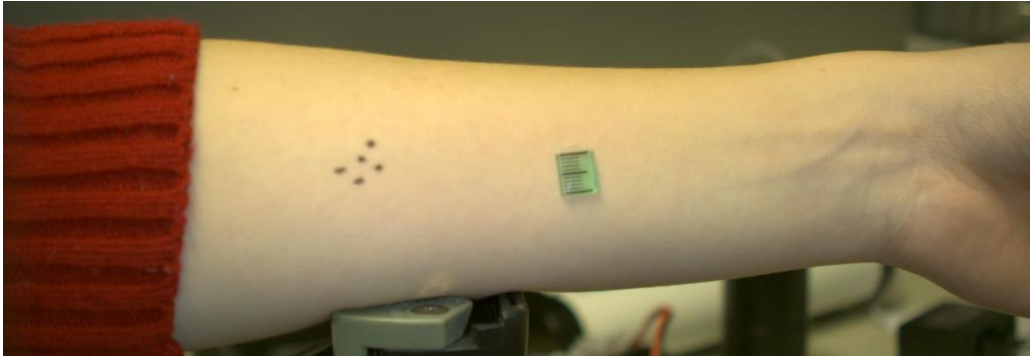


Figure 5 Colour image of a ruler of 1 cm and five dots on a test subject's arm to compare the performance of optical flow and ECC maximisation.

Comparison between both algorithms was performed in MATLAB R2022b (The Mathworks, Inc). First, the pixel size on the RGB images and on the speckle images was determined by manually measuring the 1 cm ruler on the images in MATLAB (6.2 Appendix B: Creating perfusion maps based on optical flow). This resulted in a pixel size of 77 micron in the speckle image and 159 microns in the RGB image, which was a conversion factor of 2.06. These pixel sizes differ mainly because of the diverse types of sensors within the cameras. Then, ECC maximisation was applied on the speckle frames to follow the displacements, optical flow was applied on RGB frames to follow the displacement as well and lastly, the found displacements in the RGB frames were converged to the speckle frames with the use of the conversion factor. For both algorithms, the displacements of the same starting x and y coordinate on the speckle frames were followed over time to enable comparison (6.3 Appendix C: MATLAB script ECC versus Optical flow). As the mono camera had a delay of 0.8 seconds compared to the RGB camera due to differences in hardware triggers, a second comparison was made where the optical flow algorithm was delayed with 0.8 seconds, so 24 frames.

2.2.2.2 Preparations proof-of-concept study

For the actual proof-of-concept study, one healthy female test subject of the age of 22 years was recruited for the WIPI measurements at the OR of the TechMed Centre at the University of Twente, Enschede. The aim of these measurements was to simulate a baseline measurement of the DIEP flap at the OR. To simulate the DIEP flap breast reconstruction as good as possible, the patient laid on the operating table and an example of a DIEP flap was marked on the skin in the same way as a plastic surgeon does before surgery (Figure 6). Due to privacy, the DIEP flap was drawn approximately 5 cm more cranial than the DIEP flap is normally drawn before surgery. Also, four dots were marked on the skin, representing examples of perforators as this is also common procedure before the start of the surgery. Before starting the measurements, a calibration was performed to ensure accurate perfusion measurements. The calibration was performed by measuring two areas in a calibration box; the first area was static and had a perfusion of zero (a.u.), the second area was a colloidal suspension in which the perfusion was 250 (a.u.). Following calibration, one measurement with the ruler of 1 cm on the skin was required to perform for the determination of the conversion factor between RGB frames and speckle frames for a correct alignment. Therefore, one handheld measurement with the 1 cm ruler on the abdomen was performed after which the conversion factor was determined as described in 2.2.2.1 Performance of the optical flow algorithm compared to ECC maximisation. In contrast to the HAPI, this resulted in a pixel size on RGB frames of 154.4 micron and 86.9 micron on speckle frames, leading to a conversion factor of 1.78 for the WIPI.

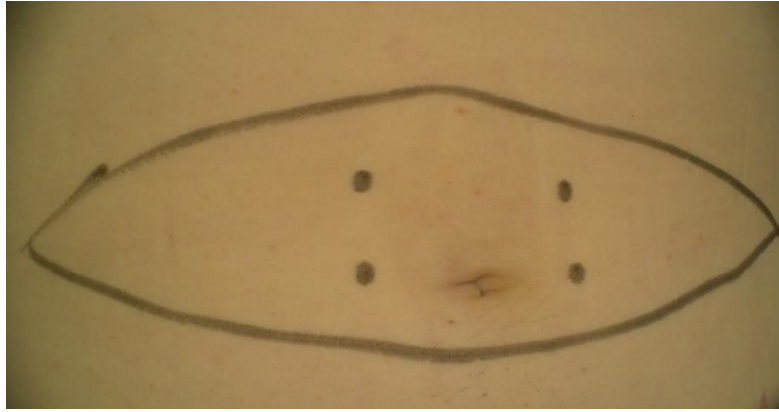


Figure 6 Colour image of the drawn DIEP flap on a healthy test subject.

2.2.2.3 Measurement protocol proof-of-concept study

Following the calibration and the measurement with the 1 cm ruler on the skin, the actual measurements could start. For this proof-of-concept study, a total of 11 measurements (4 handheld, 7 mounted) were performed by one operator. This section describes the protocol how a measurement with the use of the WIPI should be performed. Detailed measurement settings to answer the research questions are described in 2.2.2.4 The effect of background light, 2.2.2.5 Handheld versus mounted and 2.2.2.6 Perfusion distribution.

As the field of view of the WIPI has a diameter of 14 cm, three measurements were necessary to cover the entire DIEP flap. The WIPI was held 30 cm above the skin, as this is the focus distance of the colour camera. Before each measurement, the preview mode of the WIPI was used to show the current position the WIPI was measuring. During preview mode, real-time perfusion maps and colour images were previewed on the touchscreen of the WIPI by pushing a button. Previewing takes approximately one minute. When previewing or measuring the skin, the laser and LEDs on the WIPI turned on automatically and afterwards, the laser and LEDs automatically switched off. When the previewed area was visualised according to plan, the measurement could start. A measurement was started by pushing the other button on the WIPI. In contrast to the framerate of the HAPI, the framerate of both cameras in the WIPI was 16 Hz. Furthermore, 45 RGB frames and speckle frames were obtained in a synchronised way, resulting in a duration of 2.8 seconds. Additionally, the gain of both cameras was 10 dB and the exposure time was 10 ms for both cameras.

After a measurement was completed, the data were temporally saved on the raspberry pi, which took approximately 40 seconds. After saving, the data were transferred from the raspberry pi to the laptop via communication with the router. Data transfer took approximately 25 seconds. On the laptop, detailed analysis was performed in MATLAB. This is described in 2.2.2.7 The creation of an aligned and averaged perfusion map and 2.2.2.8 Additional analysis.

2.2.2.4 The effect of background light

To research the effect of ambient light in the OR and the light of the LEDs, three mounted measurements in the middle of the DIEP flap were performed. A tripod was used to hold the WIPI above the test subject (Figure 7). The first measurement was with ambient light and LEDs switched on, the second one was with ambient light switched off and LEDs switched on and the third one was with both switched off. The choice to perform mounted measurements was to do not have any influence of the operator's movement and to measure the exact same area three times.



Figure 7 The set-up of the mounted measurement at the middle of the abdomen with the WIFI held in a tripod.

2.2.2.5 Handheld versus mounted

To research the differences in perfusion in handheld and mounted measurements, six measurements were performed: handheld and mounted at the left, middle and right of the abdomen. In these six measurements, ambient light in the OR and the LEDs were switched on. Figure 8 illustrates one of the handheld measurements at the OR.



Figure 8 Image of the operator performing a handheld measurement at the OR.

2.2.2.6 Perfusion distribution

To simulate an area with higher perfusion than its surroundings, one fingertip of Midalgan cream (Remark Pharma BV; active ingredients per 100 mg: 1 mg histamine chloride, 10 mg methyl nicotinate and 100 mg glycol salicylate), which has a vasodilative effect on the microcirculatory, was applied on the skin on an area of approximately 1.5 cm² as visualised in Figure 9. The area was limited by a paper contour of a square, so the Midalgan was applied in that square only. Two measurements were performed; a mounted and a handheld measurement at the middle of the abdomen. The mounted measurement started 8 minutes after Midalgan application as the Midalgan is at its maximum effect after 8 to 10 minutes. The handheld measurement was performed as soon as possible after the

mounted measurement was performed to measure a vasodilative effect that was as similar as possible. This was approximately one minute later.

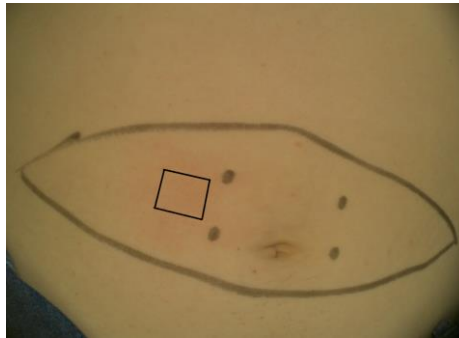


Figure 9 Drawn DIEP flap in the healthy test subject with Midalgan applied on the skin in the drawn rectangle.

2.2.2.7 The creation of an aligned and averaged perfusion map

With the use of the obtained data from the 11 measurements, 11 aligned and averaged perfusion maps were created in MATLAB (6.2 Appendix B: Creating perfusion maps based on optical flow). The first step to obtain these perfusion maps was motion detection on the RGB frames based on optical flow. Then, the found displacements on the RGB frames could be converged to speckle frames. For this conversion, the conversion factor that was found during preparation, was used (2.2.2.2 Preparations proof-of-concept study). After conversion, the 45 speckle frames of each measurement were aligned. Finally, the 45 aligned speckle frames were averaged to get one perfusion map for each measurement.

2.2.2.8 Additional analysis

Next to the creation of a perfusion map for each measurement, additional analysis in MATLAB (6.4 Appendix D: Analysis of the perfusion maps) was performed to answer the second and third research questions (Effect of background light and Handheld versus mounted). To research the effect of light, the mean intensity (I), the standard deviation of the intensity (σ_I) and the contrast (C) were calculated according to eq. (1) in the three perfusion maps in two regions of interest (ROIs): one in the centre and one in the left upper corner. In the centre, ambient light, LED light and laser light was present. In the left upper corner, ambient light and LED light were present as well, but the influence of laser light was small due to the Gaussian pattern of the laser. Furthermore, the mean perfusion and the perfusion over time in the same two ROIs were calculated.

To answer the third research question, two ROIs were placed on the perfusion maps as well: one in the centre of the image and one at the lateral side of the abdomen in case of imaging the left and right side or one in the upper left corner in case of imaging the middle of the abdomen. With the use of these ROIs, a comparison in perfusion could be made between handheld and mounted.

Furthermore, to research the differences in displacement between mounted and handheld, the displacement of the entire measurement and the displacement in the x and y direction over time were determined with the use of the optical flow algorithm and could be visualised (6.5 Appendix E: Visualisation of the displacements between handheld and mounted measurements). To quantify the differences in distance between handheld and mounted measurements, the on-surface speed was calculated by dividing the distance (d) over time (t) for each measurement according to eq. (5), after which the speed ratio was also calculated. For the quantification of the difference in displacement between handheld and mounted measurements, the mean on-surface velocity was calculated for each measurement by dividing the displacement (Δs) over time (Δt) as defined in Eq. (6), after which the ratio of on-surface velocity between handheld and mounted was calculated (6.6 Appendix F: MATLAB script for the calculations of the velocity and speed).

$$Speed = \frac{d}{t} \quad (5)$$

$$Velocity = \frac{\Delta s}{\Delta t} \quad (6)$$

Lastly, for the handheld measurement at the middle of the abdomen, the correlation between the velocity and perfusion was researched. The hypothesis was that there should be a linear correlation between these two variables. So, the perfusion should increase with an increasing velocity. However, due to the small amount of data points (45), this correlation was only researched in this handheld measurement at the middle of the abdomen.

2.3 Results

2.3.1 Performance of the optical flow algorithm compared to ECC maximisation

The left graphs of Figure 10 show the displacements in the x and y direction of ECC maximisation and the optical flow algorithm of the measurement with the ruler of 1 cm on the arm, which was performed with the use of the HAPI. As visible, the patterns of both curves are similar, but it is visible that the ECC algorithm has a delay of 24 frames (0.8 seconds) compared to the optical flow algorithm. Furthermore, there is some disagreement in especially the x direction.

The right graphs of Figure 10 show the displacement in the x and y direction of ECC maximisation and the optical flow algorithm in which the optical flow algorithm is delayed by 24 frames. This is visible as the horizontal start of the blue curve. Still, there is a difference in pixel displacement between both axes, especially in the x direction. This difference in x direction seems to stay the same over time and is approximately 40 pixels, which corresponds to 3.4 mm as the pixel size in the speckle frames was $86.9 \mu\text{m}/\text{pixel}$. In the y direction, the algorithms disagree for approximately 30 pixels at the first 150 frames of the measurement, but in the remaining part of the measurement, the displacements are more similar.

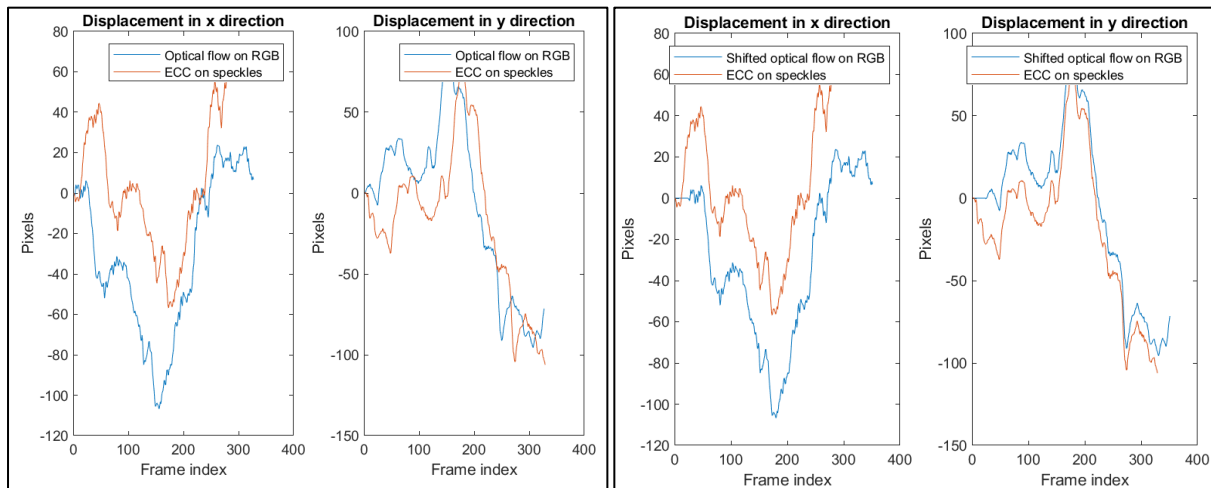


Figure 10 Displacements of optical flow on RGB frames applied on speckle frames and ECC on speckle frames directly. Left: no time adjustment on settings. Right: time adjustment by shifting optical flow data.

2.3.2 The effect of background light

In Figure 11, the RGB image (Figure 11A) and the averaged and aligned perfusion maps regarding the measurements to the effect of lights (Figure 11B, Figure 11C, Figure 11D) are shown. Figure 11B shows the perfusion map with ambient light and LEDs switched on, Figure 11C shows the perfusion map with only LEDs switched on and Figure 11D shows the perfusion map without any light switched on.

The perfusion maps have an oval of approximately 6 cm by 10 cm of lower perfusion values in the centre compared to the edges. This is primarily visible in the perfusion map with all lights switched on, suggesting ambient light plays a role in affecting the perfusion values. Moreover, at the left side of the oval, there is a clear cut-off between the region of lower perfusion in the centre and the region of higher perfusion at the edges. However, this cut-off is not as clear at the right side of the oval as at the left side. Furthermore, the peak in perfusion in all perfusion maps at the middle top of the DIEP flap (blue arrow) corresponds to the red spots at the RGB image. The peaks in perfusion just above the DIEP flap at the right and at the bottom right (green arrows), do not have a corresponding red spot on the RGB image. Both peaks have a wavy pattern, suggesting that these peaks are diffraction artefacts created by dust on the spherical lens to diverging laser beam. Lastly, the right side of each perfusion map is black because of a suboptimal position of the mono camera.

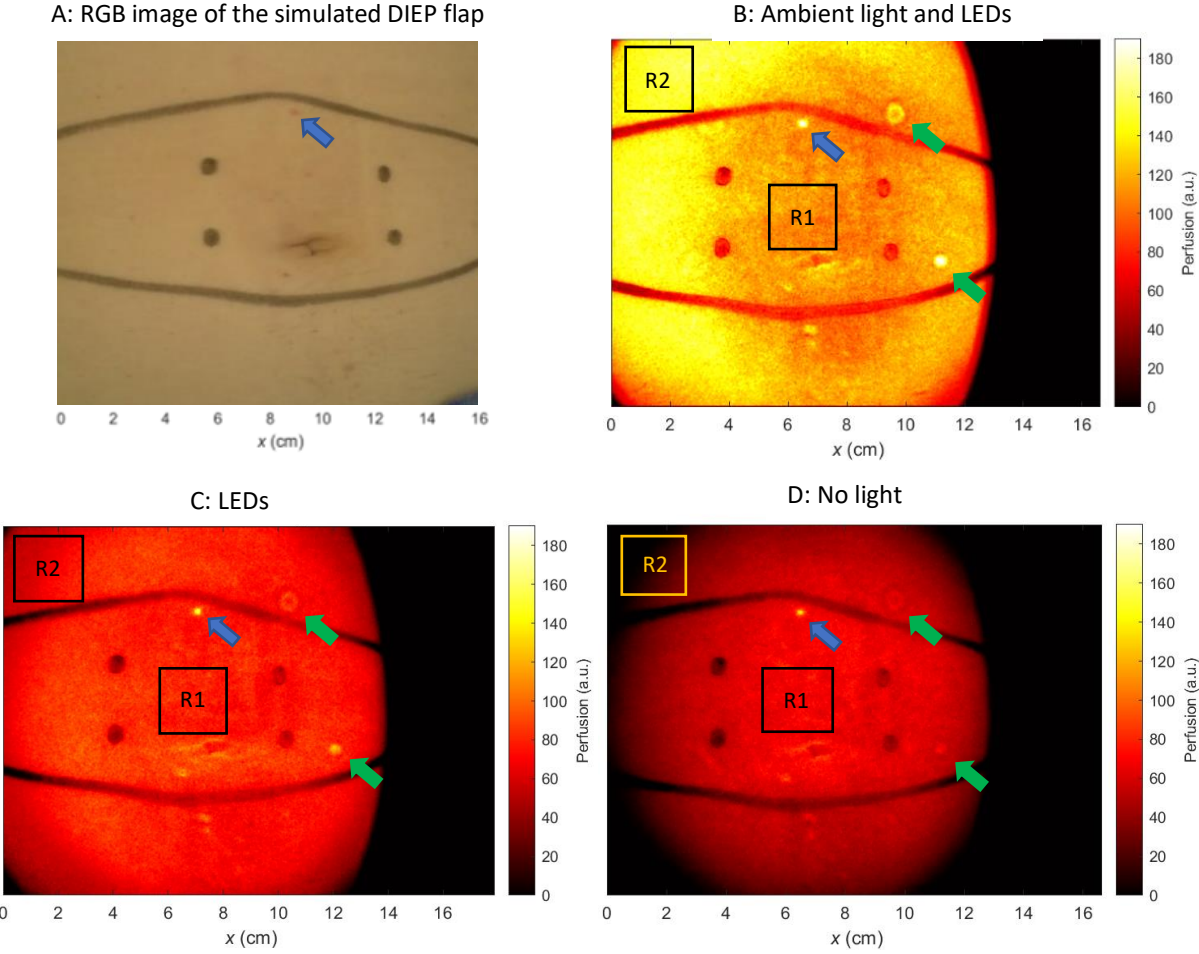


Figure 11 RGB image (A) and perfusion maps of the abdomen of a healthy test subject. B: perfusion map with ambient light and LEDs switched on. C: perfusion map with only LEDs switched on. D: ambient light and LEDs switched off. The blue arrows indicate a red spot on the skin, whereas the green arrows indicate dust artefacts.

Figure 12 shows the perfusion over time in the determined ROIs according to Figure 11. A clear rhythm of a heartbeat is visible in R1 with ambient light and LEDs switched on. A less clear heartbeat rhythm is visible in R1 with only LEDs switched on and in R1 without any light switched on, no clear heartbeat rhythm is definable. It is remarkable that the ROI with a high intensity of background light (ambient light and LED), gives the clearest heartbeat pattern, as background light primarily adds noise to the perfusion map. The perfusion in the three R2 regions, seems to be randomly defined over time, suggesting these regions are not suitable for perfusion measurements due to the low intensity of laser light in the edges.

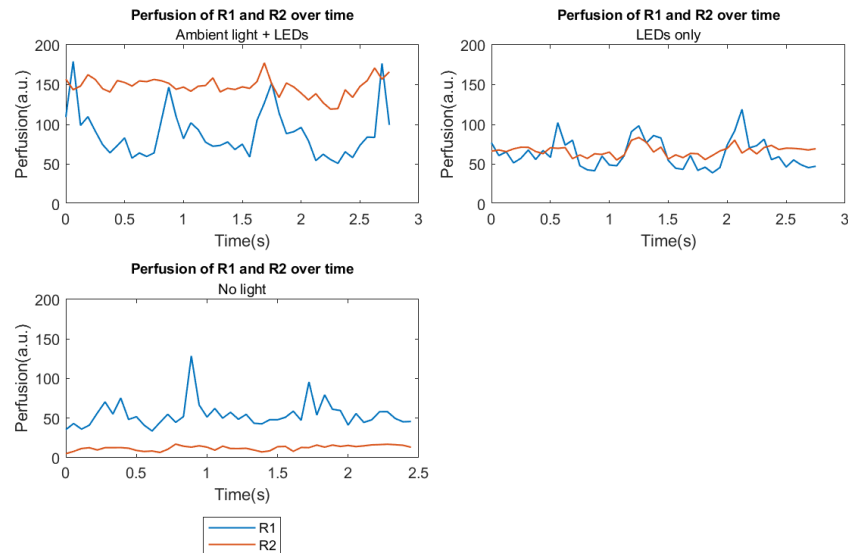


Figure 12 Perfusion of R1 and R2 (shown in Figure 11) over time in the three perfusion maps regarding the effect of light.

The calculated mean intensity, standard deviation of the intensity, speckle contrast and perfusion for the two ROIs (R1, R2) in the three perfusion maps of Figure 11 are shown in Table 1. The perfusion is the highest in R2 of the perfusion map with all lights switched on, whereas the speckle contrast is the lowest in this ROI. The perfusion and mean intensity are the lowest and the speckle contrast the highest in R2 of the perfusion map with all lights switched off. Furthermore, mean intensity and the standard deviation is in the R1 regions higher than in the R2 regions. Also, the standard deviation is the same in all R2 regions. Lastly, it is remarkable that the difference in contrast between R1 with ambient light and LEDs switched on and R1 with only LEDs switched on is 0.01, whereas the perfusion in these ROIs is respectively 110.67 and 78.98.

Table 1 The calculated mean intensity (a.u.), standard deviation of the intensity (a.u.), speckle contrast (a.u.) and perfusion (a.u.) for ROIs in Figure 11.

ROI	I_{mean}	σ_I	K	Perfusion
R1 Light + LEDs	7.6	2.6	0.34	110.67
R2 Light + LEDs	2.5	0.6	0.27	152.83
R1 LEDs only	6.6	2.2	0.33	78.98
R2 LEDs only	1.5	0.6	0.40	60.45
R1 No light	6.6	3.3	0.50	68.22
R2 No light	0.7	0.6	0.86	7.13

2.3.3 Handheld versus mounted measurements

In Figure 13, the perfusion maps of the measurements including the predefined ROIs to determine the differences in mounted and handheld measurements are shown. In the centre of each perfusion map, there is a circle or oval visible in which the perfusion is lower than in its surroundings. This results in

higher measured perfusion values in R2 than in R1 in the perfusion maps at the middle of the abdomen. However, this phenomenon is not noticeable in the perfusion maps at the right and left side of the abdomen. There, the measured perfusion value in R2 is lower than in R1. This suggests that the curvature of the abdomen plays a role in lowering the perfusion in these regions. This trend is also visible in Table 2; most of the measured perfusion values in R2 are smaller than the measured values in R1 for the measurements at the right and left side of the abdomen.

Another trend that occurs, is that handheld measurements give approximately 10% higher perfusion values than mounted measurements, which is the case in the measurements at the right and left side. The opposite is occurring for the measurements in the middle of the abdomen; handheld measurements give lower perfusion values than mounted measurements. Lastly, just as in Figure 11, circles with a wavy pattern are visible at the same locations in the perfusion map, which strengthens the presumptions that these circles are diffraction artefacts due to dust particles.

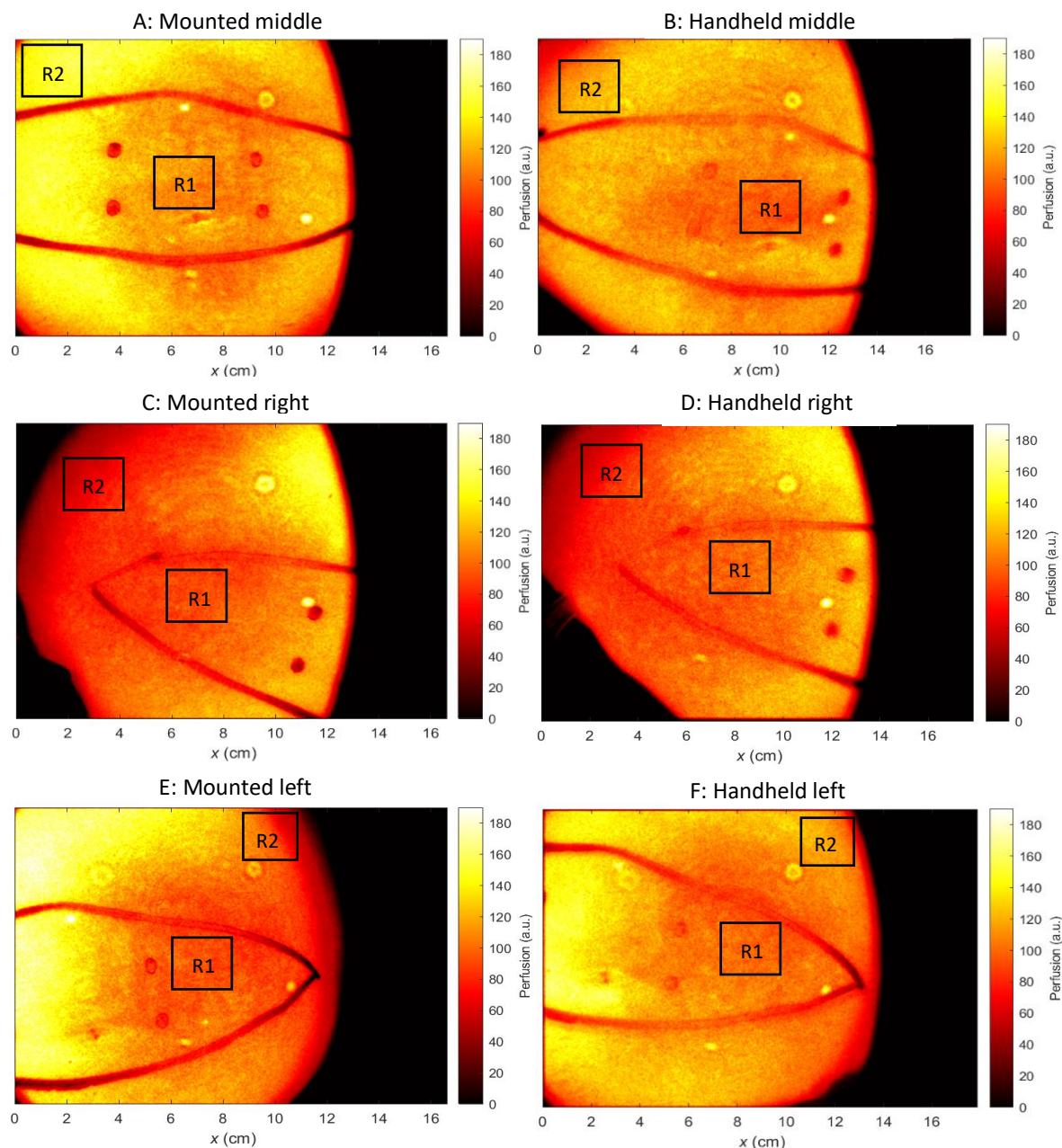


Figure 13 Perfusion maps of the six measurements regarding the differences in handheld and mounted.

Table 2 Mean perfusion in R1 and R2 of the 6 measurements to determine the differences in perfusion between handheld and mounted measurements.

	Perfusion mounted middle \pm std dev	Perfusion handheld middle \pm std dev	Perfusion mounted right \pm std dev	Perfusion handheld right \pm std dev	Perfusion mounted left \pm std dev	Perfusion handheld left \pm std dev
R1	110.67 \pm 6.65	97.07 \pm 6.42	91.39 \pm 4.93	98.42 \pm 5.52	93.88 \pm 5.74	99.79 \pm 6.04
R2	152.83 \pm 5.54	114.57 \pm 8.93	69.49 \pm 9.43	76.29 \pm 10.23	91.43 \pm 12.09	115.39 \pm 8.45

In Figure 14, the displacements on the perfusion map (the so-called Lissajous graph) and the displacement in the x and y direction over time in handheld and mounted measurements for the middle, right and left side of the abdomen are shown. It is clearly visible that handheld measurements have a larger covered distance and displacement than mounted measurements. This is also shown in Table 3, the mean on-surface speed and velocity of the handheld measurements are larger than in the mounted measurements. When comparing the velocity to the speed, the velocity is in all measurements 20 to 30 times as large as the speed, which is reasonable as the velocity takes the entire displacement into account, whereas the speed only takes the covered distance into account. Therefore, the velocity seems to be a better variable to compare handheld measurements to mounted measurements, which is three to five times as large in handheld measurements than in mounted measurements. Furthermore, the covered displacement in the x and y direction resemble, suggesting that performing measurements with the use of the WIPI results in similar operator’s movements in both directions. Lastly, a remarkable aspect is the graph of the displacement in x direction of the mounted measurement at the right side of the abdomen. This has a pattern of an arch, which could be due to breathing or due to the instability of the tripod.

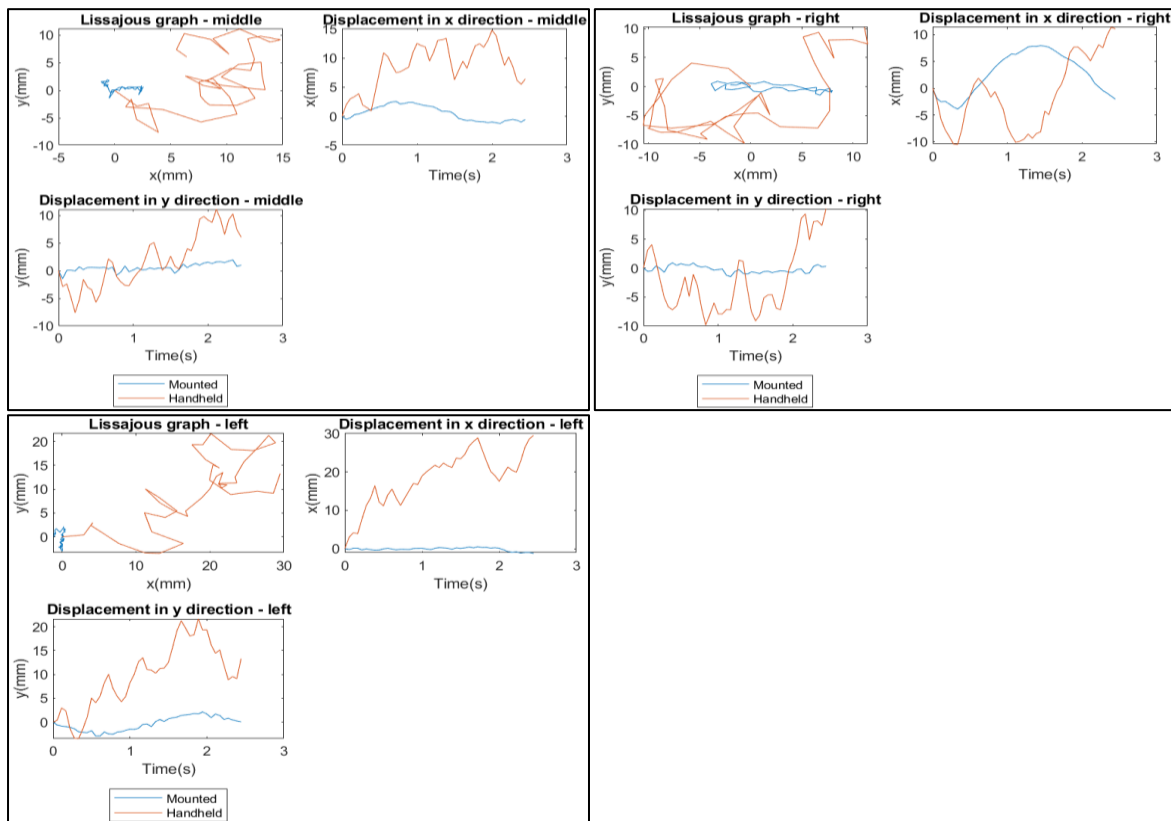


Figure 14 Displacements of mounted and handheld measurements on the perfusion maps and over time at the middle of the abdomen (top left), right side of the abdomen (top right) and left side of the abdomen (bottom left).

Table 3 Calculated mean on-surface speed, mean on-surface velocity and the corresponding ratios in handheld and mounted measurements.

Position	Mean on-surface speed handheld (mm/s)	Mean on-surface speed mounted (mm/s)	Ratio on-surface speed	Mean on-surface velocity handheld (mm/s)	Mean on-surface velocity mounted (mm/s)	Ratio on-surface velocity
Middle	1.61	0.21	7.63	28.5	5.20	5.48
Right	2.44	0.33	7.42	32.5	9.71	3.35
Left	5.89	0.22	26.52	30.8	6.22	4.95

Figure 15 shows three graphs of the handheld measurement at the middle of the abdomen. The first one is the velocity over time, the second one is the perfusion over time and the last one is the perfusion against the velocity. The velocity has a random pattern over time, which is plausible because of its handheld performance. In the second graph, the perfusion over time shows a heartbeat pattern. In the last graph, the linear fit shows the correlation between the perfusion and velocity. A horizontal fit is visible, which was not according to the hypothesis of a linear correlation. Also, the mean perfusion is plotted on the y axis, which seems to be similar as the intersection point of the linear fit at the y axis.

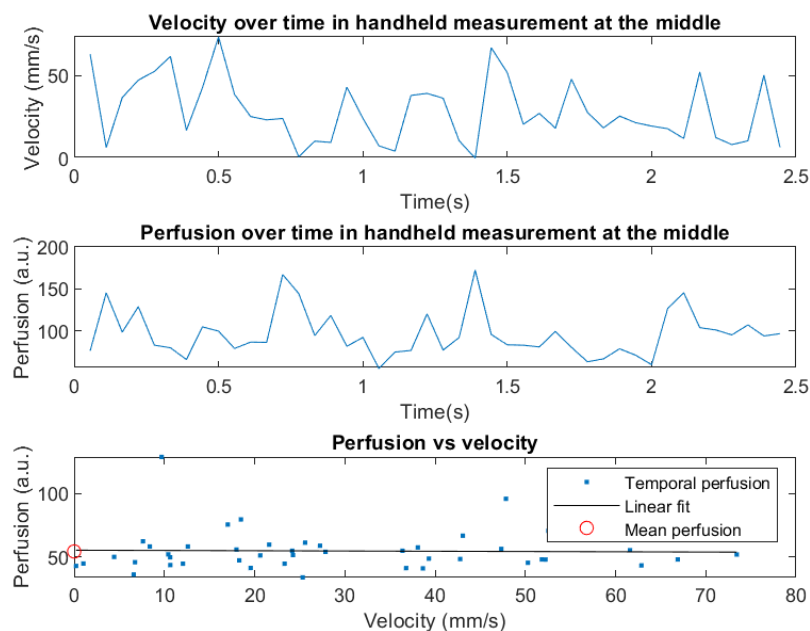


Figure 15 Three plots of the handheld measurement at the middle of the abdomen regarding the velocity over time (top), the perfusion over time (middle) and the velocity against the perfusion (bottom).

2.3.4 Perfusion distribution

Figure 16 shows the perfusion maps of the measurements at the middle of the abdomen with Midalgan applied on the skin. The area with Midalgan gives higher perfusion values than the surroundings, but it is not limited to the area of 1.5 cm² in which Midalgan was applied. The surrounding area has higher perfusion values too, which suggest that Midalgan also has some effect on the microcirculatory around the tissue that was applied with Midalgan. Furthermore, as visible in Table 4, the handheld measurement has approximately 10% higher measured perfusion values compared to the mounted measurement.

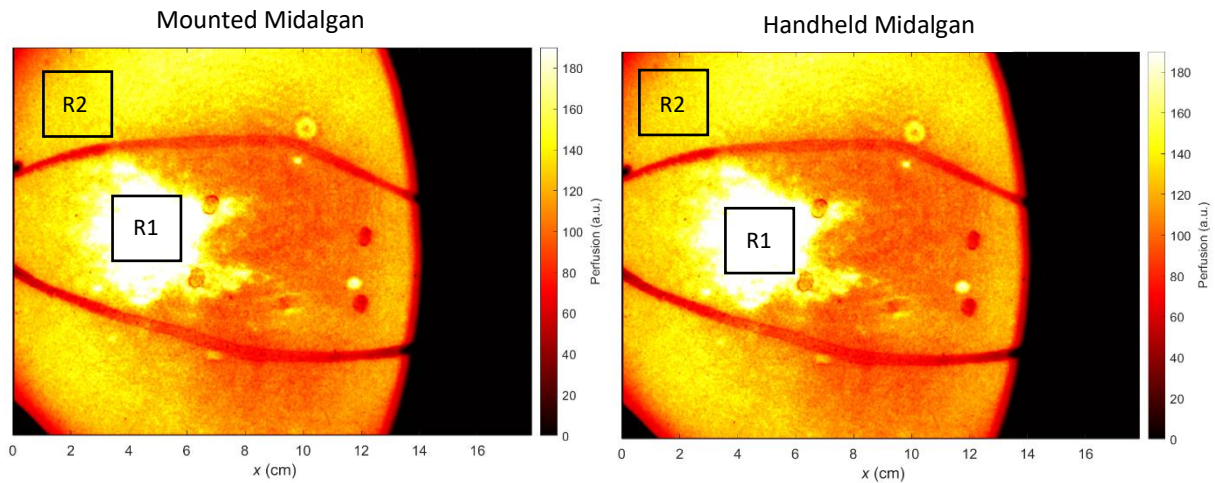


Figure 16 Mounted and handheld perfusion maps of the middle of the abdomen with Midalgan.

Table 4 Perfusion (a.u.) of R1 and R2 in the perfusion maps with Midalgan applied on the skin.

	Perfusion mounted \pm standard deviation	Perfusion handheld \pm standard deviation
R1	232.98 \pm 20.45	248.52 \pm 19.33
R2	136.12 \pm 11.34	151.14 \pm 14.55

2.4 Discussion

This proof-of-concept study can be considered as a preparation for the clinical study in which several characteristics of the WIPI and the abdominal microcirculation were researched, including the effect of light, the differences between handheld and mounted measurements, and the effect of Midalgan on the microcirculation. To investigate these characteristics, the performance of the optical flow algorithm was determined first to ensure the resulting perfusion maps were well aligned.

2.4.1 Performance of the optical flow algorithm compared to ECC maximisation

The performance of the optical flow algorithm was determined by a measurement with the use of the HAPI as the WIPI was not ready yet for performing measurements, whereas the WIPI software was already finished. The performance of the optical flow algorithm was compared to ECC maximisation, which was successfully applied for the correction of image misalignment in the HAPI study. After correction for the delay of the mono camera, the graphs of the displacement over time of ECC maximisation and optical flow had similar patterns. But there was some disagreement in exact location on the speckle frames. In the x direction, disagreement between both algorithms was approximately 40 pixels during the entire measurement, resulting in a difference of 3.4 mm. In the y direction, disagreement of about 30 pixels (2.6 mm) was present in the first 150 frames (5 seconds), after which both algorithms showed very similar displacements. These differences are small on a larger scale and therefore, a difference in the performance of optical flow and ECC maximisation is probably not noticeable on perfusion maps. Overall, optical flow is reliable enough for the correction of motion artefact in terms of spatial misalignment in this proof-of-concept study.

2.4.2 Effect of background light

To investigate the effect of background light (i.e. the portion of detected light that is not originated by the laser beam), three measurements with different light settings (ambient light and LEDs, LEDs only and no light) were performed resulting in three perfusion maps in Figure 11. There was a great difference in perfusion between the three perfusion maps. The perfusion map in which all lights are switched on, has the highest perfusion values, followed by the perfusion map with only LEDs switched on and lastly, the perfusion is the lowest in the perfusion map without any light switched on. This suggests that the presence of ambient light and LED light increases the measured perfusion value. This is explainable by Table 1 and eq.(1). The mean intensity in the centre of the image is higher than in the edge of the image, which is due to the presence of the laser light in the centre. The laser beam had a Gaussian pattern. Therefore, the intensity of the laser light is negligibly low in the edges of the perfusion map. This is confirmed by the smaller mean intensity in the edge than in the centre and by the standard deviation that is 0.6 in all R2 regions. Background light has a smaller standard deviation than laser light and it often unchangeable as it remains 0.6 in all perfusion maps. Since the standard deviation in R2 is similar in all perfusion maps, the mean intensity is the only variable affecting the contrast and so the perfusion value. The higher the intensity of the background light in the edge without laser light, the lower the contrast, the higher the perfusion. Therefore, the measured perfusion value is the highest in the edge in the perfusion map with all lights switched on. Obviously, this measured perfusion value is unreliable as no laser light is present in the edge of the perfusion map.

Reliable measurements are only possible in the centre of the perfusion map where the intensity of the laser light is high enough. The area in which reliable measurements are possible, is visible as a circle or oval with a diameter of 6 to 10 cm in the centre of the perfusion map. This is strengthened by Figure 12. In the graph of the perfusion map with all lights switched on, a clear heartbeat is visible in the centre of the perfusion map, whereas this is not visible in the corner of the perfusion map. There, the perfusion is randomly defined due to the lack of laser light. In the centre of the perfusion map with only LEDs switched on, the heartbeat is also visible, but this is a bit less clear visible and its amplitudes are smaller than in the one with all lights switched on. Still no clear heartbeat is visible in the corner of this perfusion map. Furthermore, no clear heartbeat is visible in both ROIs in the perfusion map

without any lights switched on. It is remarkable that the perfusion map in which all lights are switched on, shows the clearest heartbeat pattern. By adding background light, the perfusion measurements are affected and not pure anymore. Theoretically, only noise is added by adding background light. It would have been plausible that the measurement without any background light, would show the purest heartbeat. However, the intensity of the laser was probably not large enough to show this, resulting in small measured perfusion values. It is possible that these measured perfusion values are that small that these are 'clipped' when these become a negative value, leading to even lower measured perfusion values. Adding background light, the offset of the mean intensity is increased and this avoids clipping as the perfusion does not become negative, which eventually results in a higher measured perfusion value.

The last discussing point regarding this research question results Table 1. R1 in the perfusion map with ambient light and LEDs has a contrast of 0.34, which results in a perfusion of 110.67, whereas R1 for LEDs only has a contrast of 0.33 resulting in a perfusion of 78.98. It is remarkable that a difference of 0.01 in contrast results in a difference in perfusion of 31.69. As visible in the graph from the lookup table in Figure 2, the graph has an almost horizontal course from a perfusion of 100 to 0 and a contrast of 0.3 to 1. This course can cause large differences in perfusion for slight differences in contrast. However, the difference in perfusion of 31.69 within a difference of 0.01 in contrast is too large to fully blame the course of the graph for this difference. Additionally, there are some differences in applied software to calculate the mean intensity, standard deviation, contrast and perfusion. The mean intensity, standard deviation and contrast were calculated with the use of the software that was used for the HAPI system, whereas the perfusion was calculated with the use of the newly written software for the WIPI system. Both scripts use different look-up tables. These different look-up tables do not have to differ much from each other to create large differences in perfusion for approximately the same contrast values because of the course of the graphs.

Another reason for the small difference in contrast that results in a large difference in perfusion is the manual way of analysing the perfusion maps. It was tried to calculate the mean intensity, standard deviation and contrast at the exact same location as the perfusion. However, as different analysis software was applied for the calculation of mean intensity, standard deviation and contrast than for the calculation of the perfusion, some disagreement in location could be occurred, resulting in these differences. Moreover, the contrast in Table 1 was calculated from the all pixels in R1 and R2, whereas the perfusion in Table 1 are mean perfusion values calculated from perfusion maps that were formed by applying a sliding speckle contrast window of 9x9 pixels.

2.4.3 Handheld vs mounted measurements

In the perfusion maps regarding the difference in handheld and mounted measurements, the circle or oval in the centre in which the perfusion values are reliable, is also visible, as already discussed 2.4.2 Effect of background light. However, there are some more aspects in the perfusion maps in Figure 13 that are worth discussing. Comparing the handheld and mounted measurements at the middle of the abdomen, the handheld measurement has lower perfusion values in the centre and in the corner, which was not expected. It was expected that handheld measurements would have higher perfusion values compared to mounted measurements due to motion within the exposure time of the camera³¹. A reason for this might be the instability of the laser light. The measurements at the middle were performed before the left and right measurements were performed; possibly, the laser was not warmed up sufficiently. A solution is to let the laser stay on after the preview, so it warms up sufficiently. For the right and left measurements, the hypothesis that handheld measurements would have higher perfusion values than mounted measurements, holds true.

Another characteristic that is visible in especially Figure 13C-F, is the effect of the curvature of the abdomen. Due to the curvature, the distance between skin and WIPI increased at the lateral sides of the abdomen. Also, the created shadow because of the curvature played a role in calculating the

perfusion. The combination of both probably resulted in a lower perfusion at the lateral sides of the abdomen. To partly overcome this, measurements at the lateral sides of the abdomen should be performed perpendicular to the skin. Figure 17 graphically shows this problem and the solution to partly overcome this. The right WIPI device shows the position in which the measurements were performed. The right side of that beam has a larger distance to the skin than the left side of the beam, which makes shadow more plausible to occur. The left WIPI device shows the perpendicular position. As visible, a larger surface of the beam reaches the skin at the same distance, decreasing the influence of shadow.

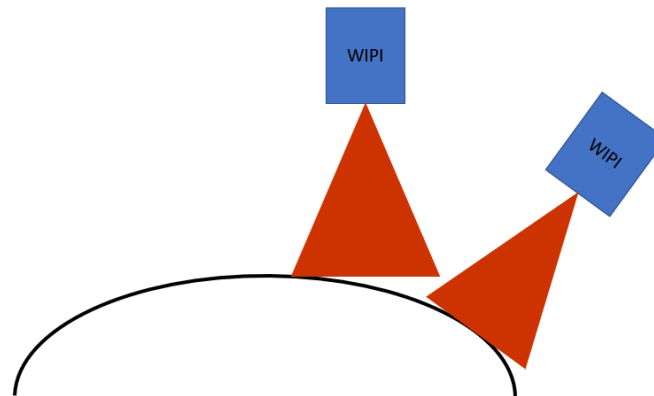


Figure 17 Graphical representation of the position of the WIPI regarding curvature artefacts. Left WIPI device: position in which the measurements were performed. Right WIPI device: position to possibly decrease curvature artefacts.

As already mentioned multiple times, in all perfusion maps is a circle or oval in the centre present in which the perfusion values are reliable. In Figure 13A, it has more the shape of an oval, in Figure 13B-F, this is a circle. The oval shape is probably caused by the position of the cameras with respect to the position of the laser, which has an angle of approximately 16 degrees. Therefore, the circle of the laser beam can become an oval, when considering it at an angle of 16 degrees. However, this oval shape is only visible in the mounted measurement at the middle of the abdomen. It is unknown why the other perfusion maps show circles as the angle between the cameras and laser remains the same. The curvature of the abdomen could have played a role in compensating this angle.

Next to the differences in the perfusion maps between handheld and mounted measurements, the differences in movements were also researched with the use of the speed, velocity and the visualisations of the movements as presented in Figure 14. The speed was determined as the covered distance divided by the duration of the measurement. However, this did not take the displacements during the measurements into account. So, when the displacement during a measurement would, for instance, have been a perfect circle, the covered distance would have been zero. Therefore, the speed was not suitable to quantify the operator's movement during a measurement. The velocity is a suitable variable, as this takes the entire path of the WIPI during a measurement into account. As shown in Table 3, the ratio in velocity between handheld and mounted measurements is 5.48, 3.35 and 4.95 for respectively measurements at the middle, right and left side of the abdomen. This is smaller than the mean on-surface velocity that was found in the research to the HAPI system, which states an increase of 8.5 of the on-surface velocity³⁷. However, in the HAPI study, the mean on-surface velocity was 1.5 mm/s and 12.7 mm/s for respectively mounted and handheld measurements, which are both two to three times smaller than in this study. One possible reason could be the experience of the operator. It is plausible that performing handheld measurements, either with HAPI or WIPI, has a learning curve. The operator in the HAPI study had probably more experience in performing handheld measurements than the operator in this study.

Lastly, the correlation of the velocity and the perfusion over time of the handheld measurement at the middle of the abdomen was researched and shown in Figure 15. The hypothesis was that a linear correlation would be findable, but the linear fit has a horizontal course. There are several variables

that could have affected this correlation from becoming linear. The first one is the framerate. In this study, the framerate was 16 Hz, which is quite large due to the limitations of the calculation power of the raspberry pi. This reduces the amount of data points, so more estimations for the displacements have to be made between two consecutive frames. Secondly, the method to obtain the velocity out of the displacements is disputable. The displacements were calculated with the use of the optical flow algorithm and the velocity was calculated out of these displacements, but there are several ways to do so. It is still unknown which method is most accurate. Thirdly, as the calculated displacement between frames is required to determine the velocity, the performance of the optical flow algorithm is an important part. When the optical flow algorithm does not perform well, the found displacement are incorrect, resulting in incorrect velocities. As fourth, the amount of data point is small. Each measurement, 45 frames were obtained, which was probably too small to enable a significant correlation. Lastly, the measured heartbeat causes fluctuations in the perfusion. The heartbeat can increase or decrease the perfusion, independently from the velocity. Probably, a combination of these defined variables affected the correlation between velocity and perfusion.

2.4.4 Perfusion distribution

As shown in Figure 16, the Midalgan is clearly visible as a region of high perfusion in the mounted perfusion maps as well as in the handheld perfusion maps. The perfusion values are approximately 10% larger in the handheld perfusion map than in the mounted perfusion map, which is according to the hypothesis that handheld measurements have larger perfusion values than mounted perfusion measurements due to motion within the exposure time of the camera. The handheld measurement was performed as soon as possible after the mounted measurement. However, it could be possible that the effect of Midalgan on the microcirculation was still increasing and that this difference in time contributed to the higher perfusion values of the handheld measurement.

2.4.5 Recommendations

This proof-of-concept study showed realistic results of what kind of results could be expected in the upcoming clinical study. However, this proof-of-concept study only included one healthy test subject. To make the results more reliable, the measurements within this proof-of-concept study should be performed again in at least three other healthy test subjects. Then, more data are available to determine for example if the optical flow algorithm is well performing as it seems to be in this study, if handheld measurements indeed tend to lead to higher perfusion values and if background light always results in higher perfusion values.

Additionally, there were some characteristics present in all perfusion maps which are undesirable for the clinical study. These were the suboptimal position of the mono camera resulting in a black area at the right side, the presence of dust artefacts due to dust particles at the laser surface and the circle or oval of 6 by 10 cm in the perfusion maps in which the perfusion values are accurate. The suboptimal position of the mono camera can easily be remedied by relocating the mono camera a bit more to the front of the device. The dust artefacts on the perfusion maps can be distinguished from red spots on the skin because of its wavy pattern due to interference and because they are present at the same location in each perfusion map. However, it still decreases the quality of the perfusion maps. Therefore it is desirable to remove these dust particles^{50,51}. To overcome the problem of the small area in the perfusion maps to reliably measure the perfusion, the diameter of the laser beam could be enlarged by increasing the laser intensity. However, this is only possible to a limited extent because of laser safety requirements. Another possibility is to flatten the Gaussian pattern of the laser beam to increase the diameter of accurate perfusion measurement. However, the laser intensity at the centre of the laser beam decreases. Therefore, further research should be performed if the laser intensity is still high enough to perform reliable measurements. Another discussion point about the laser beam is the transition from reliable to unreliable measured perfusion values in the perfusion map. As visible in Figure 11B, a clear cut-off from reliable to unreliable perfusion values is visible at the left side of the

perfusion map, but this is not the case at the right side. There, it is not clear at which position reliable measurements are still possible. To overcome this and to make the transition from reliable to unreliable measurements in the entire perfusion map clear, the pattern of the laser beam could be clipped by a diaphragm at the edges of the beam. It is recommended to flatten the Gaussian curve and to clip the beam. However, it is unknown to what extent the area in the perfusion map for reliable measurements will then increase. Therefore, this recommendation needs to be further researched.

Furthermore, background light increased the measured perfusion values, as shown in Figure 11. However, this was remarkable since background light theoretically just adds noise. To get rid of the background light, but keeping ambient light and LEDs switched on in the OR, which is preferable, the background light could be subtracted from a perfusion map with background light as well as laser light. To do so, two measurements with background light switched on should be performed; one with background light only and one with background light and laser light. Then, the perfusion map with background light only could be subtracted from the perfusion map with both background light and laser light, remaining a perfusion map with laser light only. However, this should be further researched as it is unknown if enough intensity remains after subtracting the background light.

Lastly, the method to create a perfusion map is semi-automatic. During analysis, multiple manual steps were necessary to complete the perfusion map (6.2 Appendix B: Creating perfusion maps based on optical flow). This is undesirable during the clinical study. A technical physician will perform the measurements in sterile clothes. Therefore, it is challenging to perform these manual steps as the laptop cannot be touched. However, the laptop can be controlled by a touchpad on the WIPI, but the laptop will be positioned in the corner of the OR and is therefore barely visible. It is possible to complete analysis after surgery is performed, but the obtained data can then not be checked during surgery and cannot be redone in case the measurement failed.

2.5 Conclusion

The optical flow algorithm shows good performance in aligning the perfusion maps for the application in the upcoming clinical study. The multiple perfusion maps show that background light increases the perfusion values and that handheld measurements mostly lead to 10% higher perfusion values compared to mounted measurements. In the perfusion maps, only the measured perfusion values in the centre are reliable as the laser beam has a Gaussian pattern. It is desirable to increase the area in which reliable measurements are possible before starting the clinical study by for example increasing the laser intensity or flatten the Gaussian curve. However, these solutions need to be further researched.

3. Clinical study

3.1 Introduction

In this chapter, the future clinical study will be discussed. As this study concerns medical scientific research and as participants are subject to a procedure, this study is subject to Medical Research Involving Human Subject Act⁵². Therefore, approval of the Medical Research Ethics Committee (MREC) and the advisory committee (ALU) of ZGT was necessary and this was obtained by submitting the correct documents (6.7 Appendix G: Overzicht indiening documenten aan METC en ALU). However, due to the long duration to gain approval, the clinical study could not start yet.

This clinical study aims to demonstrate that the WIPI can visualise the microcirculation of the abdominal flap and the newly reconstructed breast during DIEP flap breast reconstruction. The hypothesis is that the WIPI can detect poor skin perfusion and that the WIPI is able to demonstrate vasospasms and thromboses during surgery, which could be missed with the use of ICG. If the hypothesis holds true, the WIPI could serve as a non-invasive, real-time technique to identify poor skin perfusion and vasospasms or thromboses where the current method is not able to do so. This enables early detection of poor skin perfusion during surgery that might have resulted in postoperative necrosis, possibly caused by thromboses or a too large flap. However, as only fifteen patients will be included, this study will be limited to the visualisation of the microcirculation and the eventual correlation between the perfusion and perfusion-related complications. This is incorporated in the research questions of this study:

- i. What is the correlation between the mean perfusion of the newly reconstructed breast during DIEP flap breast reconstruction and the development of perfusion-related complications?
- ii. What is the perfusion distribution of the abdominal flap and the newly reconstructed breast during and after DIEP flap breast reconstruction measured with the WIPI?
- iii. What is the reliability and user-friendliness of the WIPI during surgery?

3.2 Methods

3.2.1 Study design

This is a prospective case series study of the multidisciplinary breast cancer treatment centre in ZGT. The first aim is to determine if there are any differences in mean perfusion of the newly reconstructed breast between two groups: patients that develop perfusion-related complications and patients that do not develop perfusion-related complications. The surgeon postoperatively determines whether perfusion-related complications did occur and its severeness. Furthermore, the perfusion distribution of the DIEP flap will be visualised multiple times with the use of the WIPI to show differences or similarities in perfusion during surgery. Lastly, as the WIPI is a newly designed device, the reliability and user-friendliness will be determined based on a questionnaire.

Fifteen patients that are willing to give informed consent and that will have a unilateral or bilateral DIEP flap breast reconstruction, either immediate or delayed, will be included. A bilateral DIEP flap breast reconstruction will be described as two separate cases. The assumption is made that the perfusion in the chosen flaps differ enough from each other to make two cases; the chosen artery and vein for both flaps will be different in length and diameter. Moreover, the flaps will not have the exact same size and weight.

3.2.2 Inclusion criteria and time schedule

All included patients will be selected from the outpatient clinic. To be eligible to participate in this study, a subject must meet all of the following criteria:

- ≥ 18 years of age,
- An indication for a unilateral or bilateral DIEP flap breast reconstruction, either immediate or delayed,

- Patients must be willing to give informed consent.

Patients that meet the inclusion criteria will be approached by their plastic surgeon before DIEP flap breast reconstruction. There are no pre-established exclusion criteria to participate in this study. During the visit in which information is given about the surgery, information about the study will also be orally provided and by means of the Subject Information Sheet (6.8 Appendix H: Proefpersoneninformatie brief). Patients will get two weeks to consider about participating in the study. After two weeks, the patient will be asked if she wants to participate and to sign the written informed consent. Patients have to sign written informed consent before surgery and enrolling into the study.

During surgery, four measurements with the use of the WIPI will be performed. Each measurement consists of digital colour images and perfusion maps. Measurement 5 takes place on the first postoperative day of the typical two to four days patient’s stay after DIEP flap breast reconstruction. Patients enrolled in this study will therefore be followed for two days (Table 5).

Table 5 Time schedule for each patient in the study

Visit before surgery	⇒ Surgery	⇒ Day after surgery
Informed consent	Measurements 1-4	Measurement 5
Patient demographics		
Medical history		

3.2.3 Study settings

3.2.3.1 Preparations

Before the measurements can start at the OR, the WIPI needs to be packed in a sterile bag (Figure 18 – E5700G Microscope Drape, Zeiss MD 51cmx165cm – 20"x65"). This sterile bag has one lens cover, which is usually applied for the coverage of the lens of the microscope at the OR. To enable the application of this sterile bag, the windows of the WIPI have the same diameter as these lens covers. Since the WIPI has two windows, one for the laser and one for both cameras, two sterile bags are required for complete packaging. For this sterile packaging, which will be done by a person at the OR that has already sterile clothes on, the following steps have to be executed:

- Click the lens cover on one of the windows of the WIPI and to pull the bag over the WIPI.
- Now, a layer of plastic covers the second WIPI window. Therefore, a small area of plastic just in front of the second window have to be cut.
- The lens cover of the second sterile bag has to be cut and will be clicked on the second WIPI window.
- As the bag is larger than the WIPI, the last part of the bag can be cut and removed.
- If necessary, the bag can be tightened with the used of the three tie straps.

In this way, the WIPI is sterile packed and the laser and cameras are not hindered by a layer of plastic (Figure 19).

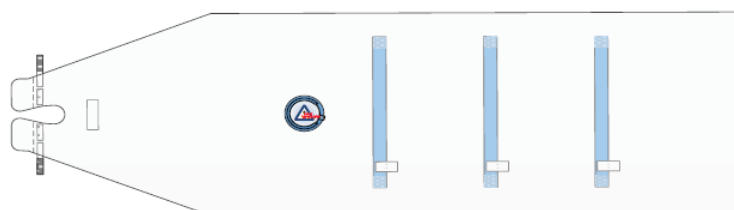


Figure 18 The sterile bag that will be applied to pack the WIPI during surgery. This bag has one lens cover, which is the circle in the figure. The three blue tie straps will be used to tighten the bag.



Figure 19 The WIPI in a sterile bag after removing the unnecessary parts of the bag.

3.2.3.2 Measurement protocol at the OR

After sterile packaging, the measurement can start. A technical physician (in training) will perform the measurements with the WIPI. The same protocol and camera settings for the performance of a measurement is applicable to this clinical study as to the proof-of-concept study (2.2.2.3 Measurement protocol proof-of-concept study). First, preview mode will be used to check the position in which the WIPI is measuring at that moment. Then the actual measurement will be performed at 30 cm. This distance can more accurately be maintained than in the proof-of-concept study as pointing lasers are attached for these measurements. These were not available for the proof-of-concept study. Just as in the proof-of-concept study, each measurement consists of 45 RGB frames and speckle frames within a duration of 2.8 seconds. Lastly, the data will be sent to the laptop to create an aligned and averaged perfusion map. The surgeon is not allowed to look at the previewed images or at the aligned and averaged perfusion map to prevent the surgeon from being influenced by these images. Therefore, the perfusion maps will not be sent to an external monitor present in the OR. For answering the research questions, five measurements in each patient will be performed:

1. BASELINE MEASUREMENT

After anaesthesia, but before the first incision, the baseline measurement will be performed to get an idea of the perfusion distribution of the entire flap. As the field of view of the WIPI has a diameter of 14 cm, three measurements will be performed to cover the entire DIEP flap. This measurement is simulated in 2. Proof-of-concept study.

2. RAISED FLAP

After the surgeon raised the abdominal flap and found the predefined perforators, the surgeon decides which perforator is going to be transplanted based on his/her own opinion. Additionally, ICG can be injected to support the surgeon's evaluation. The recommended dose of ICG is 0.1-0.3 mg/kg, which results in an intravenously administered dose of 2 ml ICG. All other perforators not used for transplantation will be sacrificed. Then, the second LSCI measurement can be performed, which will also be divided into three scanning moments. This LSCI measurement forms the reference for the LSCI measurements after breast reconstruction. It shows the tissue area that the chosen perforator perfuses and what it should approximately be after reconstruction.

3. ISCHEMIA

After the second LSCI measurement, the blood flow through the chosen perforator will be stopped with the use of a removable vascular clip, which results in ischemia. Vascular clips are part of the standard surgical instruments used DIEP flap breast reconstruction to temporarily stop the blood flow. By removing the clip, the blood flow will be restored without any complications. After one minute of ischemia, the third LSCI measurement will be performed, again divided into three scanning moments.

This measurement simulates bad perfusion of the DIEP flap and can therefore be used as reference for bad perfusion in the upcoming measurements. When this third measurement is accomplished, the vascular clip can be removed and the perfusion will be restored. Then, the perforator can be cut through to continue the surgery. This way, this measurement does not increase the time of ischemia.

4. ANASTOMOSIS

When anastomosis of the DIEP flap to the internal mammary artery is accomplished, the surgeon validates the perfusion based on his/her own opinion and additionally with the use of ICG angiography. After validation, the fourth LSCI measurement can be performed. This measurement will be performed to correlate the mean perfusion (in PU) of the newly reconstructed breast to the outcome of the surgery. The outcome is the occurrence or absence of perfusion-related complications. One scanning moment is enough as the new breast can be scanned within the field of view of the WIPI. In case the perfusion was sufficient during this LSCI measurement, but suddenly after this measurement, the surgeon does not trust it anymore, the surgeon can do additional surgical actions to restore the perfusion. An additional LSCI measurement will then be performed.

5. POSTOPERATIVE MEASUREMENT

One day after surgery, the final LSCI measurement will be performed at the newly reconstructed breast. This measurement will be performed to show if the perfusion differs from the perfusion just after anastomosis. During this measurement, no anaesthetics will be used, whereas the patient is under general anaesthesia during the other four measurements. As anaesthetics have a vasodilative effect, lowered perfusion values should be taken into account for this fifth measurement⁵³.

3.2.5 Statistical analysis

To give an answer to the first research question about the correlation between the perfusion values and the development of perfusion-related complications, the patients will be divided into two groups, as already mentioned in 3.2.1 Study design. The resulting mean perfusion values in PU of the breast \pm the standard deviation of measurement 4. Anastomosis will also be divided into these two groups to research if there will be any differences. For this purpose, an independent samples T test will be performed in IBM SPSS Statistics for Windows (Version 25, SPSS Inc., Chicago). A significant difference is proven when p value < 0.05 . Moreover, a scatter plot will be created to show the differences on a visual base. For the purpose of this thesis, an imaginary data set was created to show what the results of the future measurements might look like. As the number of participating patients is small, it is expected that no significant differences will be found in this analysis. However, the expectation is that eventual visible differences between these two groups may be explainable based on the knowledge of the (patho)physiology of the microcirculatory. These eventual visible differences could be the starting point of future research to the WIPI as a predictor of perfusion-related complications.

To answer the second research question regarding the perfusion distribution, the mean perfusion of the abdominal flap of each patient of every measurement will be determined. This means that the first three measurements result in nine mean perfusion values; three for the right, three for the middle and three for the left side of the abdominal flap due to the field of view of the WIPI. The fourth and fifth measurements result in one mean perfusion value for the fourth measurement and one for the fifth. All mean values will be compared to each other with the use of one-way analysis of variance (ANOVA) and Post Hoc Tests (Tukey) to get an idea of the perfusion distribution of the abdominal flap during surgery and afterwards. An imaginary data set was created, in which an example of the baseline measurement was added. The perfusion in the three sections in which the DIEP flap is divided due to the field of view of 14 cm of the WIPI, will be compared to each other. It is possible to add all measurements to this analysis, to get a complete overview of the perfusion during surgery and the day after surgery. Again, making a valid statistical analysis is complicated due to the small number of

participating patients. Therefore, the assumption is made to be able to interpret the results on a visual basis by keeping the knowledge of the (patho)physiology of the microcirculation into account.

To determine the reliability and user-friendliness of the WIPI according to the third research question, a User Experience Questionnaire (6.9 Appendix I: User Experience Questionnaire) will be used^{54,55}. After each measurement, this questionnaire will be filled in by the operator. When all patient measurements are performed, the 15 questionnaires will be analysed by a corresponding data analysis tool (P:\Users\Sacha Teunissen\Manuscripts\2022 METC en ALU aanvragen\2022-05 METC aanvraag ronde 2\F. Vragenlijsten\Short_UEQ_Data_Analysis_Tool).

For detailed methodology, the research protocol attached in 6.10 Appendix J: Research protocol can be consulted.

3.3 Hypothetical results

In this section, results of an imaginary data set are presented. To show hypothetical results for the first research question, an imaginary data set is made in which 3 patients developed perfusion-related complications. This was based on the complication rate of 7% - 35%. Table 6 shows the group statistics of the fifteen included patients. The mean perfusion and the standard deviation are shown for the two groups: patients that develop perfusion-related complications (N=3) and patients that do not develop these complications (N=12). Table 7 shows the results of the independent samples T test, of which the column Sig. (2-tailed) shows p value. In case the p value for the Levene's Test is significant ($p < 0.05$), the 'Equal variances assumed' output in Sig. (2-tailed) should be used, and vice versa. In this imaginary data set, no significant difference is found between the two groups as $p = 0.167$. Also, the 95% confidence interval includes 0, which indicates that there is no significant difference in mean perfusion between both groups. The results of each measurement can be plotted in a scatter plot as visualised in Figure 20.

Table 6 Group Statistics of the imaginary data set

	Complications	N	Mean	Std. Deviation	Std. Error Mean
Perfusion	Complications	3	50.0000	5.00000	2.88675
	No Complications	12	56.5000	10.81665	3.12250

Table 7 Independent Samples Test of the imaginary data set

	Levene's Test for Equality of Variances		t-test for Equality of Means				95% Confidence Interval of the Difference		
	F	Sig.	t	df	Sig. (2-tailed)	Mean Difference	Std. Error Difference	Lower	Upper
Perfusion	3.021	.106	-.993	13	.339	-6.50000	6.54619	-20.64218	7.64218
			-1.529	7.541	.167	-6.50000	4.25245	-16.41106	3.41106

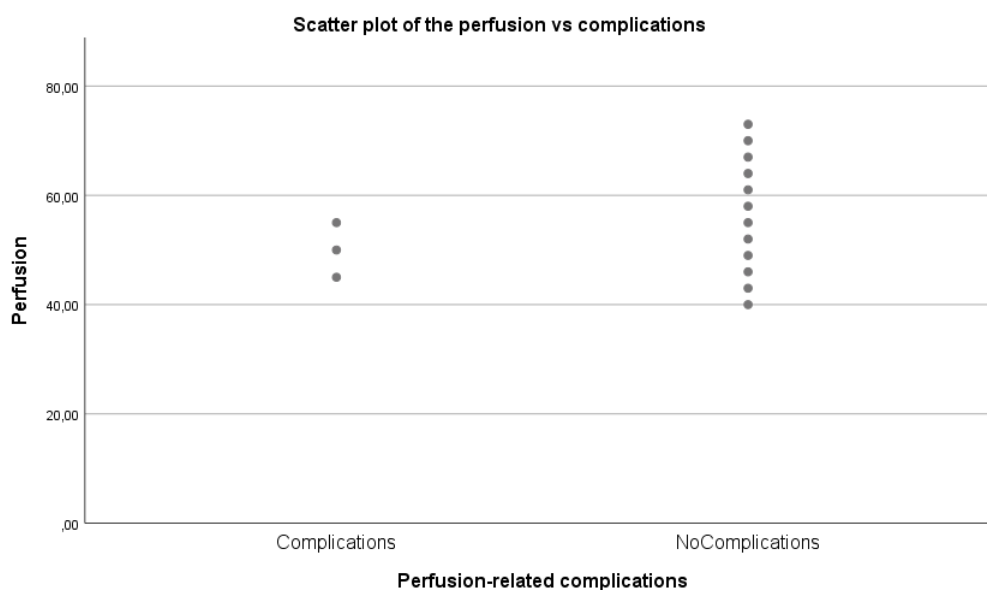


Figure 20 Scatter plot of the perfusion versus perfusion-related complications.

Table 8, Table 9 and Figure 21 show the results of an imaginary data set of a baseline measurement. The baseline measurement is divided into three measurements at the left, middle and right of the abdomen due to the field of view of the WIPI. Table 8 shows if there are any differences between these three measurements but does not tell between which groups these differences are present. The post hoc test in Table 9 shows where these differences are present. In this case, there is a significant difference between the mean perfusion of the left and middle measurements. This is visible by the asterisk in Table 9 and because the 95% confidence interval does not include 0. The results of the three times 15 perfusion measurement in this baseline measurement are visualised in the grouped scatter plot by position in Figure 21.

Table 8 ANOVA of the imaginary data set of the baseline measurement.

	Sum of Squares	df	Mean Square	F	Sig.
Between Groups	190.000	2	95.000	4.750	.014
Within Groups	840.000	42	20.000		
Total	1030.000	44			

Table 9 Multiple Comparison, Post hoc test (Tukey) of the imaginary data set of the baseline measurement.

(I) Position	(J) Position	Mean Difference (I-J)	Std. Error	Sig.	95% Confidence Interval	
					Lower Bound	Upper Bound
Left	Middle	-5.00000*	1.63299	.010	-8.9673	-1.0327
	Right	-3.00000	1.63299	.170	-6.9673	.9673
Middle	Left	5.00000*	1.63299	.010	1.0327	8.9673
	Right	2.00000	1.63299	.445	-1.9673	5.9673
Right	Left	3.00000	1.63299	.170	-.9673	6.9673
	Middle	-2.00000	1.63299	.445	-5.9673	1.9673

*. The mean difference is significant at the 0.05 level.

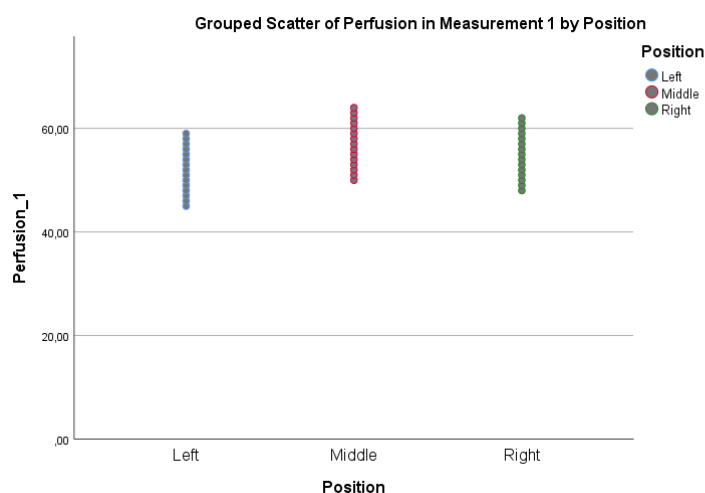


Figure 21 Grouped scatter of the perfusion (Perfusion_1) in the left, middle and right of the abdomen during the baseline measurement.

3.4 Ethical considerations

To date, little is known about the changes in the microcirculatory during DIEP flap breast reconstruction, which include the effects of thromboses and vasospasms on the microcirculatory that could result in perfusion-related complications. With the application of the WIPI, new insights will hopefully be provided into (changes in) the microcirculatory. The included patients will get the standard treatment, in which the perfusion is verified by the surgeon's assessment and additionally with the use of ICG angiography at raised flap and after anastomosis. The set-up of this future clinical study is to determine if there is a correlation between the occurrence of perfusion-related complications and the measured perfusion value. This study can end up in a larger study to the predictive value of the WIPI during DIEP flap breast reconstruction for the development of perfusion-related complications. Then, this predictive value can be compared to the predictive values of the surgeon's assessment and ICG angiography. Moreover, research can be performed if the WIPI could give a cut-off value between viable and non-viable tissue during surgery and if the WIPI could replace ICG angiography, which would be of great value given the non-invasive and easy-to-apply character of the device.

Given the potential advantages of the WIPI in the future during DIEP flap breast reconstruction, participation in this clinical study is legitimate. The duration of the surgery will be enlarged for approximately 20 to 30 minutes and only one postoperative measurement is planned that takes some time from the patient. Moreover, scanning the skin with the use of the WIPI is painless and without any discomfort.

4. Future perspectives and general conclusion

In this thesis, the proof-of-concept study and the future clinical study were described. However, the long-term aim is to distinguish viable tissue from non-viable tissue during surgery with the use of the WIPI (or an improved version of the WIPI) and so to minimise the chance of developing perfusion-related complications. Therefore, a larger study with more participating patients should be performed after the upcoming clinical study. It is desirable to include more than 30 patients to enable a reliable statistical analysis whether the WIPI is able to define a cut-off value in perfusion between viable and non-viable tissue and whether the WIPI can predict perfusion-related complications.

Furthermore, to fully incorporate the WIPI in the surgical environment, it is necessary that the perfusion maps can be created without any manual actions at the OR. The current software requires some manual steps before presenting the perfusion map. When making the creation and visualisation of the perfusion maps fully automatic, and so less time-consuming, the WIPI is more likely to be used at the OR as the planned surgeries are often on a tight time schedule.

This thesis highlighted the proof-of-concept study in which the performance of the optical flow algorithm, the effect of background light, the differences in perfusion and displacements between handheld and mounted measurements and the perfusion distribution of the abdomen in a healthy test subject were researched. The optical flow algorithm shows good performance in aligning the perfusion maps for the application in the upcoming clinical study. The multiple perfusion maps show that background light increases the perfusion values and that handheld measurements mostly lead to higher perfusion values compared to mounted measurements. In the perfusion maps, only the measured perfusion values in the centre are reliable as the laser beam has a Gaussian pattern. It is desirable to increase the area in which reliable measurements are possible before starting the clinical study by for example increasing the laser intensity or flatten the Gaussian curve. However, these solutions need to be further researched. Furthermore, this thesis highlighted the future clinical study and showed some hypothetical results based on the knowledge of the proof-of-concept study.

5. References

1. Integraal kankercentrum Nederland. Incidentie borstkanker. (2021). Available at: <https://iknl.nl/kankersoorten/borstkanker/registratie/incidentie>. (Accessed: 27th September 2021)
2. Integraal kankercentrum Nederland. Overleving borstkanker. (2021). Available at: <https://iknl.nl/kankersoorten/borstkanker/registratie/overleving>. (Accessed: 27th September 2021)
3. Costa, W. A., Eleutério, J., Giraldo, P. C. & Gonçalves, A. K. Quality of life in breast cancer survivors. *Rev. Assoc. Med. Bras.* **63**, 583–589 (2017).
4. Janssen-Heijnen, M. L. G. *et al.* Small but significant excess mortality compared with the general population for long-term survivors of breast cancer in the Netherlands. *Ann. Oncol.* **25**, 64–68 (2014).
5. Kouwenberg, C. A. E. *et al.* Long-Term Health-Related Quality of Life after Four Common Surgical Treatment Options for Breast Cancer and the Effect of Complications: A Retrospective Patient-Reported Survey among 1871 Patients. *Plast. Reconstr. Surg.* 1–13 (2020). doi:10.1097/PRS.0000000000006887
6. Hunsinger, V. *et al.* Long-Term Follow-Up of Quality of Life following DIEP Flap Breast Reconstruction. *Plast. Reconstr. Surg.* **137**, 1361–1371 (2016).
7. Heidekrueger, P. I. *et al.* Overall Complication Rates of DIEP Flap Breast Reconstructions in Germany—A Multi-Center Analysis Based on the DGPRÄC Prospective National Online Registry for Microsurgical Breast Reconstructions. *J. Clin. Med.* **10**, 1016 (2021).
8. Zötterman, J. *et al.* Intraoperative laser speckle contrast imaging in DIEP breast reconstruction: A prospective case series study. *Plast. Reconstr. Surg. - Glob. Open* 1–7 (2020). doi:10.1097/GOX.0000000000002529
9. Levine, J. L. Center for breast reconstruction. (2021). Available at: <https://centerforbreastreconstruction.com/diep-flap-surgery-and-reconstruction-procedure/%0A>. (Accessed: 21st July 2022)
10. Hamdi, M. & Rebecca, A. The Deep Inferior Epigastric Artery Perforator Flap (DIEAP) in Breast Reconstruction. *Semin. Plast. Surg.* **20**, 095–102 (2006).
11. Ben Aziz, M. & Rose, J. Breast Reconstruction Perforator Flaps. in *StatPearls* (2022).
12. Sharma, H. R., Rozen, W. M., Mathur, B. & Ramakrishnan, V. 100 Steps of a DIEP Flap - A prospective comparative cohort series demonstrating the successful implementation of process mapping in microsurgery. *Plast. Reconstr. Surg. - Glob. Open* **7**, 1–5 (2019).
13. Bhullar, H., Hunter-Smith, D. J. & Rozen, W. M. Fat Necrosis After DIEP Flap Breast Reconstruction: A Review of Perfusion-Related Causes. *Aesthetic Plast. Surg.* **44**, 1454–1461 (2020).
14. Liu, E. H. *et al.* Intraoperative SPY Reduces Post-mastectomy Skin Flap Complications: A Systematic Review and Meta-Analysis. *Plast. Reconstr. Surg. - Glob. Open* **7**, 1–8 (2019).
15. Girard, N. *et al.* Innovative DIEP flap perfusion evaluation tool: Qualitative and quantitative analysis of indocyanine green-based fluorescence angiography with the SPY-Q proprietary software. *PLoS One* **14**, 1–14 (2018).
16. Kamali, P. *et al.* Medial Row Perforators Are Associated with Higher Rates of Fat Necrosis in Bilateral DIEP Flap Breast Reconstruction. *Plast. Reconstr. Surg.* **140**, 19–24 (2017).
17. Verduijn, P. S., Michi, M., Vahrmeijer, A. L. & Mulder, B. G. S. Perfusion assessment of DIEP flaps based on near-infrared fluorescence imaging: current literature and pilot study. *SPIE* **10862**, (2019).
18. To, C. *et al.* Intraoperative Tissue Perfusion Measurement by Laser Speckle Imaging: A Potential Aid for Reducing Postoperative Complications in Free Flap Breast Reconstruction. *Plast. Reconstr. Surg.* **143**, 287e–292e (2019).
19. Zötterman, J. *et al.* Laser Speckle Contrast Imaging in Reconstructive Surgery. (Linköping University, 2020). doi:10.3384/diss.diva-164328

20. Lauritzen, E. & Damsgaard, T. E. Use of Indocyanine Green Angiography decreases the risk of complications in autologous- and implant-based breast reconstruction: A systematic review and meta-analysis. *J. Plast. Reconstr. Aesthetic Surg.* **74**, 1703–1717 (2021).
21. Alstrup, T., Christensen, B. O. & Damsgaard, T. E. ICG angiography in immediate and delayed autologous breast reconstructions: peroperative evaluation and postoperative outcomes. *J. Plast. Surg. Hand Surg.* **52**, 307–311 (2018).
22. Degett, T. H., Andersen, H. S. & Gögenur, I. Indocyanine green fluorescence angiography for intraoperative assessment of gastrointestinal anastomotic perfusion: a systematic review of clinical trials. *Langenbeck's Arch. Surg.* **401**, 767–775 (2016).
23. Hackethal, A. *et al.* Role of Indocyanine Green in Fluorescence Imaging with Near- Infrared Light to Identify Sentinel Lymph Nodes , Lymphatic Vessels and Pathways Prior to Surgery – A Critical Evaluation of Options Die Rolle von Indocyaningrün als Fluoreszenzfarbstoff in Komb. *Geburtshilfe Frauenheilk* **78**, 54–62 (2018).
24. Meira, J., Marques, M. L., Falcão-Reis, F., Gomes, E. R. & Carneiro, Â. Immediate reactions to fluorescein and indocyanine green in retinal angiography: Review of literature and proposal for patient's evaluation. *Clin. Ophthalmol.* **14**, 171–178 (2020).
25. Dupréé, A., Rieß, H., Detter, C., Debus, E. S. & Wipper, S. H. Utilization of indocyanine green fluorescent imaging (ICG-FI) for the assessment of microperfusion in vascular medicine. *Innov. Surg. Sci.* **3**, 193–201 (2018).
26. Zötterman, J., Tesselar, E. & Farnebo, S. The use of laser speckle contrast imaging to predict flap necrosis : An experimental study in a porcine flap model. *J. Plast. Reconstr. Aesthetic Surg.* 771–777 (2019). doi:10.1016/j.bjps.2018.11.021
27. Davis, M. A. & Dunn, A. K. Imaging depth and multiple scattering in laser speckle contrast imaging. *J. Biomed. Opt.* **19**, (2014).
28. Mennes, O. A., Van Netten, J. J., Van Baal, J. G. & Steenbergen, W. Assessment of microcirculation in the diabetic foot with laser speckle contrast imaging. *Physiol. Meas.* **40**, (2019).
29. Dunn, A. K. Laser speckle contrast imaging of cerebral blood flow. *Ann. Biomed. Eng.* **40**, 367–377 (2012).
30. Heeman, W., Steenbergen, W., van Dam, G. M. & Boerma, E. C. Clinical applications of laser speckle contrast imaging: a review. *J. Biomed. Opt.* **24**, 1 (2019).
31. Chizari, A. Handheld laser speckle contrast perfusion imaging. (2021).
32. Miller, D. R., Ashour, R., Sullender, C. T. & Dunn, A. K. Continuous blood flow visualization with laser speckle contrast imaging during neurovascular surgery. *Neurophotonics* **9**, 1–12 (2022).
33. Coyotl-Ocelotl, B. *et al.* Speckle contrast calculation based on pixels correlation: spatial analysis. **1074903**, 2 (2018).
34. Padmanaban, P., Chizari, A., Knop, T., Zhang, J. & Trikalitis, V. D. Assessment of flow within developing chicken vasculature and biofabricated vascularized tissues using multimodal imaging techniques. *Sci. Rep.* **11**, 1–14 (2021).
35. Mangraviti, A. *et al.* Intraoperative Laser Speckle Contrast Imaging For Real-Time Visualization of Cerebral Blood Flow in Cerebrovascular Surgery: Results From Pre-Clinical Studies. *Sci. Rep.* **10**, 1–13 (2020).
36. Kojima, S. *et al.* Laser Speckle Contrast Imaging for Intraoperative Quantitative Assessment of Intestinal Blood Perfusion During Colorectal Surgery: A Prospective Pilot Study. *Surg. Innov.* 1–9 (2019). doi:10.1177/1553350618823426
37. Chizari, A., Schaap, M. J., Knop, T., Boink, Y. E. & Seyger, M. M. B. Handheld versus mounted laser speckle contrast perfusion imaging demonstrated in psoriasis lesions. *Sci. Rep.* **11**, 16646 (2021).
38. Schaap, M. J. *et al.* Perfusion measured by laser speckle contrast imaging as a predictor for expansion of psoriasis lesions. *Ski. Res. Technol.* **28**, 104–110 (2022).
39. Chizari, A., Knop, T., Sirmacek, B., van der Heijden, F. & Steenbergen, W. Exploration of movement artefacts in handheld laser speckle contrast perfusion imaging. *Biomed. Opt.*

- Express* **11**, 2352 (2020).
40. Mahé, G. *et al.* Laser speckle contrast imaging accurately measures blood flow over moving skin surfaces. *Microvasc. Res.* **81**, 183–188 (2011).
 41. Mahe, G. *et al.* Cutaneous microvascular functional assessment during exercise: A novel approach using laser speckle contrast imaging. *Pflugers Arch. Eur. J. Physiol.* **465**, 451–458 (2013).
 42. Omarjee, L. *et al.* Optimisation of movement detection and artifact removal during laser speckle contrast imaging. *Microvasc. Res.* **97**, 75–80 (2015).
 43. Lertsakdadet, B. *et al.* Correcting for motion artifact in handheld laser speckle images. *J. Biomed. Opt.* **23**, 1 (2018).
 44. Lertsakdadet, B., Dunn, C., Bahani, A., Cruzet, C. & Choi, B. Handheld motion stabilized laser speckle imaging. *Biomed. Opt. Express* **10**, 5149–5158 (2019).
 45. Shah, S. T. H. & Xuezhhi, X. Traditional and modern strategies for optical flow: an investigation. *SN Appl. Sci.* **3**, 1–14 (2021).
 46. Aminfar, A. H., Davoodzadeh, N., Aguilar, G. & Princevac, M. Application of optical flow algorithms to laser speckle imaging. *Microvasc. Res.* **122**, 52–59 (2019).
 47. Bour, P., Cribelier, E. & Argyriou, V. *Crowd behavior analysis from fixed and moving cameras. Multimodal Behavior Analysis in the Wild: Advances and Challenges.* (Elsevier Ltd, 2018). doi:10.1016/B978-0-12-814601-9.00023-7
 48. Farneback, G. Two-Frame Motion Estimation Based on. *Lect. Notes Comput. Sci.* **2749**, 363–370 (2003).
 49. Evangelidis, G. & Psarakis, E. Parametric Image Alignment using Enhanced Correlation Coefficient Maximization. *Anesthesiology* **30**, 1858–1865 (2008).
 50. Mahé, G. *et al.* Air movements interfere with laser speckle contrast imaging recordings. *Lasers Med. Sci.* **27**, 1073–1076 (2012).
 51. Vatry, A., Grisolia, C., Delaporte, P. & Sentis, M. Removal of in vessel Tokamak dust by laser techniques. *Fusion Eng. Des.* **86**, 2717–2721 (2011).
 52. Central Committee on Research Involving Human Subjects. Your research: Is it subject to the WMO or not? (2022). Available at: <https://english.ccmo.nl/investigators/legal-framework-for-medical-scientific-research/your-research-is-it-subject-to-the-wmo-or-not>.
 53. Akata, T. General Anesthetics and Vascular Smooth Muscle. *Anesthesiology* **106**, 365–391 (2007).
 54. Schrepp, M., Hinderks, A. & Thomaschewski, J. Design and Evaluation of a Short Version of the User Experience Questionnaire (UEQ-S). *Int. J. Interact. Multimed. Artif. Intell.* **4**, 103 (2017).
 55. UEQ Team. User Experience Questionnaire. (2018). Available at: <https://www.ueq-online.org/>. (Accessed: 5th June 2022)

6. Appendix

6.1 Appendix A: Optical flow and Farneback's algorithm

With the use of Taylor series and with the assumption that the movement is small, the intensity of a point in a consecutive frame can be rewritten as⁴⁶:

$$I(x + dx, y + dy, t + dt) = I(x, y, t) + \frac{\partial I}{\partial x} dx + \frac{\partial I}{\partial y} dy + \frac{\partial I}{\partial t} dt + \text{higher - order terms} \quad (s1)$$

The higher-order terms can be neglected. Then, by dividing eq. (2) by dt and by taking eq. (1) into account, the following equation can be obtained⁴⁷:

$$\frac{\partial I}{\partial x} \frac{dx}{dt} + \frac{\partial I}{\partial y} \frac{dy}{dt} + \frac{\partial I}{\partial t} = 0 \quad (s2)$$

Where $\frac{\partial I}{\partial x}$, $\frac{\partial I}{\partial y}$ and $\frac{\partial I}{\partial t}$ are the image derivatives at (x, y, t) in the corresponding directions. To make eq. (3) more compact, the following equation is derived³⁷:

$$I_x V_x + I_y V_y = -I_t \quad (s3)$$

Where V_x and V_y are the x and y component of the velocity and where I_x , I_y and I_t are the image derivatives at (x, y, t) in the corresponding directions. Eq. (4) is an equation which cannot be solved as there are two unknown variables: V_x and V_y . To eventually find the displacement between consecutive frames, additional steps are needed. There are multiple methods to take these additional steps. The method Farneback proposed, is applied in this thesis⁴⁸.

The method Farneback proposed for the calculation of optical flow assumes that images can be represented by a second order polynomial function with matrix A, vector b and scalar c:

$$f(x) = x^T A x + b^T x + c \quad (s4)$$

Then, the consecutive image with displacement d is defined as:

$$\begin{aligned} f(x - d) &= (x - d)^T A_1 (x - d) + b_1^T (x - d) + c \\ &= x^T A_1 x + (b_1 - 2A_1 d)^T x + d^T A_1 d - b_1^T d + c_1 \\ &= x^T A_2 x + b_2^T x + c_2 \end{aligned} \quad (s5)$$

With

$$A_2 = A_1, \quad (s6)$$

$$b_2 = b_1 - 2A_1 d, \quad (s7)$$

$$c_2 = d^T A_1 d - b_1^T d + c_1 \quad (s8)$$

From eq. 8, the displacement can be calculated as follows:

$$2A_1 d = -(b_2 - b_1) \quad (s9)$$

$$d = -\frac{1}{2} A_1^{-1} (b_2 - b_1) \quad (s10)$$

In this way, the global polynomial assumption can be replaced by the local assumption which is based on second order polynomials to form the displacement for every pixel in the image. This results in

coefficients $A_1(x)$, $b_1(x)$ and $c_1(x)$ for the first image and $A_2(x)$, $b_2(x)$ and $c_2(x)$ for the consecutive image.

As it is a local problem now, A and b are dependent on location x :

$$A(x) = \frac{A_1(x) + A_2(x)}{2} \quad (s11)$$

$$\Delta b(x) = -\frac{1}{2}(b_2(x) - b_1(x)) \quad (s12)$$

Substituting eq. 12 and eq. 13 into eq. 10 gives:

$$A(x)d(x) = \Delta b(x) \quad (s13)$$

Here, $d(x)$ indicates local displacement. In eq. 14, the assumption is made that the displacement is small. Larger displacements would introduce errors in eq. 14, but this could be solved with a priori knowledge. When having a priori knowledge about the displacement, the comparison can be made between the polynomial at x in the first image and $x + \tilde{d}(x)$ in the second image, where $\tilde{d}(x)$ is the a priori displacement rounded to integer values. Then, only the relative displacement between the real value and the rounded a priori value needs to be estimated, which should be smaller. This observation can be included in this algorithm by replacing eq. 12 and eq. 13 by:

$$A(x) = \frac{A_1(x) + A_2(\tilde{x})}{2} \quad (s14)$$

$$\Delta b(x) = -\frac{1}{2}(b_2(\tilde{x}) - b_1(x)) + A(x)\tilde{d}(x) \quad (s15)$$

Where

$$\tilde{x} = x + \tilde{d}(x) \quad (s16)$$

When $\tilde{d}(x)$ is approximately zero, the above-described equations refer to eq. (s11) and eq. (s12), as expected.

6.2 Appendix B: Creating perfusion maps based on optical flow

For the application of the optical flow on the RGB images to align the perfusion map and to eventually average the perfusion maps, a GUI called clone WirelessHAPI was created in MATLAB and used in this study (P:\Projects\LASCA AND LDPI CONNECTION\3. Standard and Realtime LSCI\clone_WirelessHAPI). Figure 22 shows the interface of the GUI in which an example is given how an aligned and averaged perfusion map is created. In this example, a measurement was already loaded in the software.

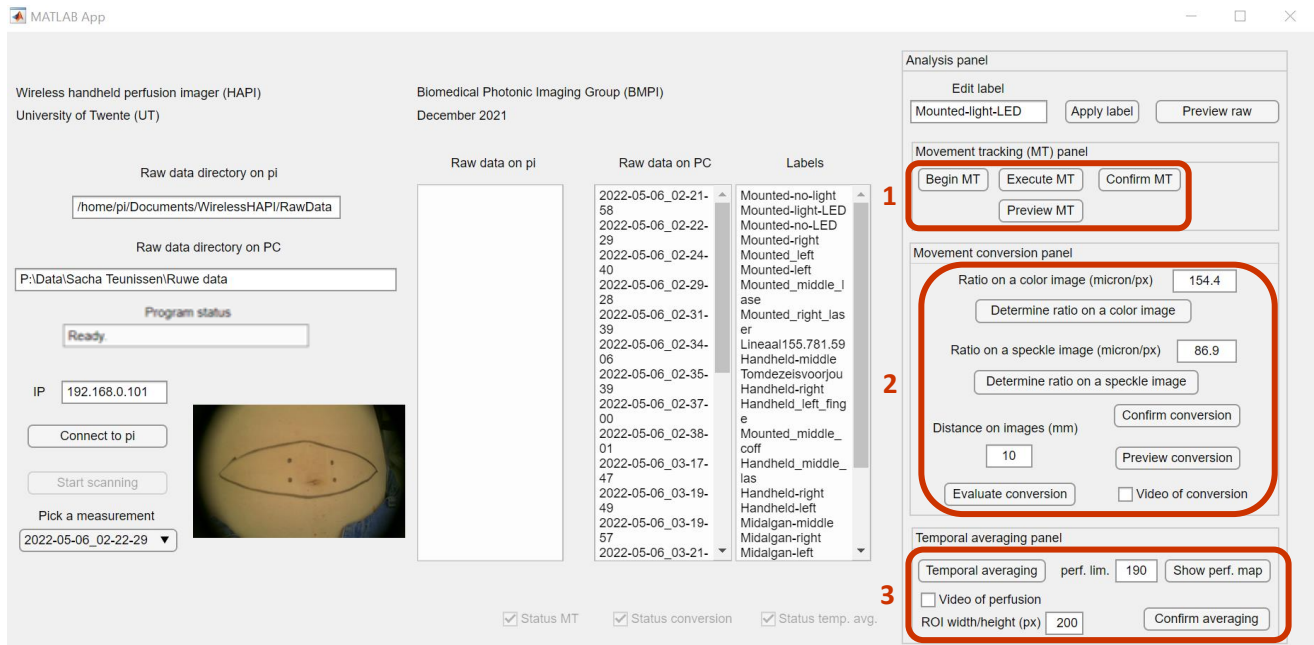


Figure 22 MATLAB GUI for motion tracking and to align and temporally average the perfusion maps.

After the measurement is loaded, the first step is to start motion tracking in the RGB frames (see first red box). By clicking begin MT and execute MT, the software runs the optical flow algorithm. After running the optical flow algorithm, the user is asked to put a crosshair somewhere in the image to visually check if the motion tracking is successful. Then the motion tracking can be confirmed and could be previewed.

The second step is to converge the found displacements in the RGB frames to speckle images. This should be done once when multiple measurements are performed, as the settings of the cameras did not change during these multiple measurements. The ratio on a colour image and speckle image can be manually determined when a ruler of 1 cm is present in the measurement by drawing a line within that 1 cm. Then, the software calculates the size of the pixel on the RGB and speckle frame in microns. The conversion can visually be evaluated whether the conversion was as expected. Afterwards, the conversion can be confirmed and previewed. Now, the speckle frames are aligned.

The last step is to average the 45 perfusion images by clicking the button temporal averaging to create an aligned and averaged perfusion map. The perfusion limit (colour bar) can be adjusted for each perfusion map. The perfusion map can be confirmed and saved by 'confirm averaging'.

6.3 Appendix C: MATLAB script ECC versus Optical flow

```

%% Analysis ECC vs optical flow
clear all
close all
clc
addpath(genpath('Functions'))

%% Loading warp optical flow
file_address_warp_optical_flow='direction';
file_name_warp_optical_flow='name.mat';
struct_warp_optical = load(strcat(file_address_warp_optical_flow,file_name_warp_optical_flow));

%% Loading warp ECC on speckles
file_address_warp_on_speckle='direction';
file_name_warp_on_speckle='name.mat';
struct_warp_optical_speckle = load(strcat(file_address_warp_on_speckle,file_name_warp_on_speckle));
struct_warp_optical_speckle.warp_matrix(1,:);
struct_warp_optical_speckle.warp_matrix(2,:);
file_name_ratio='ratio_RGB_mono.mat';
load(strcat(file_address_warp_on_speckle, file_name_ratio));

%% Loading raw speckles
file_address_speckles='direction';
file_name_speckles='gray_burst';
struct_raw_speckles=load(strcat(file_address_speckles,file_name_speckles));
load(strcat(file_address_speckles,'res_mono'));
intensity_mat=255*im2double(squeeze(struct_raw_speckles.data_raw_cam));
intensity_mat_process=intensity_mat(:, :, struct_warp_optical_speckle.ref_image_index:end);
clear intensity_mat
ROI_frames=func_crop(intensity_mat_process, round(struct_warp_optical_speckle.ROI_index_position));
clear intensity_mat_process

%% Visualise consecutive speckle frames
figure(1)
for counter=1:size(ROI_frames,3)
    imagesc(ROI_frames(:, :, counter));
    drawnow
end

optical_flow_pos_x=ratio_RGB_mono*struct_warp_optical.pos_vec_x;
optical_flow_pos_y=ratio_RGB_mono*struct_warp_optical.pos_vec_y;

%% Visualise displacements of ECC and optical flow
figure(2), clf
subplot(1, 2, 1)
plot(optical_flow_pos_x)
hold on
plot(struct_warp_optical_speckle.warp_matrix(1,:))
legend('Farneback on RGB','ECC on speckles')
title('x direction')
xlabel('pixels')
ylabel('pixels')

subplot(1, 2, 2)
plot(optical_flow_pos_y)
hold on
plot(struct_warp_optical_speckle.warp_matrix(2,:))
legend('Farneback on RGB','ECC on speckles')
title('y direction')
xlabel('pixels')
ylabel('pixels')
saveas(gcf,'Opticalflow_vs_ECC.png')

delay_px=24; % delay measured on the above plot

optical_flow_pos_x_shifted=ratio_RGB_mono*[zeros(1, delay_px),struct_warp_optical.pos_vec_x];
optical_flow_pos_y_shifted=ratio_RGB_mono*[zeros(1, delay_px),struct_warp_optical.pos_vec_y];

figure(3), clf
subplot(1, 2, 1)
plot(optical_flow_pos_x_shifted)
hold on
plot(struct_warp_optical_speckle.warp_matrix(1,:))
legend('Farneback on RGB','ECC on speckles')
title('x direction')
xlabel('pixels')
ylabel('pixels')

subplot(1, 2, 2)
plot(optical_flow_pos_y_shifted)
hold on
plot(struct_warp_optical_speckle.warp_matrix(2,:))
legend('Farneback on RGB','ECC on speckles')
title('y direction')
xlabel('pixels')
ylabel('pixels')
saveas(gcf,'Opticalflow_vs_ECC_shifted.png')

%% Visualise ECC and optical flow in consecutive speckle frames
figure(4)

```

```
crosshair_x=157.3733;
crosshair_y=106.7743;
offset_farneback_x_px=30;
offset_farneback_y_px=-28;

for counter = delay_px:size(ROI_frames,3)
    imagesc(ROI_frames(:,:,counter));
    hold on
    plot(crosshair_x+struct_warp_optical_speckle.warp_matrix(1,counter),...
        crosshair_y+struct_warp_optical_speckle.warp_matrix(2,counter),...
        'rx','markersize',20,'linewidth',1.5,'color','red')

    plot(crosshair_x+optical_flow_pos_x(counter)+offset_farneback_x_px,...
        crosshair_y+optical_flow_pos_y(counter)+offset_farneback_y_px,...
        'rx','markersize',20,'linewidth',1.5,'color','green')

    legend('ECC on speckles','Farneback on RGB', 'Location', 'southwest')
    hold off
    drawnow
end

%% Visualise ECC and shifted optical flow in consecutive speckle frames
figure(5)
crosshair_x=157.3733;
crosshair_y=106.7743;
offset_farneback_x_px=30;
offset_farneback_y_px=-28;

for counter = delay_px:size(ROI_frames,3)
    imagesc(ROI_frames(:,:,counter));
    hold on
    plot(crosshair_x+struct_warp_optical_speckle.warp_matrix(1,counter),...
        crosshair_y+struct_warp_optical_speckle.warp_matrix(2,counter),...
        'rx','markersize',20,'linewidth',1.5,'color','red')

    plot(crosshair_x+optical_flow_pos_x_shifted(counter)+offset_farneback_x_px,...
        crosshair_y+optical_flow_pos_y_shifted(counter)+offset_farneback_y_px,...
        'rx','markersize',20,'linewidth',1.5,'color','green')

    legend('ECC on speckles','Farneback on RGB', 'Location', 'southwest')
    hold off
    drawnow
end
```

6.4 Appendix D: Analysis of the perfusion maps

To analyse the perfusion maps, two interfaces in MATLAB were used (Figure 23 and Figure 24). Both were part of the software that was already applied in the research to the HAPI system. All HAPI software together was called clone HAPI (P:\Projects\LASCA AND LDPI CONNECTION\3. Standard and Realtime LSCI\clone_HAPI). Figure 23 shows the interface in which the contrast and perfusion over time of an ROI can be calculated. The applied graph of the lookup table is shown in the right upper corner. First, the raw data can be loaded at the left upper corner of the interface. The raw data will be visualised in the window 'gray frame'. All consecutive frames can be visualised by pushing the button 'play' under the gray frame. Next to the gray frame, the contrast map is calculated, in which the sliding window size can be adjusted under the contrast map. By pressing 'calculate temporal' in the work panel, the perfusion map will be shown, after which a temporally averaged perfusion map can be shown when pressing 'temporal averaging' in the work panel. A ROI can be chosen by pressing 'reset ROI' in the work panel. The ROI can be resized by 'resize' in the work panel. The graphs of temporal contrast and temporal perfusion at the top of the interface, show the contrast and perfusion over time of the chosen ROI. The analysed data can be saved by 'save averaging' in the work panel.

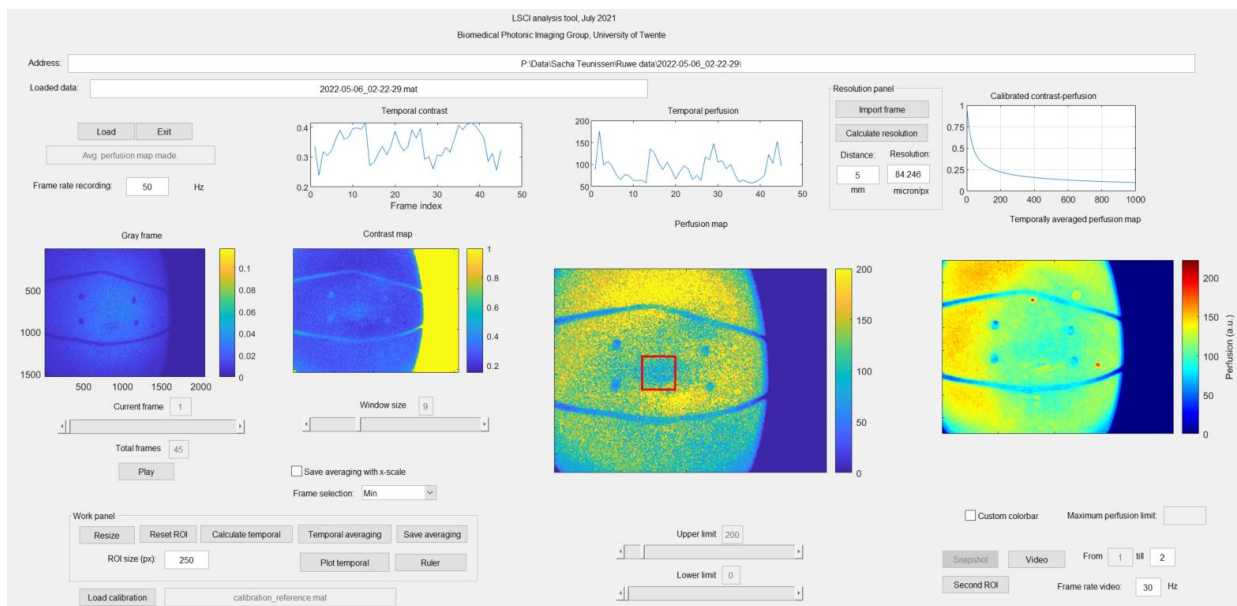


Figure 23 Analysis method to determine the perfusion over time of an ROI.

Figure 24 shows the interface to calculate the mean perfusion of an ROI in an aligned and averaged perfusion map. After loading a temporally averaged perfusion map, a first ROI can manually be placed by pressing 'place R1'. Then, the temporally averaged perfusion map will pop up to enable ROI placement, this moment is shown in Figure 24. The mean perfusion in this ROI can be calculated by pushing 'calculate mean R1', after which the result will be shown at the right of the 'calculate mean R1' button. Up to four ROIs can be placed in the perfusion map and the weighted mean value of these ROIs will be automatically calculated. The analysed data can be saved by pressing 'save' in the saving panel.

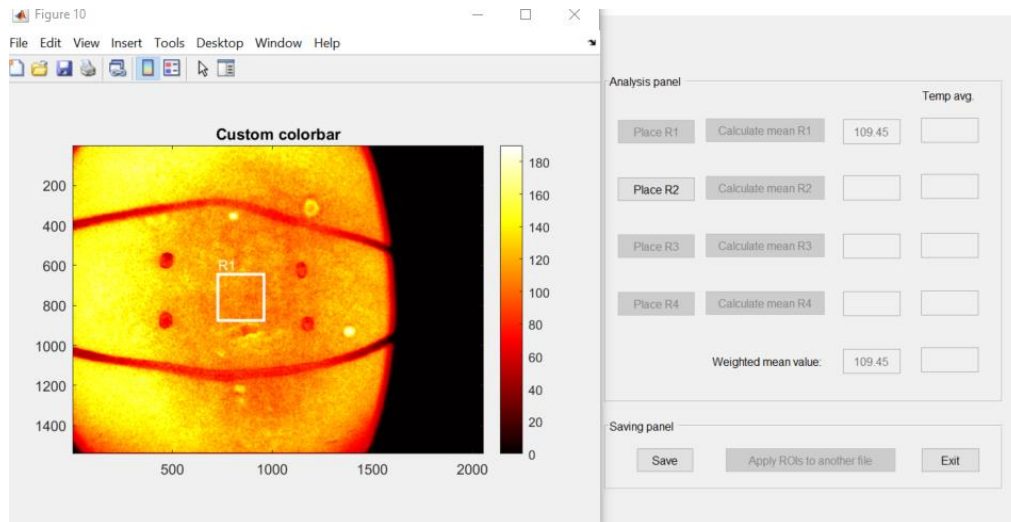


Figure 24 Analysis method to calculate the mean perfusion of an ROI.

6.5 Appendix E: Visualisation of the displacements between handheld and mounted measurements

```

%% Visualisation of the displacements between handheld and mounted measurements
clear all
close all
clc

%% Displacement handheld vs mounted - middle
mounted_middle = load ('2022-05-06_02-22-29 alignment.mat');
handheld_middle = load ('2022-05-06_03-17-47 alignment.mat');

figure(1)
tiledlayout(2,2,'TileSpacing','compact')
nexttile
line1 = plot(mounted_middle.warp_matrix(1,:),mounted_middle.warp_matrix(2,:));
xlabel('x (mm)')
ylabel('y (mm)')
title('Lissajous graph - middle')
hold on
line2 = plot(handheld_middle.warp_matrix(1,:),handheld_middle.warp_matrix(2,:));
hold on

nexttile
line3 = plot(time_vec,mounted_middle.warp_matrix(1,:));
xlabel('Time (s)')
ylabel('x (mm)')
hold on
line4 = plot(time_vec,handheld_middle.warp_matrix(1,:));
title('Displacement in x direction - middle')

nexttile
line5 = plot(time_vec,mounted_middle.warp_matrix(2,:));
xlabel('Time (s)')
ylabel('y (mm)')
title('Displacement in y direction - middle')
hold on
line6 = plot(time_vec,handheld_middle.warp_matrix(2,:));

lg = legend(nexttile(3),'Mounted','Handheld');
lg.Location = 'southoutside';
saveas(gcf,'displacement_middle.png')

%% Displacement handheld vs mounted - right
mounted_right = load ('2022-05-06_02-34-06 alignment.mat');
handheld_right = load ('2022-05-06_03-28-10 alignment.mat');
figure(2)
tiledlayout(2,2, 'TileSpacing','compact')
nexttile
line1 = plot(mounted_right.warp_matrix(1,:),mounted_right.warp_matrix(2,:));
xlabel('x (mm)')
ylabel('y (mm)')
title('Lissajous graph - right')
hold on
line2 = plot(handheld_right.warp_matrix(1,:),handheld_right.warp_matrix(2,:));

nexttile
line3 = plot(time_vec,mounted_right.warp_matrix(1,:));
xlabel('Time (s)')
ylabel('x (mm)')
hold on
line4 = plot(time_vec,handheld_right.warp_matrix(1,:));
title('Displacement in x direction - right')

nexttile
line5 = plot(time_vec,mounted_right.warp_matrix(2,:));
xlabel('Time (s)')
ylabel('y (mm)')
title('Displacement in y direction - right')
hold on
line6 = plot(time_vec,handheld_right.warp_matrix(2,:));

lg = legend(nexttile(3),'Mounted','Handheld');
lg.Location = 'southoutside';
saveas(gcf,'displacement_right.png')

%% Displacement handheld vs mounted - left
mounted_left = load ('2022-05-06_02-29-28 alignment.mat');
handheld_left = load ('2022-05-06_03-26-10 alignment.mat');
figure(3)
tiledlayout(2,2,'TileSpacing','compact');
nexttile
line1 = plot(mounted_left.warp_matrix(1,:),mounted_left.warp_matrix(2,:));
xlabel('x (mm)')
ylabel('y (mm)')
title('Lissajous graph - left')
hold on

```

```
line2 = plot(handheld_left.warp_matrix(1,:),handheld_left.warp_matrix(2,:));

nexttile
line3 = plot(time_vec,mounted_left.warp_matrix(1,:));
xlabel('Time(s)')
ylabel('x(mm)')
hold on
line4 = plot(time_vec,handheld_left.warp_matrix(1,:));
title('Displacement in x direction - left')

nexttile
line5 = plot(time_vec,mounted_left.warp_matrix(2,:));
xlabel('Time(s)')
ylabel('y(mm)')
title('Displacement in y direction - left')
hold on
line6 = plot(time_vec,handheld_left.warp_matrix(2,:));
lg = legend(nexttile(3),'Mounted','Handheld');
lg.Location = 'southoutside';
saveas(gcf,'displacement_left.png')
```

6.6 Appendix F: MATLAB script for the calculations of the velocity and speed

```

%% Calculations of the velocity and speed in handheld vs mounted
clear all
close all
clc

%% Load alignment data
mounted_middle = load ('2022-05-06_02-22-29 alignment.mat');
handheld_middle = load ('2022-05-06_03-17-47 alignment.mat');
mounted_right = load ('2022-05-06_02-34-06 alignment.mat');
handheld_right = load ('2022-05-06_03-28-10 alignment.mat');
mounted_left = load ('2022-05-06_02-29-28 alignment.mat');
handheld_left = load ('2022-05-06_03-26-10 alignment.mat');
load '2022-05-06_02-22-29 video.mat'; %gives duration of the measurements

%% velocity middle handheld
load '2022-05-06_03-1 vid perfusion hm.mat'; %gives perfusion over time
displacement_mag_handheld_middle = sqrt((handheld_middle.warp_matrix(1,:).^2+...
(handheld_middle.warp_matrix(2,:).^2));
dif_displacement_x_y_middle_handheld = diff(displacement_mag_handheld_middle);
dif_time_vec = diff(time_vec);
velocity_middle_handheld = abs(dif_displacement_x_y_middle_handheld./dif_time_vec);
mean_velocity_middle_handheld = mean(velocity_middle_handheld);
figure(10)
subplot(3,1,1)
plot(time_vec(2:end),velocity_middle_handheld)
title('Velocity over time in handheld measurement at the middle')
xlabel 'Time(s)'
ylabel 'Velocity (mm/s)'
hold on
subplot(3,1,2)
plot(time_vec(2:end),temp_perf_vec)
title('Perfusion over time in handheld measurement at the middle')
xlabel 'Time(s)'
ylabel 'Perfusion (a.u.)'
subplot(3,1,3)
plot(velocity_middle_handheld,perfusion_temporal(2:end),'.')
coeff = polyfit(velocity_middle_handheld,perfusion_temporal(2:end),1);
hold on
plot(velocity_middle_handheld,coeff(1)*velocity_middle_handheld+coeff(2),'Color','black')
hold on
plot(0, mean(perfusion_temporal), 'o','color','r')
title ('Velocity vs. perfusion')
xlabel 'Velocity (mm/s)'
ylabel 'Perfusion (a.u.)'
legend ('Temporal perfusion','Linear fit','Mean perfusion')
saveas(gcf,'velocity_vs_perfusion.png')

%% Velocity middle mounted
load '2022-05-06_02-2 vid perfusion mm.mat';
displacement_mag_mounted_middle = sqrt((mounted_middle.warp_matrix(1,:).^2+...
(mounted_middle.warp_matrix(2,:).^2));
dif_displacement_x_y_middle_mounted = diff(displacement_mag_mounted_middle);
dif_time_vec = diff(time_vec);
velocity_middle_mounted = abs(dif_displacement_x_y_middle_mounted./dif_time_vec);
mean_velocity_middle_mounted = mean(velocity_middle_mounted);

%% Velocity right mounted
load '2022-05-06_02-2 vid perfusion mr.mat'
displacement_mag_mounted_right = sqrt((mounted_right.warp_matrix(1,:).^2+...
(mounted_right.warp_matrix(2,:).^2));
dif_displacement_x_y_mounted_right = diff(displacement_mag_mounted_right);
dif_time_vec = diff(time_vec);
velocity_mounted_right = abs(dif_displacement_x_y_mounted_right./dif_time_vec);
mean_velocity_mounted_right = mean(velocity_mounted_right);

%% Velocity left mounted
load '2022-05-06_02-3 vid perfusion ml.mat';
displacement_mag_mounted_left = sqrt((mounted_left.warp_matrix(1,:).^2+...
(mounted_left.warp_matrix(2,:).^2));
dif_displacement_x_y_left = diff(displacement_mag_mounted_left);
dif_time_vec = diff(time_vec);
velocity_mounted_left = abs(dif_displacement_x_y_left./dif_time_vec);
mean_velocity_mounted_left = mean(velocity_mounted_left);

%% Velocity right handheld
load '2022-05-06_03-2 vid perfusion hr.mat'
displacement_mag_handheld_right = sqrt((handheld_right.warp_matrix(1,:).^2+...
(handheld_right.warp_matrix(2,:).^2));
dif_displacement_x_y_handheld_right = diff(displacement_mag_handheld_right);
dif_time_vec = diff(time_vec);
velocity_handheld_right = abs(dif_displacement_x_y_handheld_right./dif_time_vec);
mean_velocity_handheld_right = mean(velocity_handheld_right);

%% Velocity left handheld
load '2022-05-06_03-2 vid perfusion hl.mat';
displacement_mag_handheld_left = sqrt((handheld_left.warp_matrix(1,:).^2+...
(handheld_left.warp_matrix(2,:).^2));
dif_displacement_x_y_left_handheld = diff(displacement_mag_handheld_left);
dif_time_vec = diff(time_vec);

```



```

velocity_left_handheld = abs(dif_displacement_x_y_left_handheld./dif_time_vec);
mean_velocity_left_handheld = mean(velocity_left_handheld);

%% Speed middle
speed_mounted_middle_x = (mounted_middle.warp_matrix(1,45) -
mounted_middle.warp_matrix(1,1))./(sum(time_vec));
speed_mounted_middle_y = (mounted_middle.warp_matrix(2,45) -
mounted_middle.warp_matrix(2,1))./(sum(time_vec));
mean_speed_mounted_middle = mean(sqrt(speed_mounted_middle_x.^2+speed_mounted_middle_y.^2));
speed_handheld_middle_x = (handheld_middle.warp_matrix(1,45) -
handheld_middle.warp_matrix(1,1))./(sum(time_vec));
speed_handheld_middle_y = (handheld_middle.warp_matrix(2,45) -
handheld_middle.warp_matrix(2,1))./(sum(time_vec));
mean_speed_handheld_middle = mean(sqrt(speed_handheld_middle_x.^2+speed_handheld_middle_y.^2));
ratio_speed_mag_middle = mean_speed_handheld_middle/mean_speed_mounted_middle;

%% Speed right
speed_mounted_right_x = (mounted_right.warp_matrix(1,45)-mounted_right.warp_matrix(1,1))./(sum(time_vec));
speed_mounted_right_y = (mounted_right.warp_matrix(2,45)-mounted_right.warp_matrix(2,1))./(sum(time_vec));
mean_speed_mounted_right = mean(sqrt(speed_mounted_right_x.^2+speed_mounted_right_y.^2));
speed_handheld_right_x = (handheld_right.warp_matrix(1,45) -
handheld_right.warp_matrix(1,1))./(sum(time_vec));
speed_handheld_right_y = (handheld_right.warp_matrix(2,45) -
handheld_right.warp_matrix(2,1))./(sum(time_vec));
mean_speed_handheld_right = mean(sqrt(speed_handheld_right_x.^2+speed_handheld_right_y.^2));
ratio_speed_mag_right = mean_speed_handheld_right/mean_speed_mounted_right;

%% Speed left
speed_mounted_left_x = (mounted_left.warp_matrix(1,45)-mounted_left.warp_matrix(1,1))./(sum(time_vec));
speed_mounted_left_y = (mounted_left.warp_matrix(2,45)-mounted_left.warp_matrix(2,1))./(sum(time_vec));
mean_speed_mounted_left = mean(sqrt(speed_mounted_left_x.^2+speed_mounted_left_y.^2));
speed_handheld_left_x = (handheld_left.warp_matrix(1,45)-handheld_left.warp_matrix(1,1))./(sum(time_vec));
speed_handheld_left_y = (handheld_left.warp_matrix(2,45)-handheld_left.warp_matrix(2,1))./(sum(time_vec));
mean_speed_handheld_left = mean(sqrt(speed_handheld_left_x.^2+speed_handheld_left_y.^2));
ratio_speed_mag_left = mean_speed_handheld_left/mean_speed_mounted_left;

```

6.7 Appendix G: Overzicht indiening documenten aan METC en ALU

In deze appendix wordt een overzicht gegeven van de documenten die zijn goedgekeurd door de METC (Table 10) en ALU (Table 11). De proefpersoneninformatie brief (6.8 Appendix H: Proefpersoneninformatie brief) en het protocol (6.10 Appendix J: Research protocol) bijgevoegd in deze thesis. De overige documenten zijn raad te plegen via P:\Users\Sacha Teunissen\Manuscripts\2022 METC en ALU aanvragen.

Table 10 Documenten met versie nummer welke zijn goedgekeurd door de METC.

Sectie	Document	Versie/datum	Opmerkingen
A	A1	Aanbiedingsbrief	01-03-2022
	A2	Machtiging van de verrichter als de indiener niet de verrichter is	n.v.t.
	A3	Ontvangstbewijs EudraCT-nummer	n.v.t.
B	B1	ABR-formulier	23-05-2022
	B3	EudraCT aanvraagformulier	n.v.t.
	B4	Gentherapie/GGO-formulier	n.v.t.
C	C1	Onderzoeksprotocol	04-05-2022
	C2	Amendementen	n.v.t.
D	D1	Investigator's Brochure en overzicht SUSAR's na IB-datum	n.v.t.
	D2	IMPD of SPC en overzicht relevante studies	n.v.t.
	D2	IMDD	09-06-2022 Gemaakt door Tom
	D3	Voorbeeldetiket in het Nederlands	n.v.t.
	D4	Vergunningen/verklaringen onderzoeksmiddel	n.v.t.
	D5	Productgegevens ziekenhuisapotheker	n.v.t.
	D6	Aanvullende productgegevens	n.v.t.
E	E1	Proefpersoneninformatie	04-05-2022
	E2	Toestemmingsformulier(en)	04-05-2022
	E3	Eventuele advertentieteksten of ander wervingsmateriaal	n.v.t.
	E4	Eventueel overig voorlichtingsmateriaal	n.v.t.
F	F1	Vragenlijsten (UEQ)	06-04-2022
	F2	Patiëntendagboek	n.v.t.
	F3	Patiëntenkaart	n.v.t.
G	G1	Verklaring proefpersonenverzekering	n.v.t.
	G1	Certificaat WMO-proefpersonenverzekering	n.v.t.
	G2	Bewijs dekking aansprakelijkheid	17-12-2021
H	H1	CV onafhankelijke deskundige(n)	15-02-2022
	H2	CV coördinerend onderzoeker (bij multicenteronderzoek)	24-01-2022
I	I1	Lijst van deelnemende centra met hoofdonderzoeker	n.v.t.
	I2	Onderzoeksverklaring van het afdelingshoofd, de zorggroepmanager of een persoon in een equivalente positie per centrum	16-02-2022
	I3	CV hoofdonderzoeker per centrum	n.v.t.
	I3	GCP-/BROK-certificaat hoofdonderzoeker	12-09-2019 Bijgevoegd in sectie H
	I4	Eventuele overige centruminformatie	n.v.t.
J	J1	Aanvullende informatie financiële vergoedingen aan proefpersonen	n.v.t.

Sectie	Document	Versie/datum	Opmerkingen
	J2	Aanvullende informatie financiële vergoedingen aan onderzoekers en deelnemende centra	n.v.t.
K	K1	Kopie beoordeling door andere instanties (peer-review), bijvoorbeeld subsidiegever, advies registratieautoriteit	01-02-2021
	K2	Overzichtslijst bevoegde instanties in het buitenland (bij internationaal onderzoek) & kopie van beoordeling door andere METC's/bevoegde instanties (inclusief VHP)	n.v.t.
	K3	Onderzoekscontract van verrichter (sponsor) met de onderzoeker en/of instelling	01-06-2022
	K4	Ingediende publicaties	2019/2021
	K5	Data Safety Monitoring Board (DSMB) – samenstelling en charter	n.v.t.
	K6	Overige documenten, bijv. brief aan huisarts/specialist/apotheek of formulier stralingsbelasting	n.v.t.

Table 11 Overzicht van goedgekeurde documenten door de ALU.

Documenten	Versie	Toelichting
Trialverrichtingenformulier, bestaand uit:	25-05-2022	
<i>Deel 1: Algemene informatie studie</i>		
<i>Deel 2: Verzekering en contracten</i>		
<i>Deel 3: Overzichtspagina: Medewerking, kosten & budget</i>		
<i>Deel 4: Trialverrichtingen en medewerking formulier ondersteunende afdelingen</i>		n.v.t.
<i>Deel 5: Personeelskosten afdeling lokale hoofdonderzoeker</i>		
<i>Deel 6: Offertes</i>		n.v.t.
VGO Deel A of onderzoeksverklaring	16-02-2022	
Begroting studie	25-05-2022	
Onderzoeksprotocol	04-05-2022	Dezelfde als voor METC aanvraag
Vragenlijsten / dagboekjes	06-04-2022	
Datamanagementplan Prospectief onderzoek (DMP)	25-05-2022	
Eventuele amendementen		n.v.t.
Volledig ingevuld ABR-formulier van de hoofdonderzoeker (met vermelding van ZGT als deelnemende ziekenhuis).	23-05-2022	Dezelfde als voor METC aanvraag
Informatiebrief(-ven) voor de proefpersoon (PIF)	04-05-2022	Dezelfde als voor METC aanvraag
Toestemmingsformulier(en) (informed consent)	04-05-2022	Dezelfde als voor METC aanvraag
Informatiebrief aan huisarts		n.v.t.

Verzekeringcertificaat proefpersonenverzekering (geldig gedurende het hele onderzoek)		Onheffing is verleend.
Goedkeuringsbrief van de primair toetsende commissie	05-07-2022	
Kopie van geldig GCP certificaat (conform EMWO) van hoofdonderzoeker in ZGT	12-09-2019	
Gebruik medische apparatuur / medische technologie	25-05-2022	
Gebruik materialen / medische hulpmiddelen (<i>alle steriele/onsteriele verbruiksartikelen, disposables, reusables, implantaten, prothesen, wearables</i>)		n.v.t.
Gebruik ICT/Software/apps		n.v.t.
Onderzoekscontract (CTA)	01-06-2022	
Verwerkersovereenkomst (VWO)		n.v.t.
Data transfer agreement / Material transfer agreement		n.v.t.
Monitorplan	20-06-2022	
Data Protection Impact assessment (DPIA) / Gegevensbeschermingseffectbeoordeling (GBEB)		n.v.t.

Proefpersoneninformatie voor deelname aan medisch-wetenschappelijk onderzoek

Titel van het onderzoek:

Vergroten van het inzicht in het ontstaan van complicaties en het voorspellen van complicaties na een DIEP borstreconstructie door het scannen van de oppervlakkige bloedvaten in de huid.

Officiële titel: Draadloos Laser Speckle Contrast Imaging Apparaat voor de visualisatie van de microcirculatie tijdens DIEP flap borstreconstructie.

Inleiding

Geachte mevrouw,

Met deze informatiebrief willen we u vragen of u wilt meedoen aan medisch-wetenschappelijk onderzoek. Meedoen is vrijwillig. U krijgt deze brief omdat u borstkanker heeft of heeft gehad en omdat u binnenkort een DIEP borstreconstructie ondergaat. U leest hier om wat voor onderzoek het gaat, wat het voor u betekent, en wat de voordelen en nadelen zijn. Het is veel informatie. Wilt u de informatie doorlezen en beslissen of u wilt meedoen? U heeft twee weken de tijd om na te denken of u wilt meedoen. Als u wilt meedoen, kunt u het formulier invullen dat u vindt in bijlage B.

Stel uw vragen

U kunt uw beslissing nemen met de informatie die u in deze informatiebrief vindt. Daarnaast raden we u aan om dit te doen:

- Stel vragen aan de onderzoeker die u deze informatie geeft.
- Praat met uw partner, familie of vrienden over dit onderzoek.
- Stel vragen aan de onafhankelijk deskundige, drs. G.M. van Couwelaar
- Lees de informatie op www.rijksoverheid.nl/mensenonderzoek.

1. Algemene informatie

Dit onderzoek wordt uitgevoerd door de afdeling plastische chirurgie van het ZGT. Voor dit onderzoek zijn wij op zoek naar vijftien proefpersonen die een DIEP borstreconstructie ondergaan. De medisch-ethische toetsingscommissie uit Nieuwegein heeft dit onderzoek goedgekeurd.

2. Wat is het doel van het onderzoek?

Door de Universiteit Twente is een apparaat ontwikkeld dat de kleine bloedvaatjes in de huid in beeld kan brengen. Dit apparaat heet voluit het 'Wireless Laser Speckle Contrast Imaging (LSCI) Device'. In de verdere tekst zullen wij dit apparaat het 'LSCI apparaat' noemen. Het doel van deze studie is om te

onderzoeken of het in beeld brengen van de kleine bloedvaatjes tijdens de operatie ons meer kan vertellen over eventuele complicaties die zouden kunnen ontstaan na de DIEP operatie. Hierdoor willen we erachter komen of door middel van het LSCI apparaat het aantal complicaties na de DIEP operatie omlaag kan worden gebracht.

3. Wat is de achtergrond van het onderzoek?

De DIEP borstreconstructie wordt in Nederland steeds vaker uitgevoerd en vrouwen zijn over het algemeen tevreden met de uitkomst van de operatie. Helaas komt het nog steeds wel eens voor dat er complicaties optreden, zoals (gedeeltelijke) afsterving van de borst of een zeer traag wondherstel. Dit komt doordat de doorbloeding niet goed is. Tijdens de operatie wordt de doorbloeding vaak gecontroleerd om zulke complicaties te voorkomen. Dit gebeurt op basis van het oordeel van de chirurg en door het gebruik van een fluorescente vloeistof (contrastvloeistof). Met die fluorescente vloeistof kunnen we echter alleen de doorbloeding kort na het inspuiten zien. Dus wanneer de doorbloeding op meerdere momenten tijdens de operatie wordt gecontroleerd, moet de fluorescente vloeistof meerdere keren in worden gespoten. Daarnaast geeft de fluorescente vloeistof geen informatie over bijvoorbeeld de stroomsnelheid van het bloed. De fluorescente vloeistof laat het bloed oplichten, maar daarvoor hoeft het niet te stromen. Hierdoor is het lastiger om eventuele veranderingen in de vaten die zorgen dat de bloedstroom vermindert of stopt, te ontdekken. Dit soort veranderingen zouden bijvoorbeeld een bloedprop of een (plotselinge) vernauwing van het bloedvat kunnen zijn. We denken dat het LSCI apparaat dat wel snel kan ontdekken. Door de huid op verschillende momenten tijdens de operatie met het LSCI apparaat te bekijken, willen we eventuele veranderingen van de kleine bloedvaatjes in de huid volgen. We willen daarnaast kijken of we het ontstaan van complicaties tijdens de operatie kunnen voorspellen. Hopelijk kunnen we de complicaties voorkomen door het gebruik van het LSCI apparaat. Uiteindelijk is het doel om het ontstaan van complicaties na een DIEP borstreconstructie beter te begrijpen door de kleine bloedvaatjes in beeld te brengen en om het aantal complicaties te verminderen.

4. Hoe verloopt het onderzoek?

Hoelang duurt het onderzoek?

Als u meedoet, vindt het onderzoek plaats tijdens de operatie. Ook wordt er nog een meting uitgevoerd één dag na de operatie.

Stap 1: bent u geschikt om mee te doen?

Iedere vrouw die een DIEP borstreconstructie ondergaat, is geschikt om mee te doen.

Stap 2: onderzoeken en metingen

Tijdens de operatie kijken we naar de kleine bloedvaatjes in de huid door vier metingen met het LSCI apparaat te verrichten. Daarbij maken we ook foto's van de huid. Eén dag na de operatie doen we de laatste, vijfde meting aan uw bed in het ziekenhuis. Elke meting duurt hooguit enkele minuten. Het LSCI apparaat scant de huid door middel van laserlicht. De onderzoeker houdt het LSCI apparaat vast in de handen en scant op een afstand van ongeveer 30 centimeter van de huid. Dit is niet schadelijk voor uw huid. Het apparaat raakt uw huid tijdens het scannen niet aan. Het LSCI apparaat heeft nog geen CE markering. Dat betekent dat als het apparaat waardevol blijkt te zijn voor de dagelijkse praktijk in het ziekenhuis, het nog niet direct in de reguliere zorg mag worden gebruikt. Wel is het zeker dat het LSCI apparaat veilig is om te gebruiken in het ziekenhuis. Hiervoor zijn berekeningen voor de veiligheid van de laser uitgevoerd. Deze berekeningen zijn gecontroleerd door de Universiteit Twente

en de afdeling Zorgtechnologie van ZGT. Op de scans en foto's is alleen de huid dat wordt gebruikt voor de DIEP borstreconstructie zichtbaar. U bent niet herkenbaar.

Wat is er anders dan bij gewone zorg?

Er is bij dit onderzoek niet zoveel anders dan bij gewone zorg. De standaard DIEP borstreconstructie wordt uitgevoerd. Dat betekent dat de beoordeling van de doorbloeding tijdens de operatie op basis van het oordeel van de chirurg en door het gebruik van de fluorescente vloeistof zal zijn. Alleen de metingen met het LSCI apparaat zijn extra. Wel wordt hierdoor de operatietijd langer met ongeveer 20 tot 30 minuten. Mocht het LSCI apparaat een ander oordeel over de doorbloeding aangeven dan blijkt op basis van het oordeel van de chirurg en de fluorescente vloeistof, zal het oordeel van de chirurg en de fluorescente vloeistof altijd leidend zijn voor het uitvoeren van de DIEP borstreconstructie.

5. Welke afspraken maken we met u?

We willen graag dat het onderzoek goed verloopt. Daarom maken we de volgende afspraken met u:

- U doet tijdens dit onderzoek niet ook nog mee aan een ander medisch-wetenschappelijk onderzoek.
- U komt naar iedere afspraak.
- U neemt contact op met de onderzoeker in deze situaties:
 - U wilt andere medicijnen gaan gebruiken. Ook als dit homeopathische middelen zijn, natuurgeneesmiddelen, vitaminen of geneesmiddelen van de drogist.
 - U wordt in een ziekenhuis opgenomen of behandeld voor iets anders.
 - U krijgt plotseling problemen met uw gezondheid.
 - U wilt niet meer meedoen met het onderzoek.
 - Uw telefoonnummer, adres of e-mailadres verandert.

6. Van welke bijwerkingen, nadelige effecten of ongemakken kunt u last krijgen?

Bij het scannen van de huid met het LSCI apparaat wordt het apparaat boven de huid gehouden. Met behulp van laserlicht brengt het apparaat kleine bloedvaatjes in beeld. Dat is niet schadelijk voor de huid en u zult hier geen hinder van ondervinden.

7. Wat zijn de voordelen en de nadelen als u meedoet aan het onderzoek?

Meedoen aan het onderzoek kan voordelen en nadelen hebben. Hieronder zetten we ze op een rij. Denk hier goed over na, en praat erover met anderen.

Mogelijke voordelen van deelname aan dit onderzoek

U heeft zelf geen voordeel van meedoen aan dit onderzoek. Maar met uw deelname helpt u de onderzoekers meer inzicht te krijgen in de eventuele toegevoegde waarde van het LSCI apparaat om het aantal complicaties na DIEP borstreconstructie te verminderen.

Mogelijke nadelen van deelname aan dit onderzoek

Doordat de LSCI metingen tijdens de operatie plaatsvinden, zal de operatietijd met ongeveer 20 tot 30 minuten worden verlengd. Daarnaast kost de vijfde meting met het LSCI apparaat de dag na de

operatie enkele minuten van uw tijd. Verder ondervindt u van deelname aan dit onderzoek geen nadelen.

Wilt u niet meedoen?

U beslist zelf of u meedoet aan het onderzoek. Deelname is geheel vrijwillig. Als u besluit om niet mee te doen, hoeft u verder niets te doen. U hoeft niets te tekenen. U hoeft ook niet te zeggen waarom u niet wilt meedoen.

8. Wanneer stopt het onderzoek?

De onderzoeker laat het u weten als er nieuwe informatie over het onderzoek komt die belangrijk voor u is. De onderzoeker vraagt u daarna of u blijft meedoen.

In deze situaties stopt voor u het onderzoek:

- Alle onderzoeken volgens het schema zijn voorbij.
- U wilt zelf stoppen met het onderzoek. Dat mag op ieder moment. Meld dit dan meteen bij de onderzoeker. U hoeft er niet bij te vertellen waarom u stopt. U zult dan de reguliere DIEP borstreconstructie ondergaan zonder LSCI metingen.
- De onderzoeker vindt het beter voor u om te stoppen.
- Een van de volgende instanties besluit dat het onderzoek moet stoppen:
 - afdeling plastische chirurgie van het ZGT
 - de overheid, of
 - de medisch-ethische commissie die het onderzoek beoordeelt.

Wat gebeurt er als u stopt met het onderzoek?

De onderzoekers gebruiken de gegevens die tot het moment van stoppen zijn verzameld.

9. Wat gebeurt er na het onderzoek?

Krijgt u de resultaten van het onderzoek?

Ongeveer een half jaar na uw deelname laat de onderzoeker u weten wat de belangrijkste uitkomsten zijn van het onderzoek.

10. Wat doen we met uw gegevens?

Doet u mee met het onderzoek? Dan geeft u ook toestemming om uw gegevens te gebruiken en te bewaren.

Welke gegevens bewaren we?

We bewaren deze gegevens:

- uw naam
- uw geslacht
- uw adres

- uw geboortedatum
- gegevens over uw gezondheid
- (medische) gegevens die we tijdens het onderzoek verzamelen

Waarom verzamelen, gebruiken en bewaren we uw gegevens?

We verzamelen, gebruiken en bewaren uw gegevens om de vragen van dit onderzoek te kunnen beantwoorden. En om de resultaten te kunnen publiceren.

Hoe beschermen we uw privacy?

Om uw privacy te beschermen geven wij uw gegevens een code. Op al uw gegevens zetten we alleen deze code. De sleutel van de code bewaren we op een beveiligde plek in het ziekenhuis. Als we uw gegevens verwerken, gebruiken we steeds alleen die code. Ook in rapporten en publicaties over het onderzoek kan niemand terughalen dat het over u ging.

Wie kunnen uw gegevens zien?

Sommige personen kunnen wel uw naam en andere persoonlijke gegevens zonder code inzien. Dit zijn mensen die controleren of de onderzoekers het onderzoek goed en betrouwbaar uitvoeren. Deze personen kunnen bij uw gegevens komen:

- Leden van de commissie die de veiligheid van het onderzoek in de gaten houdt.
- Een controleur die voor het ZGT werkt.
- Nationale en internationale toezichthoudende autoriteiten. Bijvoorbeeld de Inspectie Gezondheidszorg en Jeugd.

Deze personen houden uw gegevens geheim. Wij vragen u voor deze inzage toestemming te geven.

Hoelang bewaren we uw gegevens?

We bewaren uw gegevens 15 jaar in het ziekenhuis.

Mogen we uw gegevens gebruiken voor ander onderzoek?

Uw gegevens kunnen na afloop van dit onderzoek ook nog van belang zijn voor ander wetenschappelijk onderzoek op het gebied van doorbloeding tijdens en na een DIEP borstreconstructie. Daarvoor zullen uw gegevens 15 jaar worden bewaard in het ziekenhuis. In het toestemmingformulier geeft u aan of u dit goed vindt. Geeft u geen toestemming? Dan kunt u nog steeds meedoen met dit onderzoek. U krijgt dezelfde zorg.

Kunt u uw toestemming voor het gebruik van uw gegevens weer intrekken?

U kunt uw toestemming voor het gebruik van uw gegevens op ieder moment intrekken. Maar let op: trekt u uw toestemming in, en hebben onderzoekers dan al gegevens verzameld voor een onderzoek? Dan mogen zij deze gegevens nog wel gebruiken.

Wilt u meer weten over uw privacy?

- Wilt u meer weten over uw rechten bij de verwerking van persoonsgegevens? Kijk dan op www.autoriteitpersoonsgegevens.nl.
- Heeft u vragen over uw rechten? Of heeft u een klacht over de verwerking van uw persoonsgegevens? Neem dan contact op met degene die verantwoordelijk is voor de verwerking van uw persoonsgegevens. Voor uw onderzoek is dat:
 - Ziekenhuis ZGT. Zie bijlage A voor contactgegevens, en website.
- Als u klachten heeft over de verwerking van uw persoonsgegevens, raden we u aan om deze eerst te bespreken met het onderzoeksteam. U kunt ook naar de Functionaris Gegevensbescherming van ZGT gaan. Of u dient een klacht in bij de Autoriteit Persoonsgegevens.

11. Krijgt u een vergoeding als u meedoet aan het onderzoek?

De extra LSCI metingen voor het onderzoek kosten u niets. U krijgt ook geen vergoeding als u meedoet aan dit onderzoek. Wel krijgt u een vergoeding als u extra reiskosten maakt.

12. Bent u verzekerd tijdens het onderzoek?

U bent niet extra verzekerd door dit onderzoek. Want meedoen aan dit onderzoek heeft geen extra risico's. Daarom hoeft de afdeling plastische chirurgie van de medisch-ethische toetsingscommissie geen extra verzekering af te sluiten.

13. Heeft u vragen?

Vragen over het onderzoek kunt u stellen aan dr. H.A. Rakhorst (plastisch chirurg), dr. D.J. Evers (chirurg) of S.E.M. Teunissen (technisch geneeskundige in opleiding). Wilt u advies van iemand die er geen belang bij heeft? Ga dan naar drs. G.M. van Couwelaar (plastisch chirurg). Hij weet veel over het onderzoek, maar werkt niet mee aan dit onderzoek.

Heeft u een klacht? Bespreek dit dan met de onderzoeker of de arts die u behandelt. Wilt u dit liever niet? Ga dan naar klachtenbemiddeling van het ZGT. In bijlage A staan alle contactgegevens.

14. Hoe geeft u toestemming voor het onderzoek?

U kunt eerst rustig nadenken over dit onderzoek. Daarna vertelt u de onderzoeker of u de informatie begrijpt en of u wel of niet wilt meedoen. Wilt u meedoen? Dan vult u het toestemmingsformulier in dat u bij deze informatiebrief vindt. U en de onderzoeker krijgen allebei een getekende versie van deze toestemmingsverklaring.

Dank voor uw tijd.

15. Bijlagen bij deze informatie

- A. Contactgegevens
- B. Toestemmingsformulier

Bijlage A: Contactgegevens

Hoofdonderzoekers
Dr. H.A. Rakhorst, plastisch chirurg Mailadres: h.rakhorst@zgt.nl Telefoonnummer: 088 708 52 45
Dr. D.J. Evers, chirurg Mailadres: d.evers@zgt.nl Telefoonnummer: 088 708 52 43
S.E.M. Teunissen BSc., Technisch Geneeskundige in opleiding Mailadres: s.teunissen@zgt.nl
Onderzoekskoördinator
Ing. T. Knop Mailadres: t.knop@utwente.nl
Onafhankelijke deskundige
G.M. van Couwelaar MSc., plastisch chirurg Mailadres: g.vcouwelaar@zgt.nl Telefoonnummer: 088 708 52 45
Klachten
U kunt uw onvrede of klacht digitaal, telefonisch of op papier indienen bij de klachtenbemiddelaar. Daarnaast is het mogelijk een afspraak met de klachtenbemiddelaar te maken voor een persoonlijk gesprek. Postadres: ZGT, t.a.v. Klachtenbemiddeling Postbus 7600 7600 SZ Almelo Telefoonnummer: 088 708 57 83 Mailadres: klachten@zgt.nl
Functionaris voor de Gegevensbescherming van de instelling
Functionaris Gegevensbescherming, t.a.v. mw. E.A. Jolink of dhr. A.S. Hashemi (FG i.o.) Postbus 546 7550 AM Hengelo Mailadres: gegevensbescherming@zgt.nl
Voor meer informatie over uw rechten
Functionaris Gegevensbescherming, t.a.v. mw. E.A. Jolink of dhr. A.S. Hashemi (FG i.o.) Postbus 546 7550 AM Hengelo Mailadres: gegevensbescherming@zgt.nl Website: www.zgt.nl/zgt-privacyverklaring-website/

Bijlage B: toestemmingsformulier proefpersoon

Behorende bij: Vergroten van het inzicht in het ontstaan van complicaties en het voorspellen van complicaties na een DIEP flap borstreconstructie door het scannen van de oppervlakkige bloedvaten in de huid.

- Ik heb de informatiebrief gelezen. Ook kon ik vragen stellen. Mijn vragen zijn goed genoeg beantwoord. Ik had genoeg tijd om te beslissen of ik meedoe.
- Ik weet dat meedoen vrijwillig is. Ook weet ik dat ik op ieder moment kan beslissen om toch niet mee te doen met het onderzoek. Of om ermee te stoppen. Ik hoef dan niet te zeggen waarom ik wil stoppen.
- Ik geef de onderzoekers toestemming om mijn gegevens te verzamelen en gebruiken. De onderzoekers doen dit alleen om de onderzoeksvraag van dit onderzoek te beantwoorden.
- Ik weet dat voor de controle van het onderzoek sommige mensen al mijn gegevens kunnen inzien. Die mensen staan in deze informatiebrief. Ik geef deze mensen toestemming om mijn gegevens in te zien voor deze controle.
- Ik geef toestemming om mijn gegevens te bewaren om dit te gebruiken voor ander onderzoek, zoals in de informatiebrief staat
 - Ja
 - Nee
- Ik geef toestemming om mij eventueel na dit onderzoek te vragen of ik wil meedoen met een vervolgonderzoek
 - Ja
 - Nee
- Ik wil meedoen aan dit onderzoek.

Mijn naam is (proefpersoon):

Handtekening:

Datum : __ / __ / __

Ik verklaar dat ik deze proefpersoon volledig heb geïnformeerd over het genoemde onderzoek.

Wordt er tijdens het onderzoek informatie bekend die de toestemming van de proefpersoon kan beïnvloeden? Dan laat ik dit op tijd weten aan deze proefpersoon.

Naam onderzoeker (of diens vertegenwoordiger):.....

Handtekening:.....

Datum: __ / __ / __

6.9 Appendix I: User Experience Questionnaire

For the assessment of the product, please fill out the following questionnaire. The questionnaire consists of pairs of contrasting attributes that may apply to the product. The circles between the attributes represent gradation between the opposites. You can express your agreement with the attributes by ticking the circle that most closely reflects your impression.

Example:

Attractive	<input type="radio"/>	<input checked="" type="radio"/>	<input type="radio"/>	<input type="radio"/>	<input type="radio"/>	<input type="radio"/>	<input type="radio"/>	Unattractive
------------	-----------------------	----------------------------------	-----------------------	-----------------------	-----------------------	-----------------------	-----------------------	--------------

This response would mean that you rate the application as more attractive than unattractive.

Please decide spontaneously. Do not think too long about your decision to make sure that you convey your original impression.

Sometimes you may not be completely sure about your agreement with a particular attribute or you may find that the attribute does not apply completely to the particular product. Nevertheless, please tick a circle in every line.

It is your personal opinion that counts. Please remember: there is no wrong or right answer.

1	Annoying	<input type="radio"/>	<input type="radio"/>	<input type="radio"/>	<input type="radio"/>	<input type="radio"/>	<input type="radio"/>	Enjoyable
2	Not understandable	<input type="radio"/>	<input type="radio"/>	<input type="radio"/>	<input type="radio"/>	<input type="radio"/>	<input type="radio"/>	Understandable
3	Creative	<input type="radio"/>	<input type="radio"/>	<input type="radio"/>	<input type="radio"/>	<input type="radio"/>	<input type="radio"/>	Dull
4	Easy to learn	<input type="radio"/>	<input type="radio"/>	<input type="radio"/>	<input type="radio"/>	<input type="radio"/>	<input type="radio"/>	Difficult to learn
5	Valuable	<input type="radio"/>	<input type="radio"/>	<input type="radio"/>	<input type="radio"/>	<input type="radio"/>	<input type="radio"/>	Inferior
6	Boring	<input type="radio"/>	<input type="radio"/>	<input type="radio"/>	<input type="radio"/>	<input type="radio"/>	<input type="radio"/>	Exciting
7	Not interesting	<input type="radio"/>	<input type="radio"/>	<input type="radio"/>	<input type="radio"/>	<input type="radio"/>	<input type="radio"/>	Interesting
8	Unpredictable	<input type="radio"/>	<input type="radio"/>	<input type="radio"/>	<input type="radio"/>	<input type="radio"/>	<input type="radio"/>	Predictable
9	Fast	<input type="radio"/>	<input type="radio"/>	<input type="radio"/>	<input type="radio"/>	<input type="radio"/>	<input type="radio"/>	Slow
10	Inventive	<input type="radio"/>	<input type="radio"/>	<input type="radio"/>	<input type="radio"/>	<input type="radio"/>	<input type="radio"/>	Conventional
11	Obstructive	<input type="radio"/>	<input type="radio"/>	<input type="radio"/>	<input type="radio"/>	<input type="radio"/>	<input type="radio"/>	Supportive
12	Good	<input type="radio"/>	<input type="radio"/>	<input type="radio"/>	<input type="radio"/>	<input type="radio"/>	<input type="radio"/>	Bad
13	Complicated	<input type="radio"/>	<input type="radio"/>	<input type="radio"/>	<input type="radio"/>	<input type="radio"/>	<input type="radio"/>	Easy
14	Unlikable	<input type="radio"/>	<input type="radio"/>	<input type="radio"/>	<input type="radio"/>	<input type="radio"/>	<input type="radio"/>	Pleasing
15	Usual	<input type="radio"/>	<input type="radio"/>	<input type="radio"/>	<input type="radio"/>	<input type="radio"/>	<input type="radio"/>	Leading edge
16	Unpleasant	<input type="radio"/>	<input type="radio"/>	<input type="radio"/>	<input type="radio"/>	<input type="radio"/>	<input type="radio"/>	Pleasant
17	Secure	<input type="radio"/>	<input type="radio"/>	<input type="radio"/>	<input type="radio"/>	<input type="radio"/>	<input type="radio"/>	Not secure
18	Motivating	<input type="radio"/>	<input type="radio"/>	<input type="radio"/>	<input type="radio"/>	<input type="radio"/>	<input type="radio"/>	Demotivating
19	Meets expectations	<input type="radio"/>	<input type="radio"/>	<input type="radio"/>	<input type="radio"/>	<input type="radio"/>	<input type="radio"/>	Does not meet expectations
20	Inefficient	<input type="radio"/>	<input type="radio"/>	<input type="radio"/>	<input type="radio"/>	<input type="radio"/>	<input type="radio"/>	Efficient
21	Clear	<input type="radio"/>	<input type="radio"/>	<input type="radio"/>	<input type="radio"/>	<input type="radio"/>	<input type="radio"/>	Confusing
22	Impractical	<input type="radio"/>	<input type="radio"/>	<input type="radio"/>	<input type="radio"/>	<input type="radio"/>	<input type="radio"/>	Practical
23	Organised	<input type="radio"/>	<input type="radio"/>	<input type="radio"/>	<input type="radio"/>	<input type="radio"/>	<input type="radio"/>	Cluttered
24	Attractive	<input type="radio"/>	<input type="radio"/>	<input type="radio"/>	<input type="radio"/>	<input type="radio"/>	<input type="radio"/>	Unattractive
25	Friendly	<input type="radio"/>	<input type="radio"/>	<input type="radio"/>	<input type="radio"/>	<input type="radio"/>	<input type="radio"/>	Unfriendly
26	Conservative	<input type="radio"/>	<input type="radio"/>	<input type="radio"/>	<input type="radio"/>	<input type="radio"/>	<input type="radio"/>	Innovative

6.10 Appendix J: Research protocol

The research protocol approved by the MREC is attached on the next pages.

NL80104.100.22 / Wireless LSCI device during DIEP flap breast reconstruction

RESEARCH PROTOCOL

Wireless Laser Speckle Contrast Imaging Device for the visualisation of the microcirculatory during DIEP flap breast reconstruction

Dossiernummer: NL80104.100.22

NL80104.100.22 / Wireless LSCI device during DIEP flap breast reconstruction

PROTOCOL TITLE: Wireless Laser Speckle Contrast Imaging for the visualisation of the microcirculatory during DIEP flap breast reconstruction.

Protocol ID	NL80104.100.22
Short title	Wireless LSCI device during DIEP flap breast reconstruction
EudraCT number	Not applicable
Version	2.0
Date	4 May 2022
Coordinating investigator/project leader	Ing. T. Knop University of Twente Faculty of Science and Technology Horst Complex ZH273 P.O. Box 217, 7500 AE Enschede The Netherlands E-mail: t.knop@utwente.nl
Principal investigators (in Dutch: hoofdonderzoeker/ uitvoerder)	Dr. H.A. Rakhorst (plastic surgeon) Department of Plastic Surgery Ziekenhuisgroep Twente P.O. Box 546, 7550 AM Hengelo The Netherlands E-mail: h.rakhorst@zgt.nl Phone: + 31 88 708 52 45 Dr. D.J. Evers (surgeon) Department of Surgery Ziekenhuisgroep Twente P.O. Box 546, 7550 AM Hengelo The Netherlands E-mail: d.evers@zgt.nl Phone: +31 88 708 52 43 S.E.M. Teunissen, BSc (Technical Physician in training) Department of plastic surgery Ziekenhuisgroep Twente P.O. Box 546, 7550 AM Hengelo The Netherlands E-mail: s.teunissen@zgt.nl
Technical staff	Ing. T. Knop Dr. A. Chizari

NL80104.100.22 / Wireless LSCI device during DIEP flap breast reconstruction

	University of Twente Faculty of Science and Technology Horst Complex ZH264 P.O. Box 217, 7500 AE Enschede The Netherlands E-mail: a.chizari@utwente.nl
Sponsor (in Dutch: verrichter/opdrachtgever)	University of Twente
Subsidising party	Not applicable.
Independent expert (s)	G.M. van Couwelaar, MSc. Department of plastic surgery Ziekenhuisgroep Twente P.O. Box 546, 7550 AM Hengelo The Netherlands E-mail: g.vcouwelaar@zgt.nl
Laboratory sites	Not applicable.
Pharmacy	Not applicable.

PROTOCOL SIGNATURE SHEET




Name	Signature	Date
Sponsor or legal representative: Prof. dr. ir. W. Steenbergen University of Twente Faculty of Science and Technology Horst Complex ZH263 P.O. Box 217, 7500 EA Enschede The Netherlands E-mail: w.steenbergen@utwente.nl Phone: +31534893160		15-02-2022
Coordinating Investigator: Ing. T. Knop		15-02-2022
Principal Investigator: Dr. H.A. Rakhorst		01-03-2022

TABLE OF CONTENTS

1.	INTRODUCTION AND RATIONALE	9
1.1	Breast cancer and breast reconstructions	9
1.2	Current assessment of the microcirculation during DIEP flap breast reconstruction	9
1.3	Laser Speckle Contrast Imaging	10
1.4	Results from previous LSCI studies	10
1.5	Study rationale	11
2.	OBJECTIVES	11
3.	STUDY DESIGN	12
4.	STUDY POPULATION	14
4.1	Population (base)	14
4.2	Inclusion criteria	14
4.3	Exclusion criteria	14
4.4	Sample size calculation	14
5.	TREATMENT OF SUBJECTS	14
5.1	Investigational product/treatment	15
5.2	Use of co-intervention	15
5.3	Escape medication	15
6.	INVESTIGATIONAL PRODUCT	15
6.1	Name and description of investigational product(s)	15
6.2	Summary of findings from non-clinical studies	15
6.3	Summary of findings from clinical studies	15
6.4	Summary of known and potential risks and benefits	15
6.5	Description and justification of route of administration and dosage	15
6.6	Dosages, dosage modifications and method of administration	15
6.7	Preparation and labelling of Investigational Medicinal Product	15
6.8	Drug accountability	15
7.	NON-INVESTIGATIONAL PRODUCT	15
7.1	Name and description of non-investigational product	15
7.2	Summary of findings from non-clinical studies	16
7.3	Summary of findings from clinical studies	16
7.4	Summary of known and potential risks and benefits	16
7.5	Description and justification of route of administration and dosage	16
7.6	Dosages, dosage modifications and method of administration	16
7.7	Preparation and labelling of Non Investigational Medicinal Product	16
7.8	Drug accountability	16
8.	METHODS	16
8.1	Study parameters/endpoints	16
8.1.1	Main study parameter/endpoint	16
8.1.2	Secondary study parameters/endpoints (if applicable)	16
8.1.3	Other study parameters (if applicable)	17
8.2	Randomisation, blinding and treatment allocation	17

NL80104.100.22 / Wireless LSCI device during DIEP flap breast reconstruction

8.3	Study procedures	17
8.4	Withdrawal of individual subjects	17
8.4.1	Specific criteria for withdrawal	17
8.5	Replacement of individual subjects after withdrawal	17
8.6	Follow-up of subjects withdrawn from treatment	18
8.7	Premature termination of the study	18
9.	SAFETY REPORTING	18
9.1	Temporary halt for reasons of subject safety	18
9.2	AEs, SAEs and SUSARs	18
9.2.1	Adverse events (AEs)	18
9.2.2	Serious adverse events (SAEs)	18
9.2.3	Suspected unexpected serious adverse reactions (SUSARs)	19
9.3	Annual safety report	19
9.4	Follow-up of adverse events	19
9.5	Data Safety Monitoring Board (DSMB) / Safety Committee	19
10.	STATISTICAL ANALYSIS	19
10.1	Primary study parameter(s)	19
10.2	Secondary study parameter(s)	19
10.3	Other study parameters	19
10.4	Interim analysis	20
11.	ETHICAL CONSIDERATIONS	20
11.1	Regulation statement	20
11.2	Recruitment and consent	20
11.3	Objection by minors or incapacitated subjects	20
11.4	Benefits and risks assessment, group relatedness	20
11.5	Compensation for injury	20
11.6	Incentives	21
12.	ADMINISTRATIVE ASPECTS, MONITORING AND PUBLICATION	21
12.1	Handling and storage of data and documents	21
12.2	Monitoring and Quality Assurance	21
12.3	Amendments	21
12.4	Annual progress report	21
12.5	Temporary halt and (prematurely) end of study report	21
12.6	Public disclosure and publication policy	22
13.	STRUCTURED RISK ANALYSIS	22
13.1	Potential issues of concern	22
13.2	Synthesis	23
14.	REFERENCES	23

LIST OF ABBREVIATIONS AND RELEVANT DEFINITIONS

AE	Adverse Event
CCMO	Central Committee on Research Involving Human Subjects; in Dutch: Centrale Commissie Mensgebonden Onderzoek
DIEP	Deep Inferior Epigastric Perforator
DSMB	Data Safety Monitoring Board
EU	European Union
EudraCT	European drug regulatory affairs Clinical Trials
GDPR	General Data Protection Regulation; in Dutch: Algemene Verordening Gegevensbescherming (AVG)
IB	Investigator's Brochure
IC	Informed Consent
ICG	Indocyanine Green (Contrast agent)
IMP	Investigational Medicinal Product
IMPD	Investigational Medicinal Product Dossier
LSCI	Laser Speckle Contrast Imaging
METC	Medical research ethics committee (MREC); in Dutch: medisch-ethische toetsingscommissie (METC)
PU	Perfusion Units
(S)AE	(Serious) Adverse Event
SPC	Summary of Product Characteristics; in Dutch: officiële productinformatie IB1-tekst
Sponsor	The sponsor is the party that commissions the organisation or performance of the research, for example a pharmaceutical company, academic hospital, scientific organisation or investigator. A party that provides funding for a study but does not commission it is not regarded as the sponsor, but referred to as a subsidising party.
SUSAR	Suspected Unexpected Serious Adverse Reaction
UAVG	Dutch Act on Implementation of the General Data Protection Regulation; in Dutch: Uitvoeringswet AVG
WIPI	Wireless Perfusion Imager
WMO	Medical Research Involving Human Subjects Act; in Dutch: Wet Medisch-wetenschappelijk Onderzoek met Mensen
ZGT	Ziekenhuisgroep Twente

SUMMARY

Rationale: Perfusion-related complications are reported to occur in 7%-35% of the patients that have a Deep Inferior Epigastric Perforator (DIEP) flap breast reconstruction. Currently, the microcirculation is intraoperatively assessed with the use of Indocyanine green (ICG) angiography and by the surgeon's intraoperative evaluation. However, these methods have some disadvantages. A promising technique that could overcome these disadvantages is Laser Speckle Contrast Imaging (LSCI). This study aims to demonstrate that the newly designed LSCI device, the Wireless Perfusion Imager (WIPI), is able to visualise the microcirculation of the abdominal flap and the newly reconstructed breast during DIEP flap breast reconstruction. The WIPI could be used in the future as a non-invasive method to predict the development of perfusion-related complications.

Objective: The primary objective is to determine if there are any differences in mean perfusion of the newly reconstructed breast during DIEP flap breast reconstruction between patients that develop perfusion-related complications and patients that do not develop perfusion-related complications. Secondary objectives include the visualisation of the abdominal flap and newly reconstructed breast during and after DIEP flap breast reconstruction with the use of the WIPI (i), the establishment of a method to create robustness against motion artefacts (ii) and the development of a wireless system that can operate reliably and preview perfusion frames with a relatively fast rate (iii).

Study design: This is a prospective case series study of the multidisciplinary breast cancer treatment centre in Ziekenhuisgroep Twente (ZGT) hospital.

Study population: Fifteen (former) breast cancer patients that will undergo a DIEP flap breast reconstruction (either immediate or delayed) will be included.

Main study parameters/endpoints: The main study parameter is the mean perfusion (in PU) of the newly reconstructed breast in correlation with the development of perfusion-related complications.

Nature and extent of the burden and risks associated with participation, benefit and group relatedness: There are no immediate benefits for patients participating in this study, but this study could unravel new methods to visualise the microcirculation during DIEP flap breast reconstruction and for the potential prevention of perfusion-related complications afterwards. Given the non-invasive nature of the WIPI, we estimate the study risks as negligible. Scanning the skin with the use of the WIPI is painless and without any discomfort.

1. INTRODUCTION AND RATIONALE

1.1 Breast cancer and breast reconstructions

Breast cancer is responsible for 26% of all malignancies in the Netherlands and is therefore the most frequently diagnosed malignancy among Dutch females¹. As the 10-year survival rate has significantly increased in the last decades due to improved treatments, surgical decisions regarding the improvement of the quality of life have become more important²⁻⁴. One of the treatments which is related to a good quality of life is skin-sparing mastectomy followed by breast reconstruction⁵. Breast reconstructions can be performed with autologous tissue or with breast implants^{5,6}. Autologous breast reconstructions are superior to implants regarding the aesthetic outcome, long-term satisfaction and quality of life⁷. Moreover, autologous breast reconstructions are recommended in case the remaining breast tissue is of bad quality due to, for example, radiotherapy⁸. The standard for autologous breast reconstruction is the Deep Inferior Epigastric Perforator (DIEP) flap reconstruction, referring to the feeding artery⁶. During this reconstruction, abdominal fat and skin, which are fed by the aforementioned perforator, are dissected⁹. Subsequently, the DIEP flap is reconnected to the internal mammary artery¹⁰.

Fortunately, most patients have a postoperative recovery without any severe complications. However, perfusion-related complications, such as wound healing delay or necrosis, are reported to occur in 7%-35% of the patients^{7,11-14}. Necrosis could develop in the skin envelope, in the fatty tissue or in the skin of the transplanted flap. Perfusion-related complications could occur when the transplanted flap is too large or as a result of thrombosis in the flap or the pedicle. It is important to reduce these complications to an absolute minimum as these complications cause a decrease in the patient's satisfaction and quality of life⁵. Moreover, necessary revision surgeries lead to the increase of costs, hospital stay and can lead to serious stress for the surgeon⁶.

1.2 Current assessment of the microcirculation during DIEP flap breast reconstruction

Currently, the microcirculation is intraoperatively assessed by the surgeon by evaluating the skin colour and temperature, capillary refill time and dermal edge bleeding^{8,15}. However, these methods depend on the surgeon's experience and subjective opinion, resulting in potential intra- and inter-observer variabilities¹⁶. For a more objective assessment, indocyanine green (ICG) angiography can be applied for additional evaluation of the perfusion of the DIEP flap¹⁷. ICG can give a real-time prediction of the perfusion of tissue that is going to be transplanted and to make an assessment of the perfusion of the newly reconstructed breast. The assessment of the perfusion with the use of ICG is based on the area that becomes green on the angiogram and its intensity level. The intensity level corresponds to the amount of ICG and therefore to the amount of blood that perfuses the tissue. The application of ICG has resulted in a decrease in perfusion-related complications¹⁸. Therefore, nowadays in Ziekenhuisgroep Twente (ZGT), the current assessment of the microcirculatory consists of the combination of the application of ICG and the subjective assessment of the surgeon.

Nevertheless, ICG has some disadvantages^{19,20}. First, it requires the administration of a contrast agent. Due to the washout of 20 minutes and a half-life time of 150 to 180 seconds, it takes several minutes after inflow to visualise the outflow of ICG out of the arterial and venous system^{20,21}. This means that the intensity signal gradually decreases over time after ICG administration. However, changes in perfusion after the inflow of ICG due to for example vasospasm or thrombosis can hardly be visualised as the ICG is already present in the vascular system. Thus, it is hard to detect an occlusion that is caused by vasospasms or thrombosis just after the inflow of ICG. Another disadvantage is that the assessment of the fluorescence intensity does not have a cut-off value (yet) for under-perfused tissue, which makes the assessment subjective¹⁹. Finally, as ICG is a contrast agent that has often to be administered multiple times during surgery, adverse reactions can occur. However, these are rare and are reported to develop in 0.2% of the exposed patients²².

1.3 Laser Speckle Contrast Imaging

A promising technique that could overcome the aforementioned disadvantages of ICG is Laser Speckle Contrast Imaging (LSCI). LSCI is a real-time and non-contact imaging technique for perfusion measurements. It does not need any contrast agents, the measurements could take place at any convenient time and the measurements only take a few seconds^{15,23}. The principle of LSCI is that it uses backscattered light from tissue that is illuminated with coherent laser light to create a random interference pattern. This is also known as the speckle pattern²⁴. Moving particles in tissue, for example red blood cells, cause fluctuations in this speckle pattern, which results in blurring speckles²⁴. The degree of blurring can be correlated to the blood flow, and so to perfusion. With the use of this technique, perfusion at a depth of about 300 µm can be visualised. In the skin, this corresponds to dermal microcirculation^{8,25}.

1.4 Results from previous LSCI studies

In several studies, LSCI is already evaluated and considered as a promising technique for perioperative assessment of the microcirculation in colorectal surgery, cerebrovascular surgery and reconstructive surgery^{8,15,16,23,26,27}. The results in reconstructive surgery are of particular interest to this study. Zötterman et al. performed multiple studies regarding the assessment of perfusion in reconstructive surgery, of which a cut-off value was lacking for under-perfused tissue^{8,16,23}. First, their aim was to investigate whether LSCI could be perioperatively applied to identify areas with compromised circulation and thereby to predict areas that have a high risk of developing postoperative necrosis²³. They concluded that perfusion below 25 Perfusion Units (PU, arbitrary unit) was a predictor for tissue morbidity within 72 hours after surgery in porcine flap models. Consecutive research started on the perfusion distribution and perfusion-related postoperative complications during DIEP flap breast reconstruction^{8,23}. That study also showed a cut-off value for tissue morbidity, but this was a cut-off value of 30 PU for postoperative flap necrosis.

However, a limitation of these studies was the use of mounted LSCI devices. Due to the inflexibility of these devices, it is complicated to use them in the operating theatre. Therefore, the Biomedical Photonic Imaging group of the University of Twente is developing

a handheld and wireless system. The previous version of this LSCI system, known as handheld perfusion imager (HAPI), was applied in the research to psoriasis lesions (NL69174.091.19) and this showed that handheld measurements give similar visual results compared to mounted measurements²⁸. Even though a statistically significant difference was found between mounted and handheld measurements because of movement artefacts in handheld measurements, the handheld device is of additionally clinical value in terms of comfortability and flexibility for medical staff and patients. However, the HAPI system still had some disadvantages in terms of manual postprocessing to correct motion artefacts, which was time-consuming.

1.5 Study rationale

This study aims to demonstrate that the new generation of the HAPI, the Wireless Perfusion Imager (WIPI) is able to visualise the microcirculation of the abdominal flap and the newly reconstructed breast during DIEP flap breast reconstruction. The hypothesis is that the WIPI is able to detect poor skin perfusion and that the WIPI is able to demonstrate vasospasms and thromboses during surgery, which could be missed with the use of ICG. If the hypothesis holds true, the WIPI could serve as a non-invasive, real-time technique to identify poor skin perfusion and vasospasms or thromboses where the current method is not able to do so. This enables early detection of poor skin perfusion during surgery that might have resulted in postoperative necrosis, possibly caused by thromboses or a too large flap. However, as this is a proof of concept study, this study will be limited to the visualisation of the microcirculation and the eventual correlation between the perfusion and perfusion-related complications.

In conclusion, our vision is that the WIPI could be used in the future as a non-invasive technique to visualise poor skin perfusion and thereby minimise perfusion-related complications in an objective manner. The compactness and handheld nature of this technique are of particular interest with regard to the application in the operating theatre.

2. OBJECTIVES

Primary objective:

The correlation between the mean perfusion of the newly reconstructed breast during DIEP flap breast reconstruction and the development of perfusion-related complications.

Secondary Objectives:

- i. The visualisation of the perfusion of the abdominal flap and the newly reconstructed breast during and after DIEP flap breast reconstruction with the use of the WIPI.
- ii. Establish a method to create robustness against motion artefacts. To do so, a colour camera will be used to track the movement during a measurement and align the perfusion maps afterwards using imaging processing.
- iii. Develop a wireless system that can operate reliably and preview perfusion frames with a relatively fast rate.

3. STUDY DESIGN

Study design:

This is a prospective case series study and a proof of concept study of the multidisciplinary breast cancer treatment centre in ZGT. The aim is determine if there are any differences in mean perfusion of the newly reconstructed breast between two groups: patients that develop perfusion-related complications and patients that do not develop perfusion-related complications. The surgeon postoperatively determines whether perfusion-related complications did occur and its severeness. We will include 15 patients. We will include patients that will have a unilateral or a bilateral DIEP flap breast reconstruction. A bilateral DIEP flap breast reconstruction will be described as two cases. We assume the perfusion in the chosen flaps differ enough from each other to make two separate cases; the chosen artery and vein for both flaps will be different in length and diameter. Moreover, the flaps will not have the exact same size and weight.

Duration of the study:

Patients enrolled in this study will be followed for two days. Measurements take place during DIEP flap breast reconstruction and the day after surgery (Table 1). Prior to participating in this study, patients have to meet inclusion criteria and must be willing to give written informed consent. There are no pre-established exclusion criteria to participate in this study.

Settings:

Prior to each measurement, real-time perfusion maps (existing of speckle images) and colour images will be previewed on the screen of the WIPI by pushing a button during surgery. A technical physician (in training) will perform the measurements with the WIPI. The previews make it easier for the technical physician to check which area of the skin will be scanned at the current position and if this is according to plan. To make sure the surgeon will not be influenced by the perfusion maps made with the WIPI, the perfusion maps will only be visualised at the screen of the WIPI itself and the laptop in the corner of the operating room. The perfusion maps will not be sent to an external monitor. The surgeon is not allowed to look at the perfusion maps at the WIPI or at the laptop during surgery.

After previewing, the actual measurement can start. Some of the measurements consists of three scanning moments. During each scanning moment, multiple colour images and speckle images will be obtained. The front side of the WIPI will be held at a distance of 30 cm of the skin as this is the focus distance of the colour camera. Each scanning moment takes five seconds, after which the data have to be saved and have to be send to a laptop to visualise the perfusion maps. Saving the data takes 40 to 60 seconds and data transfer takes 20 to 30 seconds, depending on the exact duration of the measurement. The collected data (colour images and speckle images) will immediately be processed. The results of each measurement for further evaluation will be a colour image and an averaged and aligned perfusion map. These two images will be shown on the screen of the laptop. Still, the surgeon is not allowed to already look at the results during surgery. The measurement protocol will be applied to each patient and consists of the following five measurements:

1. Baseline measurement: After anaesthesia, but before the first incision, the baseline measurement will be performed to get an idea of the perfusion distribution of the entire flap. As the field of view of the WIPI has a diameter of about 14 cm, three measurements will be performed to cover the entire DIEP flap. This is schematically visualised in Figure 1.

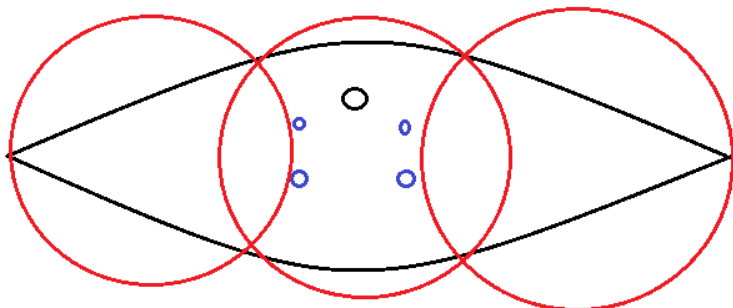


Figure 1 Schematic representation of the baseline measurement. The DIEP flap is visualised including the belly button (black circle). The blue circles are examples of perforators, which are located in depth. The red circles are examples of the field of view of the WIPI.

2. Raised flap: After the surgeon raised the flap and found the predefined perforators, (s)he makes the decision which perforator is going to be transplanted based on ICG angiography and her/his own evaluation. All other perforators are clamped or cut through. Then, the second LSCI measurement can take place, which will also be divided into three scanning moments according to Figure 1. This LSCI measurement forms the reference for the LSCI measurement after breast reconstruction. It shows what area of tissue the chosen perforator perfuses and what it should approximately be after reconstruction.

3. Ischemia: After the second LSCI measurement is performed, the blood flow through the chosen perforator can be stopped using a removable vascular clip, which results in ischemia. Vascular clips are often used during different types of surgery for different reasons to temporarily stop the blood flow. By removing the clip, the blood flow will be restored without any complications. After one minute of ischemia, the third LSCI measurement will be performed, again divided into three scanning moments. This measurement simulates bad perfusion of the DIEP flap and could therefore be used as a reference for bad perfusion in the upcoming measurements. When this third measurement is completed, the vascular clip can be removed and the perfusion will be restored. Then, the perforator can be cut through to continue the surgery. This way, this measurement does not increase the time of ischemia.

4. Anastomosis: When anastomosis is accomplished, the surgeon validates whether the perfusion is good enough with the use of ICG angiography and based on capillary refill etc. After validation, the fourth LSCI measurement DIEP can be performed. This measurement will be performed to correlate the mean perfusion (in PU) of the newly reconstructed breast to the outcome of the surgery. The outcome is the occurrence or absence of perfusion-related complications. One scanning moment is enough as the new breast can be scanned in the field of view with a diameter of 14 cm. In case the perfusion was sufficient during this LSCI measurement, but suddenly after this measurement, the surgeon does not trust it anymore,

the surgeon can do additional surgical actions to restore the perfusion. An additional LSCI measurement will then be performed.

5. Postoperative: One day after surgery, the last LSCI measurement will be performed at the breast. This measurement will be performed to show if the perfusion in PU differs from the perfusion in PU during surgery or if the perfusion will approximately be the same.

Table 1 Time schedule of the study for each patient

Visit before surgery	Surgery	Day after surgery
Informed consent	Measurements 1-4	Measurement 5
Patient demographics		
Medical history		

4. STUDY POPULATION

4.1 Population (base)

For this study, we will include 15 adult patients that will undergo a DIEP flap breast reconstruction. (Former) breast cancer patients in the department of (plastic) surgery will be asked to participate in this research if they fulfil the following inclusion criteria.

4.2 Inclusion criteria

In order to be eligible to participate in this study, a subject must meet all of the following criteria:

- ≥ 18 years of age.
- An indication for a unilateral or bilateral DIEP flap breast reconstruction, either immediate or delayed.
- Patients must be willing to give informed consent.

4.3 Exclusion criteria

A potential subject who meets any of the following criteria will be excluded from participation in this study:

- Patients unwilling or unable to give informed consent.

4.4 Sample size calculation

As a case series study is a descriptive study, it is impossible to determine the number of participants based on a sample size calculation.

5. TREATMENT OF SUBJECTS

Not applicable.

5.1 Investigational product/treatment

Not applicable.

5.2 Use of co-intervention

Not applicable.

5.3 Escape medication

Not applicable.

6. INVESTIGATIONAL PRODUCT

6.1 Name and description of investigational product(s)

The WIPI consists of two parts: a camera system with two cameras and a laser beam. The skin is illuminated by the laser beam and white light emitting diodes. One camera captures backscattered light from tissue (speckle pattern). The other camera captures the scanned area by means of colour photograph. This enables to correct for motion artefacts afterwards and to overlap the perfusion maps on colour images. The WIPI noninvasively measures relative skin perfusion. Detailed information about the WIPI is attached in the 'Investigational Medicinal Device Dossier'.

6.2 Summary of findings from non-clinical studies

Not applicable.

6.3 Summary of findings from clinical studies

Not applicable.

6.4 Summary of known and potential risks and benefits

The application of the WIPI is without any discomfort and is painless.

6.5 Description and justification of route of administration and dosage

Not applicable.

6.6 Dosages, dosage modifications and method of administration

Not applicable.

6.7 Preparation and labelling of Investigational Medicinal Product

Not applicable.

6.8 Drug accountability

Not applicable.

7. NON-INVESTIGATIONAL PRODUCT

7.1 Name and description of non-investigational product

Indocyanine green (ICG) is a fluorescent dye applied as contrast agent in medical diagnostics. ICG has been used for decades in retinal angiography and more recently in perfusion diagnostics of organs and tissues²⁹. It is part of the standard care in autologous breast reconstruction in ZGT. The principle of ICG angiography is as follows: after administration of ICG in the blood circulation, tissue of interest is illuminated with light of a

wavelength of about 780 nm, which is the excitation wavelength of ICG. Longer emission wavelengths of over 800 nm are subsequently emitted by ICG and can be observed with the use of cameras that can record wavelengths in the near-infrared (NIR) spectrum. With the use of ICG angiography, information about deeper lying blood vessels can be obtained. This is because ICG angiography operates in the NIR spectrum, in which human tissue is more translucent than in the visual spectrum.

7.2 Summary of findings from non-clinical studies

Not applicable.

7.3 Summary of findings from clinical studies

Not applicable.

7.4 Summary of known and potential risks and benefits

Please refer to section 1.2 for the benefits and potential risks of ICG.

7.5 Description and justification of route of administration and dosage

Not applicable.

7.6 Dosages, dosage modifications and method of administration

An ampul of 25 mg ICG in 5 ml water is available in ZGT for ICG angiography. The recommended dose is 0.1-0.3 mg/kg (max < 5 mg/kg), which often results in an administered bolus of 2 ml ICG solution. It is administered via the intravenous drip and is visible after around 30 seconds with the use of NIR cameras.

7.7 Preparation and labelling of Non Investigational Medicinal Product

Please refer to 7.6.

7.8 Drug accountability

Not applicable.

8. METHODS

8.1 Study parameters/endpoints

8.1.1 Main study parameter/endpoint

The main study endpoint will be:

The mean perfusion in PU of the newly reconstructed breast correlated to the occurrence of absence of perfusion-related complications.

8.1.2 Secondary study parameters/endpoints (if applicable)

The secondary study endpoints will be:

1. Visualisation of the perfusion of the abdominal flap during five moments the measurements will be performed.
2. Applicability and efficiency of the method against motion artefacts.
3. Feasibility and applicability of the WIPI that operates wireless and can preview perfusion frames in daily clinical practice.

8.1.3 Other study parameters (if applicable)

Not applicable.

8.2 Randomisation, blinding and treatment allocation

Not applicable.

8.3 Study procedures

All included patients will be selected from the outpatient clinic, please refer to chapter four for inclusion criteria. For the scheme of the performed procedures and measurements in this study, please refer to chapter three. In this paragraph, a detailed description of all measurements and procedures is given.

Study procedure

Patients that meet the inclusion criteria will be approached by their (plastic) surgeon before the DIEP flap breast reconstruction. During the visit in which information is given about the surgery, information about the study will also be orally provided and by means of the Subject Information Sheet (in Dutch: proefpersonen informatiebrief). Patients will get some time for consideration. A second meeting, either in person or by phone, will be planned to ask the patient if she wants to participate and to sign a written informed consent. Patients have to sign a written informed consent before surgery and enrolling into the study. Each patient will undergo a DIEP flap breast reconstruction, either immediate or delayed. DIEP flap breast reconstruction can be unilateral or bilateral.

Each LSCI measurement will consist of digital colour images and perfusion maps made by the WIPI. Measurements 2 (raised flap) and measurement 4 (anastomosis) will also contain ICG angiograms, which are nowadays used to be performed during DIEP flap breast reconstruction. Measurement 5 takes place on the first postoperative day of the typical two to four days patient's stay after DIEP flap breast reconstruction.

Measurements with the WIPI

The WIPI will be held above the skin at a distance of approximately 30 cm as this is the focus distance of the cameras. Due to the low output of the laser beam, no protective darkened spectacles will be needed during the scanning procedure. Performing measurements with the WIPI is painless, non-invasive and without any discomfort.

8.4 Withdrawal of individual subjects

Subjects can leave the study at any time for any reason if they wish to do so without any consequences. The investigator can decide to withdraw a subject from the study for urgent medical reasons.

8.4.1 Specific criteria for withdrawal

Not applicable.

8.5 Replacement of individual subjects after withdrawal

If a subjects decides to leave the study before the end of the study period, we will try to replace this subject by another subject.

8.6 Follow-up of subjects withdrawn from treatment

Follow-up of withdrawn subjects will be guaranteed by regular treatment.

8.7 Premature termination of the study

No reasons for premature termination of the study are foreseen.

9. SAFETY REPORTING

9.1 Temporary halt for reasons of subject safety

In accordance to section 10, subsection 4, of the WMO, the sponsor will suspend the study if there is sufficient ground that continuation of the study will jeopardise subject health or safety. The sponsor will notify the accredited METC without undue delay of a temporary halt including the reason for such an action. The study will be suspended pending a further positive decision by the accredited METC. The investigator will take care that all subjects are kept informed.

9.2 AEs, SAEs and SUSARs

9.2.1 Adverse events (AEs)

Adverse events are defined as any undesirable experience occurring to a subject during the study, whether or not considered related to [the investigational product / trial procedure/ the experimental intervention]. All adverse events reported spontaneously by the subject or observed by the investigator or his staff will be recorded.

9.2.2 Serious adverse events (SAEs)

A serious adverse event is any untoward medical occurrence or effect that

- results in death;
- is life threatening (at the time of the event);
- requires hospitalisation or prolongation of existing inpatients' hospitalisation;
- results in persistent or significant disability or incapacity;
- is a congenital anomaly or birth defect; or
- any other important medical event that did not result in any of the outcomes listed above due to medical or surgical intervention but could have been based upon appropriate judgement by the investigator.

An elective hospital admission will not be considered as a serious adverse event.

The sponsor will report the SAEs through the web portal *ToetsingOnline* to the accredited METC that approved the protocol, within 7 days of first knowledge for SAEs that result in death or are life threatening followed by a period of maximum of 8 days to complete the initial preliminary report. All other SAEs will be reported within a period of maximum 15 days after the sponsor has first knowledge of the serious adverse events.

9.2.3 Suspected unexpected serious adverse reactions (SUSARs)

Not applicable.

9.3 Annual safety report

Not applicable.

9.4 Follow-up of adverse events

All AEs will be followed until they have abated, or until a stable situation has been reached. Depending on the event, follow up may require additional tests or medical procedures as indicated, and/or referral to the general physician or a medical specialist.

SAEs need to be reported till end of study within the Netherlands, as defined in the protocol.

9.5 Data Safety Monitoring Board (DSMB) / Safety Committee

A DSMB is not necessary as this is a study with negligible risk.

10. STATISTICAL ANALYSIS

10.1 Primary study parameter(s)

The primary study parameter will be the mean perfusion in PU of the breast \pm the standard deviation, separated into two groups: patients that develop perfusion-related complications and patients that do not develop perfusion-related complications. As the number of participating patients is small, it is expected that no significant differences will be found in this analysis. However, we assume we can explain eventual visible differences between these two groups based on the knowledge of the (patho)physiology of the microcirculatory, which matches the proof of concept idea of this study. These eventual visible differences could be the starting point of future research to the WIPI as a predictor for perfusion-related complications, for example.

10.2 Secondary study parameter(s)

i. Five measurements will be performed on the abdominal flap that will be used for reconstruction. The mean perfusion in PU of the flap of each patient will be determined for each measurement. Then, we could get an idea of the way the perfusion in the flap differs or remains the same during surgery and after surgery. Again, we probably have a too small number of data points to make a valid statistical analysis. Therefore, we assume to be able to interpret the results based on visible differences and/or similarities with the use of the knowledge of the (patho)physiology of the microcirculatory.

ii. iii. The method against motion artefacts and the system that can preview perfusion maps during surgery will both be evaluated with the use of the User Experience Questionnaire (questionnaire attached as "UEQ_Dutch.pdf").

iv. Description of the population. A table will be made for the descriptive statistics of the population including: age (mean \pm standard deviation), type of tumour, type of DIEP flap breast reconstruction (immediate or delayed, unilateral or bilateral) and smoking.

10.3 Other study parameters

Not applicable.

10.4 Interim analysis

Not applicable.

11. ETHICAL CONSIDERATIONS

11.1 Regulation statement

This study will be conducted according to the Medical Research Involving Human Subjects Act (WMO) and to the principles of the Declaration of Helsinki (version 10, October 2013).

11.2 Recruitment and consent

(Former) breast cancer patients will be selected from the outpatient clinic at the department of plastic surgery of Ziekenhuisgroep Twente. Patients will be approached by their treating plastic surgeon. If patients are willing to receive more information about the study, one of the principal investigators will inform them, provide written information and ask for informed consent. If necessary, patients can take as long as they need within the inclusion period to give informed consent. No research procedures will take place before informed consent is obtained.

11.3 Objection by minors or incapacitated subjects

Not applicable.

11.4 Benefits and risks assessment, group relatedness

To date, little is known about the changes in the microcirculatory during DIEP flap breast reconstruction, which include the effects of thromboses and vasospasms on the microcirculatory that could result in perfusion-related complications. With the WIPI, we hope to provide new insights into this device as an imaging technique for the visualisation of the microcirculatory and changes within the microcirculatory. We aim to define the predictive value for the development of perfusion-related complications and to find a cut-off value in perfusion for perfusion-related complications to, hopefully, reduce these complications in the future.

The included patients will undergo the standard treatment, in which the perfusion is verified twice (raised flap and after anastomosis) by ICG angiography. The set-up of this study is to determine the predictive value of LSCI for the development of perfusion-related complications, to compare this to the predictive value of ICG and the surgeon's intraoperative assessment and to determine whether LSCI may be able to replace ICG angiography. That would be of great value, given the non-invasive and easy-to-apply character of the device.

Given the potential advantages of the WIPI during DIEP flap breast reconstruction in the future, we are of the opinion that participation in this study with only one postoperative measurement and the application of the non-invasive imaging technique is legitimate. Scanning the skin with the use of the WIPI is painless and without any discomfort.

11.5 Compensation for injury

The sponsor/investigator has a liability insurance which is in accordance with article 7 of the WMO. The sponsor (also) has an insurance which is in accordance with the legal

requirements in the Netherlands (Article 7 WMO). This insurance provides cover for damage to research subjects through injury or death caused by the study.

The insurance applies to the damage that becomes apparent during the study or within 4 years after the end of the study.

11.6 Incentives

Not applicable.

12. ADMINISTRATIVE ASPECTS, MONITORING AND PUBLICATION

12.1 Handling and storage of data and documents

A registry will be developed that contains the LSCI images and colour images obtained from the five LSCI measurements. During surgery, LSCI images and colour images will be stored at an external hard drive, which is secured by a password. After surgery, the data will be saved in a coded manner in a secured ZGT map, which is only accessible for the principal investigators working for ZGT. A separate registry will include the subject numbers and their corresponding personal data. The key to the code will be kept in a registry safeguarded and is only accessible for the principal investigators working for ZGT. Pseudonymised data will be transferred to the University of Twente for data analysis and will be stored in a map for patient data only, which is accessible for the coordinating investigator, principal investigator working for the University of Twente and technical staff.

The colour images will be taken close to the skin at approximately 30 cm, so patients cannot be recognised. Moreover, the head of the patient is covered by the sterile field during surgery. All data will be handled comply with EU General Data Protection Regulation and the Dutch Act on Implementation of the General Data Protection Regulation (in Dutch: Uitvoeringswet AVG, UAVG).

12.2 Monitoring and Quality Assurance

Not applicable.

12.3 Amendments

Amendments are changes made to the research after a favourable opinion by the accredited METC has been given. All amendments will be notified to the METC that gave a favourable opinion.

12.4 Annual progress report

The sponsor/investigator will submit a summary of the progress of the trial to the accredited METC once a year. Information will be provided on the date of inclusion of the first subject, numbers of subjects included and numbers of subjects that have completed the trial, serious adverse events/ serious adverse reactions, other problems, and amendments.

12.5 Temporary halt and (prematurely) end of study report

The investigator/sponsor will notify the accredited METC of the end of the study within a period of 8 weeks. The end of the study is defined as the last patient's last visit.

The sponsor will notify the METC immediately of a temporary halt of the study, including the reason of such an action. In case the study is ended prematurely, the sponsor will notify the accredited METC within 15 days, including the reasons for the premature termination.

Within one year after the end of the study, the investigator/sponsor will submit a final study report with the results of the study, including any publications/abstracts of the study, to the accredited METC.

12.6 Public disclosure and publication policy

The results of this study will be published in an international journal for plastic surgery. The CCMO statement on publication policy will be followed.

13. STRUCTURED RISK ANALYSIS

13.1 Potential issues of concern

No risks are foreseen with microcirculation imaging during DIEP flap breast reconstruction in tissue of interest by the WIPI. It is a non-invasive imaging device with a low-output laser beam.

a. Level of knowledge about mechanism of action

Not applicable.

b. Previous exposure of human beings with the test product(s) and/or products with a similar biological mechanism

The WIPI is produced and tested within the University of Twente. The device used in this study is a successor to the HAPI system (NL69174.091.19). Previous study with the HAPI system in sixteen patients showed that the application of this non-invasive system was without any discomfort to the patients.

c. Can the primary or secondary mechanism be induced in animals and/or in *ex-vivo* human cell material?

Not applicable.

d. Selectivity of the mechanism to target tissue in animals and/or human beings

Not applicable.

e. Analysis of potential effect

Not applicable.

f. Pharmacokinetic considerations

Not applicable.

g. Study population

Please refer to chapter four.

h. Interaction with other products

ICG does not interact with the WIPI. The emitted light from ICG is around 800 nm, whereas the laser beam has a wavelength of 671 nm. The camera that receives the reflected laser light, can only receive light of that particular wavelength due to the filter within the camera.

NL80104.100.22 / Wireless LSCI device during DIEP flap breast reconstruction

So wavelengths of 800 nm do not interact with the reflected light of a wavelength of 671 nm within the camera.

i. Predictability of effect

Not applicable.

j. Can effects be managed?

Not applicable.

13.2 Synthesis

As the WIPI is non-invasive, we estimate the study risks as negligible. We are of the opinion that participating in this study with four measurements during surgery, one measurement after surgery and the application of a non-invasive imaging technique is legitimate. Scanning the skin with the use of the WIPI is painless and without any discomfort.

14. REFERENCES

1. Integraal kankercentrum Nederland. Incidentie borstkanker. (2021). Available at: <https://iknl.nl/kankersoorten/borstkanker/registratie/incidentie>. (Accessed: 27th September 2021)
2. Integraal kankercentrum Nederland. Overleving borstkanker. (2021). Available at: <https://iknl.nl/kankersoorten/borstkanker/registratie/overleving>. (Accessed: 27th September 2021)
3. Costa, W. A., Eleutério, J., Giraldo, P. C. & Gonçalves, A. K. Quality of life in breast cancer survivors. *Rev. Assoc. Med. Bras.* **63**, 583–589 (2017).
4. Janssen-Heijnen, M. L. G. *et al.* Small but significant excess mortality compared with the general population for long-term survivors of breast cancer in the Netherlands. *Ann. Oncol.* **25**, 64–68 (2014).
5. Kouwenberg, C. A. E. *et al.* Long-Term Health-Related Quality of Life after Four Common Surgical Treatment Options for Breast Cancer and the Effect of Complications: A Retrospective Patient-Reported Survey among 1871 Patients. *Plast. Reconstr. Surg.* 1–13 (2020). doi:10.1097/PRS.0000000000006887
6. Hunsinger, V. *et al.* Long-Term Follow-Up of Quality of Life following DIEP Flap Breast Reconstruction. *Plast. Reconstr. Surg.* **137**, 1361–1371 (2016).
7. Heidekrueger, P. I. *et al.* Overall Complication Rates of DIEP Flap Breast Reconstructions in Germany—A Multi-Center Analysis Based on the DGPRÄC Prospective National Online Registry for Microsurgical Breast Reconstructions. *J. Clin. Med.* **10**, 1016 (2021).
8. Zötterman, J. *et al.* Intraoperative laser speckle contrast imaging in DIEP breast reconstruction: A prospective case series study. *Plast. Reconstr. Surg. - Glob. Open* 1–7 (2020). doi:10.1097/GOX.0000000000002529
9. Sharma, H. R., Rozen, W. M., Mathur, B. & Ramakrishnan, V. 100 Steps of a DIEP Flap - A prospective comparative cohort series demonstrating the successful implementation of process mapping in microsurgery. *Plast. Reconstr. Surg. - Glob. Open* **7**, 1–5 (2019).
10. Bhullar, H., Hunter-Smith, D. J. & Rozen, W. M. Fat Necrosis After DIEP Flap Breast Reconstruction: A Review of Perfusion-Related Causes. *Aesthetic Plast. Surg.* **44**, 1454–1461 (2020).
11. Liu, E. H. *et al.* Intraoperative SPY Reduces Post-mastectomy Skin Flap Complications: A Systematic Review and Meta-Analysis. *Plast. Reconstr. Surg. - Glob. Open* **7**, 1–8 (2019).
12. Girard, N. *et al.* Innovative DIEP flap perfusion evaluation tool: Qualitative and quantitative analysis of indocyanine green-based fluorescence angiography with the SPY-Q proprietary software. *PLoS One* **14**, 1–14 (2018).
13. Kamali, P. *et al.* Medial Row Perforators Are Associated with Higher Rates of Fat Necrosis in Bilateral DIEP Flap Breast Reconstruction. *Plast. Reconstr. Surg.* **140**, 19–24 (2017).
14. Verduijn, P. S., Michi, M., Vahrmeijer, A. L. & Mulder, B. G. S. Perfusion assessment of DIEP flaps based on near-infrared fluorescence imaging: current literature and pilot study. *SPIE* **1086213**, (2019).
15. To, C. *et al.* Intraoperative Tissue Perfusion Measurement by Laser Speckle Imaging: A Potential Aid for Reducing Postoperative Complications in Free Flap Breast Reconstruction. *Plast. Reconstr. Surg.* **143**, 287e-292e (2019).
16. Zötterman, J. *et al.* Laser Speckle Contrast Imaging in Reconstructive Surgery. (Linköping University,

NL80104.100.22 / Wireless LSCI device during DIEP flap breast reconstruction

- 2020). doi:10.3384/diss.diva-164328
17. Lauritzen, E. & Damsgaard, T. E. Use of Indocyanine Green Angiography decreases the risk of complications in autologous- and implant-based breast reconstruction: A systematic review and meta-analysis. *J. Plast. Reconstr. Aesthetic Surg.* **74**, 1703–1717 (2021).
 18. Alstrup, T., Christensen, B. O. & Damsgaard, T. E. ICG angiography in immediate and delayed autologous breast reconstructions: peroperative evaluation and postoperative outcomes. *J. Plast. Surg. Hand Surg.* **52**, 307–311 (2018).
 19. Degett, T. H., Andersen, H. S. & Gögenur, I. Indocyanine green fluorescence angiography for intraoperative assessment of gastrointestinal anastomotic perfusion: a systematic review of clinical trials. *Langenbeck's Arch. Surg.* **401**, 767–775 (2016).
 20. Hackethal, A. *et al.* Role of Indocyanine Green in Fluorescence Imaging with Near- Infrared Light to Identify Sentinel Lymph Nodes , Lymphatic Vessels and Pathways Prior to Surgery – A Critical Evaluation of Options Die Rolle von Indocyaningrün als Fluoreszenzfarbstoff in Komb. *Geburtshilfe Frauenheilk* **78**, 54–62 (2018).
 21. Dupréé, A., Rieß, H., Detter, C., Debus, E. S. & Wipper, S. H. Utilization of indocyanine green fluorescent imaging (ICG-FI) for the assessment of microperfusion in vascular medicine. *Innov. Surg. Sci.* **3**, 193–201 (2018).
 22. Meira, J., Marques, M. L., Falcão-Reis, F., Gomes, E. R. & Carneiro, Â. Immediate reactions to fluorescein and indocyanine green in retinal angiography: Review of literature and proposal for patient's evaluation. *Clin. Ophthalmol.* **14**, 171–178 (2020).
 23. Zötterman, J., Tesselaar, E. & Farnebo, S. The use of laser speckle contrast imaging to predict flap necrosis : An experimental study in a porcine flap model. *J. Plast. Reconstr. Aesthetic Surg.* 771–777 (2019). doi:10.1016/j.bjps.2018.11.021
 24. Heeman, W., Steenbergen, W., van Dam, G. M. & Boerma, E. C. Clinical applications of laser speckle contrast imaging: a review. *J. Biomed. Opt.* **24**, 1 (2019).
 25. Mennes, O. A., Van Netten, J. J., Van Baal, J. G. & Steenbergen, W. Assessment of microcirculation in the diabetic foot with laser speckle contrast imaging. *Physiol. Meas.* **40**, (2019).
 26. Mangraviti, A. *et al.* Intraoperative Laser Speckle Contrast Imaging For Real-Time Visualization of Cerebral Blood Flow in Cerebrovascular Surgery: Results From Pre-Clinical Studies. *Sci. Rep.* **10**, 1–13 (2020).
 27. Kojima, S. *et al.* Laser Speckle Contrast Imaging for Intraoperative Quantitative Assessment of Intestinal Blood Perfusion During Colorectal Surgery: A Prospective Pilot Study. *Surg. Innov.* 1553350618823426 (2019). doi:10.1177/1553350618823426
 28. Chizari, A., Schaap, M. J., Knop, T., Boink, Y. E. & Seyger, M. M. B. Handheld versus mounted laser speckle contrast perfusion imaging demonstrated in psoriasis lesions. *Sci. Rep.* **11**, 16646 (2021).
 29. Alander, J. T. *et al.* A review of indocyanine green fluorescent imaging in surgery. *Int. J. Biomed. Imaging* **2012**, 940585 (2012).